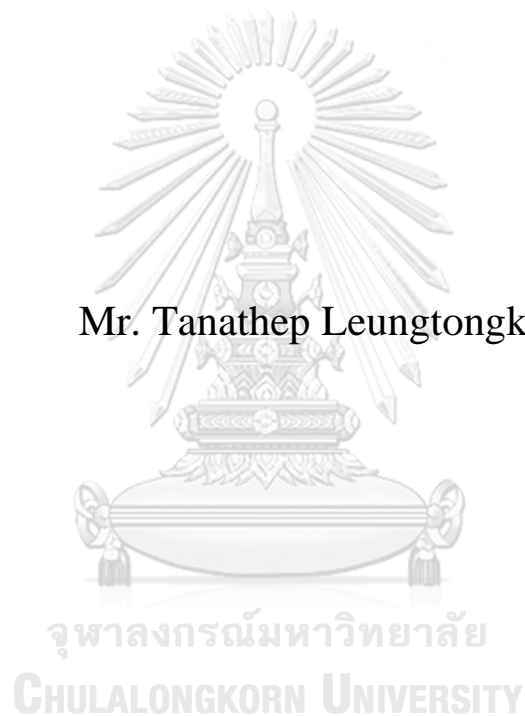# NUMERICAL SIMULATION AND OPTIMIZATION OF COMMERCIAL STERILIZATION OF LIQUID ENTERAL NUTRITION USING BATCH MICROWAVE HEATING

Mr. Tanathep Leungtongkum

จุฬาลงกรณ์มหาวิทยาลัย
CHULALONGKORN UNIVERSITY

A Thesis Submitted in Partial Fulfillment of the Requirements
for the Degree of Master of Science in Food Technology
Department of Food Technology
Faculty of Science
Chulalongkorn University
Academic Year 2018
Copyright of Chulalongkorn University

การจำลองเชิงตัวเลขและการหาค่าเหมาะที่สุดของการฆ่าเชื้อทางการค้าอาหารเหลวทางสายให้อาหารด้วยการให้ความร้อนด้วยไมโครเวฟแบบกะ

นายธนเทพ เหลืองทองคำ

Thesis Title	NUMERICAL SIMULATION AND OPTIMIZATION OF COMMERCIAL STERILIZATION OF LIQUID E NTERAL NUTRITION USING BATCH MICROWAV E HEATING
By	Mr. Tanathep Leungtongkum
Field of Study	Food Technology
Thesis Advisor	Associate Professor Jirarat Anuntagool, Ph.D.
Thesis Co Advisor	Associate Professor Jean-Claude Laguerre, Ph.D.

Accepted by the Faculty of Science, Chulalongkorn University in Partial Fulfillment of the Requirement for the Master of Science

.... Dean of the Faculty of Science
(Professor POLKIT SANGVANICH, Ph.D.)

THESIS COMMITTEE

.... Chairman
(Assistant Professor SASIKAN KUPONGSAK, Ph.D.)
.... Thesis Advisor
(Associate Professor Jirarat Anuntagool, Ph.D.)
.... Thesis Co-Advisor
(Associate Professor Jean-Claude Laguerre, Ph.D.)
.... Examiner
(Assistant Professor THANACHAN MAHAWANICH, Ph.D.)
.... External Examiner
(Assistant Professor Suthida Akkarachaneeyakorn, Ph.D.)

จุฬาลงกรณ์มหาวิทยาลัย

CHULALONGKORN UNIVERSITY

ธนเทพ เหลืองทองคำ : การจำลองเชิงตัวเลขและการหาค่าเหมาะที่สุดของการฆ่าเชื้อทางการค้าอาหารเหลวทางสายให้อาหาร ด้วยการให้ความร้อนด้วยไมโครเวฟแบบกะ. (
NUMERICAL SIMULATION AND OPTIMIZATION OF COMMERCIAL STE
RILIZATION OF LIQUID ENTERAL NUTRITION USING BATCH MICROW
AVE HEATING) อ.ที่ปรึกษาหลัก : รศ. ดร.จิรารัตน์ อนันตกูล, อ.ที่ปรึกษาร่วม : รศ. ดร.Jean-Claude Laguerre

วิทยานิพนธ์ประกอบด้วย 3 ส่วน โดยส่วนที่หนึ่งนำเสนอการศึกษาอิทธิพลขององค์ประกอบและหาสูตรที่เหมาะสมของอาหารเหลว สำหรับผู้ป่วยชนิดให้ทางปาก ซึ่งเป็นอาหารที่มีความเข้มข้นของพลังงานสูง เนื่องจากมีคาร์โบไฮเดรต โปรตีนและไขมันในปริมาณมาก ดังนั้นอาหาร ชนิดนี้จึงมักมีความหนืดที่สูงและ/หรือเกิดการแยกชั้นได้ง่าย ดังนั้นทางผู้วิจัยจึงแปร 9 ปัจจัยคือความเข้มข้นของพลังงาน ชนิดของน้ำมัน ความเข้มข้น ของเลซิทิน อัตราส่วนของน้ำเชื่อมฟรุกโทสกับกรด ร้อยละของเวย์โปรตีนชนิดไฮโดรไลซ์ต่อโปรตีนทั้งหมด ร้อยละของพลังงานจากไขมันต่อพลังงาน ทั้งหมด ร้อยละของพลังงานจากน้ำเชื่อมฟรุกโทสต่อพลังงานทั้งหมด ความเข้มข้นของเวย์โปรตีนเชิงซ้อนและอัตราส่วนของเวย์โปรตีนสกัดต่อเวย์ โปรตีนเชิงซ้อนทั้งหมด เพื่อให้อาหารมีค่าความหนืดเชิงซ้อนที่วัดที่ความถี่ 50 เฮิรตซ และอุณหภูมิ 25 องศาเซลเซียส กับร้อยละการแยกชั้นของ อิมัลชันที่เหมาะสม พบว่าเทคนิคความสัมพันธ์เชิงไอคอนรูปภาพเสนอแผนการทดลองเพื่อหาสูตรที่เหมาะสมจำนวน 17 การทดลอง ในขณะที่เทคนิค การตอบสนองเชิงพื้นผิวร่วมกับโดห์เลอร์เมทริกซ์ต้องใช้ 524 การทดลอง แบบจำลองเชิงตรรกะที่ได้จากเทคนิคความสัมพันธ์เชิงไอคอนรูปภาพซึ่ง แสดงถึงความสัมพันธ์ระหว่างพจน์ทางตรรกะระหว่าง 2 ปัจจัยใดๆ ที่มีความสำคัญต่อตัวแปรตามที่สนใจสามารถอธิบายแนวโน้มของตัวแปรตามได้ดี (R^2_{adj} = 0.99 และ 0.93 สำหรับค่าความหนืดและร้อยละการแยกชั้นของอิมัลชันตามลำดับ) วิทยานิพนธ์ส่วนที่สองนำเสนอการศึกษาอิทธิพลของ ตัวแปรในการให้ความร้อนด้วยไมโครเวฟและหาสภาวะที่เหมาะสมของกระบวนการดังกล่าวสำหรับอาหารเหลวสำหรับผู้ป่วยชนิดให้ทางสายให้อาหาร โดยศึกษาการให้ความร้อนผลิตภัณฑ์ปริมาตร 150 มิลลิลิตรในถุงเพาช์ที่มีความเข้มข้นของพลังงานเป็น 1 กิโลแคลอรีต่อมิลลิลิตร ซึ่งประกอบด้วย พลังงานจากคาร์โบไฮเดรต ไขมันและโปรตีนในอัตราส่วน 50: 30: 20 ด้วยไมโครเวฟที่แปรเวลาในการให้ความร้อน 5 ระดับตั้งแต่ 35 วินาทีถึง 60 วินาที และกำลังไมโครเวฟจำเพาะ 3 ระดับตั้งแต่ 3 วัตต์ต่อมิลลิลิตรถึง 7 วัตต์ต่อมิลลิลิตรด้วยแผนการทดลองแบบโดห์เลอร์เมทริกซ์ต่อค่า อุณหภูมิพื้นผิวเฉลี่ยที่วัดด้วยกล้องอินฟราเรด ค่าร้อยละการสูญเสียทริปโตแฟน และค่าดัชนี FAST ที่วิเคราะห์ด้วยเทคนิคสเปกโตรสโกปีแบบฟลูออ เรสเซนส์ พบว่าเวลาในการให้ความร้อนมีอิทธิพลต่อดัชนี FAST ส่วนกำลังไมโครเวฟจำเพาะมีอิทธิพลต่อค่าอุณหภูมิพื้นผิวเฉลี่ย และแบบจำลองที่ได้ จากเทคนิคการตอบสนองเชิงพื้นผิวดีกว่าแบบจำลองที่ได้จากเทคนิคความสัมพันธ์เชิงไอคอนรูปภาพสำหรับตัวแปรตามส่วนใหญ่ วิทยานิพนธ์ส่วน สุดท้ายนำเสนอการใช้การจำลองเชิงตัวเลขในการศึกษาการให้ความร้อนด้วยไมโครเวฟ โดยทางผู้วิจัยศึกษาองค์ประกอบทางเคมี สมบัติทางกายภาพ ความร้อน การไหลและไดอิเล็กทริกของตัวอย่างอาหารเหลวที่มีความเข้มข้นพลังงานเป็น 1 กิโลแคลอรีต่อมิลลิลิตร 2.5 กิโลแคลอรีต่อมิลลิลิตรและ 3.78 กิโลแคลอรีต่อกรัม แล้วจึงศึกษาการให้ความร้อนผลิตภัณฑ์ในถุงเพาช์ที่กำลัง 450 วัตต์หรือ 850 วัตต์ ด้วยการให้ความร้อนแบบต่อเนื่องหรือ เป็นจังหวะ ที่เวลาต่างๆ กัน โดยใช้ระบบไมโครเวฟที่มีความถี่ 2,450 เมกะเฮิรตซ พบว่าอัตราการให้ความร้อนและความไม่สม่ำเสมอของอุณหภูมิสูง ในตัวอย่างที่มีความเข้มข้นของพลังงานสูง และการให้ความร้อนแบบเป็นจังหวะทำให้การกระจายของอุณหภูมิสม่ำเสมอมากขึ้น แต่การให้ความร้อนไม่ ทำให้ดัชนี FAST เพิ่มขึ้น กระบวนการจำลองเชิงตัวเลขโดยใช้วิธี Finite Element ร่วมกับสมการที่อธิบายพฤติกรรมคลื่นแม่เหล็กไฟฟ้า และ การนำความร้อนแบบพาเสนอกระบวนการให้ความร้อนในระดับการฆ่าเชื้อทางการค้า โดยสามารถทำนายอุณหภูมิเฉลี่ยที่พื้นผิวด้านบนของตัวอย่างและ ดัชนี FAST ได้ แต่รูปแบบการกระจายอุณหภูมิของตัวอย่างและผลการให้ความร้อนแบบเป็นจังหวะจากการจำลองเชิงตัวเลขแตกต่างจากผลการ ทดลองจริง

5972148323 : MAJOR FOOD TECHNOLOGY

Tanathep   Leungtongkum   :
NUMERICAL SIMULATION AND OPTIMIZATION OF COMMERCIAL STERILIZA
TION OF LIQUID ENTERAL NUTRITION USING BATCH MICROWAVE HEATIN
G. Advisor: Assoc. Prof. Jirarat Anuntagool, Ph.D. Co-advisor: Assoc. Prof. Jean-Claude
Laguerre, Ph.D.

This thesis contains 3 parts. The first part was to investigate the effect of ingredients on product's stability and to find optimized oral-feeding enteral nutrition formulas. Since oral-feeding enteral nutrition is high in caloric density, it contains a high amount of calorie sources. Thus, it is likely to have either too high viscosity and/or unstable emulsion. Consequently, 9 factors which are caloric content, oil type, lecithin concentration, fructose syrup to acid ratio, percentage of hydrolyzed whey protein to total protein, percentage of calorie from fat and from fructose syrup to total calorie, complex whey protein concentration, and percentage of whey protein isolate to total complex whey protein were optimized. The desired responses were the complex viscosity at 50 Hz and 25 ℃, and the percentage of emulsion separation. By using the Iconographic Correlation method (IC), the number of experiment was reduced from 524 treatments for classical response surface methodology (RSM) with Doehlert matrix (DM) to 17 treatments. IC proposed models described of significant logical interactions between factors and responses with excellent correlation (R^2_{adj} = 0.99, and 0.93 for complex viscosity, and emulsion separation, respectively). The second part aimed to investigate the effect of microwave heating on the enteral nutrition and finding optimal conditions for heating tube-feeding formula. DM with 5 heating times (35 s to 60 s) and 3 specific powers (3 W/mL to 7 W/mL) was assigned to investigate the effect of microwave heating for a pouch of 150-mL product contained 1 kcal/mL and had the caloric distribution from carbohydrate: fat: protein at 50: 30: 20. The surface temperature measured by an infrared camera, relative tryptophan loss and FAST index by fluorometric spectroscopy were determined as responses. The FAST index and the change in average surface temperature were correlated with heating time and specific power, respectively. Comparing the models proposed by RSM and IC, RSM gave more predictive models than those of IC did for most responses. The last part involved the development of numerical simulation for microwave heating process. Proximate composition, physical, thermal, rheological, and dielectric properties of 1 kcal/mL, 2.5 kcal/mL, and 3.78 kcal/g liquid enteral nutrition products were determined. Products in a retortable pouch were heated at 450 W or 850 W by continuous heating or intermittent heating at different heating times by a 2,450-MHz microwave oven. Higher caloric density had higher heating rate and heterogeneity in temperature distribution while intermittent heating enhanced the homogeneity of heating. In addition, heating did not increase the FAST index of the samples. A numerical model was developed by using the Finite Element Method to solve a convective heat transfer in fluid coupling with electromagnetic propagation. The model proposed the conditions reaching the commercial sterilization for the products. Moreover, it can predict the average surface temperature for continuous heating and the FAST index, but not the temperature distribution and the temperature profile from intermittent heating.

Field of Study:	Food Technology	Student's Signature ....
Academic Year:	2018	Advisor's Signature ....
		Co-advisor's Signature ....

ACKNOWLEDGEMENTS

Tanathep Leungtongkum

TABLE OF CONTENTS

Page

จุฬาลงกรณ์มหาวิทยาลัย

CHULALONGKORN UNIVERSITY

LIST OF TABLES

Page

LIST OF FIGURES

Page

LIST OF SYMBOLS

Abbreviations

Time   Heating time (s)

Spec_Power   Specific power (W/mL)

FAST_index   FAST index

Trp_loss   Relative tryptophane loss (%)

CML   Carboxymethyllysine content (µg/g)

Lysine   Lysine content (mg/g)

Mean_Temp   Average of bottom surface temperature (°C)

P5_Temp   5-Percentile of bottom surface temperature (°C)

SD_Temp   Standard deviation of bottom surface temperature (°C)

Symbols

C_p Specific heat (J/kg·K)

E   Electric field (V/m)

E_a Activation energy (kJ/mol)

F   Volume force vector (N/m^3)

g   Gravity force (N)

h_c Convective heat transfer (W/m^2·K)

J   Current density (A/m^2)

k   Thermal conductivity (W/m·K)

K   Consistency index (Pa·s)

p   Pressure (Pa)

q   Heat flux by convection (W/m^2)

R   Gas constant (8.314×10^{-3} kJ/mol·K)

T   Temperature (°C)

t   Time (s)

T_0 Reference temperature (25 °C)

u   Velocity vector (m/s)

x   Weight fraction

Greek letters

$\dot{\gamma}$ Shear rate (Hz)

ε Permittivity (F/m)

ε_0 Permittivity of vacuum (8.85×10^{-12} F/m)

ε_r Relative permittivity

η Dynamic viscosity (Pa·s)

μ Permeability (H/m)

μ_0 Permeability of vacuum ($4\pi \times 10^{-7}$ H/m)

μ_r Relative permeability

ρ Density (kg/m^3)

σ Electric conductivity (S/m)

τ Shear stress (Pa)

τ_0 Yield stress (Pa)

ω Angular frequency (rad/s)

Chapter 1 Introduction

Currently, aging society is one of the challenging issues all over the world and around half of the elderly suffers from dysphagia. They need enteral nutrition products to maintain adequate nutrient intake. It can be either a homemade blenderized or a commercial enteral nutrition product and in the form of powder or liquid. Considering a liquid enteral nutrition product, it can be classified into 2 types by their viscosities, which are viscous types and liquid types. Viscous enteral nutrition types are for patients who can swallow food, but have a problem with aspiration, while liquid types, usually be fed through a tube, are for patients who completely lose the ability to swallow.

Thermal sterilization is one kind of the food processing techniques in producing commercial liquid enteral nutrition formula to extend its shelf-life. Microwave heating has been proven to having faster heating rate than traditional method by generating heat within the products. Considering household and in-hospital usages, microwave heating is generally accomplished by microwave ovens. However, heating food by microwave ovens is still cumbersome because the composition, the geometry of food products, and the position of products in microwave ovens result in uneven temperature distribution within products. To study heating behavior, either experiment or numerical simulation has been widely used. Concerning studying resource, numerical simulation can reduce time and labor in studying microwave heating. By far, no studies on microwave sterilization of enteral nutrition to ensure safety while maintain its nutritional quality have been carried out

The objectives of this thesis were to:

- Obtain enteral nutrition formulas which satisfy the need of patients without specific conditions and have good organoleptic qualities.
- Determine appropriate conditions for microwave heating of liquid enteral nutrition products to maximize their safety and quality.
- Develop numerical models for commercial sterilization of liquid enteral nutrition products using a batch microwave oven.

Chapter 2 A comprehensive review

2.1 Enteral nutrition

Enteral nutrition is the nutrition supports, which is introduced to patients either by tube or oral, containing specific combination of protein, carbohydrates, fat, mineral, and vitamin. There are numerous formulas for patients with different diseases (Rufián-Henares, Guerra-Hernandez, & García-Villanova, 2006).

This product can be categorized by various criteria, e.g. composition and application. There are 3 categories of enteral nutrition formula by composition, which are detailed as following:

1) Standard formula, which mainly contains carbohydrates, protein, fat source and water to formulate the exact caloric density.
2) Fiber supplemented formula, which is mostly the standard formula with fiber addition.
3) Specialize formula for diverse conditions, e.g. formula for renal disease patients, formula for hepatic disease patients (Malone, 2005).

Moreover, it can also be classified by application, which includes the following:

1) Tube-feeding formula, which is usually thin liquid, normally be instructed by tube such as a nasogastric tube. This kind of formula is for patients who totally lose swallowing ability.
2) Spoon-feeding formula which is more viscous than the other formula. It is for patients who only have problems with aspiration, but they are still capable of swallowing.

The main consideration for the classification of the formula is viscosity. Gallegos, Brito-de la Fuente, Clavé, Costa, and Assegehegn (2017) stated that the viscosity of spoon-feeding formula should be higher than 1,750 cP at 50 Hz and 25 °C. Flow curves of some thickened fluid are shown in Figure 2.1.
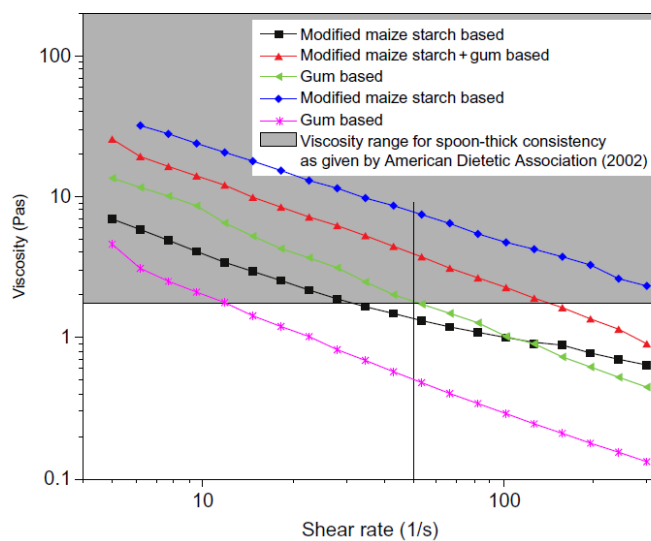
Figure 2.1 Flow curves of thickened fluid with different thickening powders

(Gallegos et al., 2017)

2.2 Microwave theory

Microwave is an electromagnetic wave whose frequency ranges from 300 MHz to 3,000 MHz (Hitchcock, 2004). In food application, only 915 MHz and 2,450 MHz microwave are allowed as per US Federal Communications Commission for microwave heating applications' guidelines. The electromagnetic spectrum and allocated microwave frequency is illustrated in Figure 2.2.
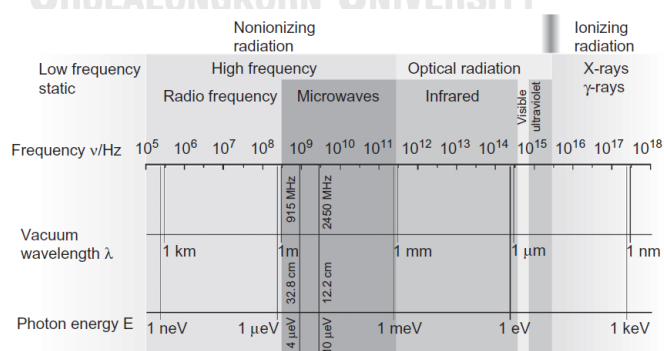
Figure 2.2 Electromagnetic spectrum and two allocated microwave frequencies are indicated

(Regier, Knoerzer, & Schubert, 2017)

2.2.1 Interaction between microwave and materials

When microwave is applied to materials, it can be reflected, refracted and absorbed inside the food load, and transmitted (Fellows, 2009) as shown in Figure 2.3.
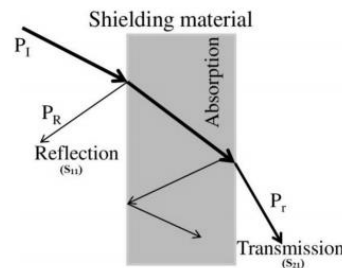
Figure 2.3 The interaction of incident microwave on a food material

(Mishra, Nath, & Mishra, 2018)

Heat generation due to microwave is from the absorbed radiation. The mechanisms for heat generation include ionic polarization and dipole rotation (Fellows, 2009). Ionic polarization or ionic conduction can be found in ionic substances such as NaCl. The dissolved ions move forward and backward repeatedly in the electromagnetic field. Dipole rotation or dipolar polarization occurs in dipole molecules, which are primarily free water presented in food materials. Dipoles rotate in the electromagnetic field. These two mechanisms induce collision between particles; thus, heat is produced. Figure 2.4 depicts the stated mechanisms.
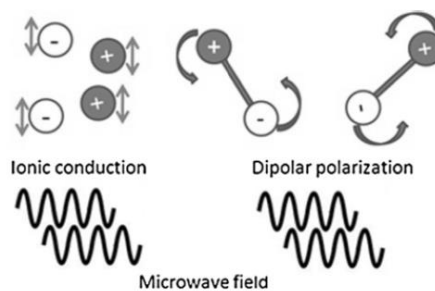
Figure 2.4 Two mechanisms arisen during microwave heating

(Gude, Patil, Martinez-Guerra, Deng, & Khandan, 2013)

2.2.2 Dielectric properties and penetration depth (d_p)

Dielectric properties explain the ability of a material to change microwave energy to heat (Chandrasekaran, Ramanathan, & Basak, 2013). There are 2 parts, which are dielectric constant and dielectric loss factor. The dielectric constant (ε') describes the capability of a material to store electric energy. The dielectric loss factor (ε'') depicts how well a material converts absorbed electric energy to heat (Chandrasekaran et al., 2013).

Penetration depth (d_p) indicates the depth in the sample where microwave loses 63% of its energy comparing with microwave at the surface (Fellows, 2009) as shown in Equation 2.1.

$$d_{p=} \frac{\lambda_o \sqrt{\varepsilon'}}{2\pi\varepsilon''} \tag{2.1}$$

Where λ_0 is the constant equals to 33 cm at 915 MHz microwave and 12 cm at 2,450 MHz microwave.

2.2.3 Factors affecting heat transfer during microwave heating

2.2.3.1 Microwave distribution facilitators

Temperature distribution in the material in the microwave field is impacted by microwave distribution. As a result, designers or researchers try to make microwave spreading as uniform as possible. In domestic microwave ovens, a stirrer mode and a rotatable plate are installed within the equipment (Figure 2.5).
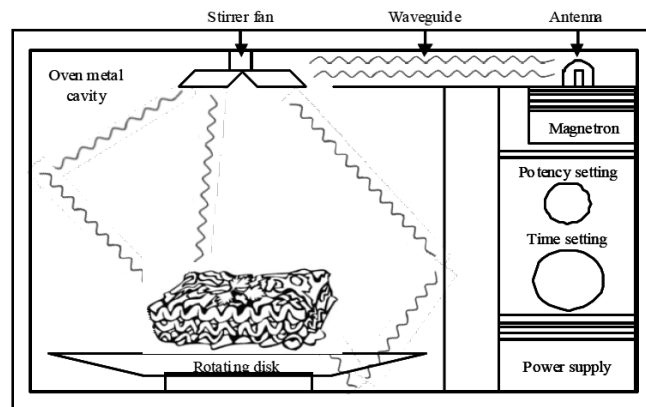
Figure 2.5 Simplified schematic drawing of a microwave oven showing a stirrer fan and a rotating plate

(Malheiro, Casal, Ramalhosa, & Pereira, 2011)

There is also an attempt to improve heating uniformity in a continuous microwave system. Koskiniemi, Truong, Simunovic, and McFeeters (2011) investigated the effect of package rotation on the heating uniformity for pasteurization of various packaged acidified vegetable and found that it significantly improved the homogeneity.

2.2.3.2 Material's dielectric properties

Dielectric properties play a major role for microwave heating. There are several factors influencing these properties, for example, microwave frequency, product's temperature, product's composition.

2.2.3.2.1 Microwave frequency

Different frequencies affect heat generation in materials differently due to various interactions in microwave absorption and heat generation and their dielectric properties (Meda, Orsat, & Raghavan, 2017). Figure 2.6 elaborates the influence of different mechanisms on the loss factors at different electromagnetic wave frequencies. It also confirms that main heat generation mechanisms during microwave heating of food materials at allocated frequency are ionic conduction and free water relaxation.
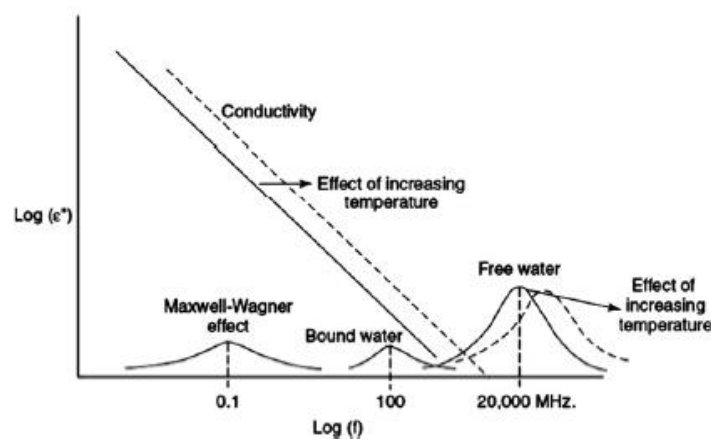
Figure 2.6 Different mechanisms to dielectric loss factor at various frequencies
(Sosa-Morales, Valerio-Junco, López-Malo, & García, 2010)

Considering the frequency effect on dielectric properties, ε' value seems to be decreasing with increasing frequency. There are several studies with various kinds of food to affirm this point. This finding is in accordance with the works from Hu and Mallikarjunan (2005), Wang, Tang, Rasco, Kong, and Wang (2008), and Zheng, Huang, Nelson, Bartley, and Gates (1998) on dielectric constant of various kinds of seafood at different frequencies. Dev, Raghavan, and Gariepy (2008) and Zhang, Liu, Nindo, and Tang (2013) reported the impact of frequency on ε' of egg and its component. The works by Franco, Tadini, and Wilhelms Gut (2017) and Peng, Tang, Jiao, Bohnet, and Barrett (2013) also pointed out this finding for fruit and vegetable products and their juice.

However, the effect of frequency on dielectric loss factor is more complicated since there are two main terms consisting in this variable (Muñoz, Gou, Picouet, Barlabé, & Felipe, 2018) as shown in Equation 2.2.

$$\varepsilon'' = \varepsilon_d'' + \varepsilon_\sigma''$$ (2.2)

Where, ε_d'' is dipole loss resulted by dipole molecules.

ε_σ'' is ionic loss affected from ionic particles.

Dipole loss has a positive correlation with frequency among allocated spectrum while ionic loss negatively correlates with it (Zhang et al., 2015) as shown in Equation 2.3.

$$\varepsilon_\sigma'' = \frac{\sigma}{2\pi f \varepsilon_0}$$ (2.3)

Where, σ is ionic conductivity (S/m), f is frequency (Hz), and ε_0 is electrical energy stored in vacuum (8.8542×10^{-12} F/m).

Accordingly, there are either positive or negative trend of ε'' with frequency depending on food composition. Hu and Mallikarjunan (2005), Wang et al. (2008), and Zheng et al. (1998) found that dielectric loss factor of seafood was lower at higher frequency. Zhang et al. (2013) and Peng et al. (2013) also pointed out this trend for egg and tomatoes, respectively. On the contrary, Okiror and Jones (2012) and Zhang et al. (2015) reported that increasing frequency led to higher dielectric loss factor of gellan gel. The work from Franco et al. (2017) on citrus juice stated the same finding at low temperature.

2.2.3.2.2 Product's temperature

Temperature is also an essential factor that has an impact on dielectric properties since it impacts the particles' movements. Therefore, the ability to absorb microwave energy and convert it to heat is remarkably changed.

Dielectric constant is generally lower at higher temperature because intermolecular vibration among water molecules leads to reduced orderliness of water (Al-Holy, Wang, Tang, & Rasco, 2005). Okiror and Jones (2012) and Zhang et al. (2015) indicated that ε′ of gellan gel was lower at an elevated temperature. The works on dielectric constant on egg from Dev et al. (2008) and Zhang et al. (2013) were also in agreement with this. Franco et al. (2017), Muñoz et al. (2018), and Peng et al. (2013) found the same trend for ε′ of citrus juice, milk, and tomatoes, respectively.

Unlike dielectric constant, the effect of temperature on dielectric loss factor is diverted. Increasing temperature results in lower dipole loss but higher ionic loss (Al-Holy et al., 2005). Therefore, temperature effect on ε″ primarily depends on the kind of food. Dev et al. (2008) showed that the dielectric loss factor of eggs was lower with increasing temperature. While the work from Auksornsri, Tang, Tang, Lin, and Songsermpong (2018) and Muñoz et al. (2018) pointed out that higher temperature yielded an increase in ε″ for rice and milk, respectively.

Moreover, microwave frequency plays a dominant role on dielectric loss factor at different temperature too. Franco et al. (2017) indicated that dielectric loss factor of citrus juice increased with elevated temperature at low frequency; whereas, at high frequency, the trend was inverted. This phenomena was also reported for ε′ of gellan gel by Zhang et al. (2015). The result of the effect of temperature and frequency on dielectric properties of Pera orange juice is shown in Figure 2.7.
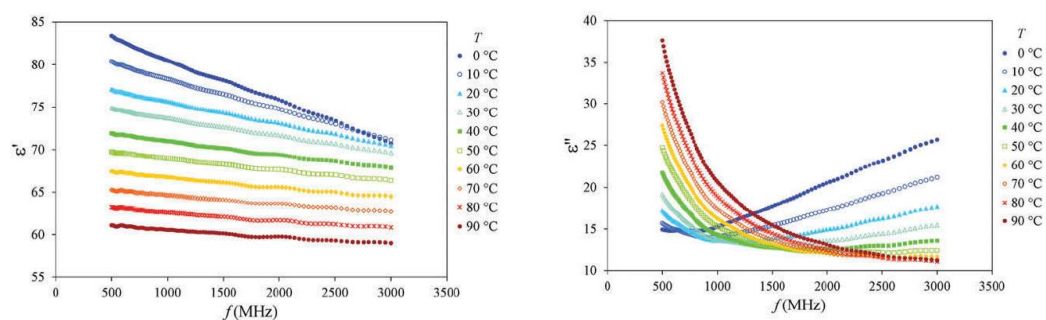
Figure 2.7 Dielectric properties of Pera orange juice at various frequencies and temperature levels

(Franco et al., 2017)

2.2.3.2.3 Product's composition

Because different food compositions have different interactions under the electromagnetic wave, composition of a material is the main consideration of dielectric properties as well. Among various kinds of ingredients in food system, water and salt are major constituents affecting dielectric properties of food (Venkatesh & Raghavan, 2004).

Moisture content is positively correlated with dielectric constant as described in Ahmed, Ramaswamy, and Raghavan (2007), Liao, Raghavan, Dai, and Yaylayan (2003), and Muñoz et al. (2018) for ε′ of Basmatic rice flour dispersion, glucose solutions, and milk, respectively. On the other hand, dielectric loss factor appears to be decreasing with rising moisture content. Negative relationship between moisture content and dielectric loss factor for glucose solutions, hydrocolloid powders, and gellan gel were investigated in the work by Liao et al. (2003), Prakash, Nelson, Mangino, and Hansen (1992), and Zhang et al. (2015), respectively. While the study from Ahmed et al. (2007) concluded that the impact of moisture content on dielectric loss factor of Basmati rice slurry was not clear. Figure 2.8 shows the impact of sucrose concentration on dielectric properties of gellan gel.
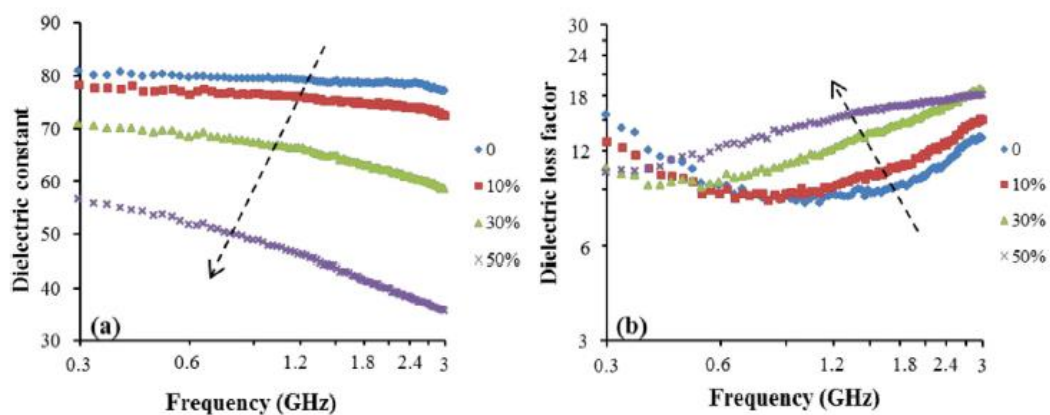
Figure 2.8 Dielectric properties of gellan gel at various sucrose concentraion at 22 °C
(Zhang et al., 2015)

The other ingredients influencing dielectric properties is salt. There are several works that investigated the effect of salt content on dielectric properties of various food. Al-Holy et al. (2005) and Zheng et al. (1998) pointed out that marination can significantly decrease ε' for oyster and shrimp, respectively. The reverse effect of salt concentration on dielectric constant was also studied in Sakai, Mao, Koshima, and Watanabe (2005) and Zhang et al. (2015) for NaCl solutions and gellan gels, respectively. However, Llave, Mori, Kambayashi, Fukuoka, and Sakai (2016) did not find any clear relationship between salt concentration and dielectric constant for tylose-water pastes.

On the contrary, dielectric loss factor increases with increasing salt content. Al-Holy et al. (2005), Sakai et al. (2005), Wang et al. (2009), Zhang et al. (2015), and Zheng et al. (1998) showed that ε'' value was higher with higher salt concentration in oyster, NaCl solutions, salmon, gellan gel, and shrimp, respectively. Figure 2.9 shows the effect of marination on dielectric properties of shrimp.
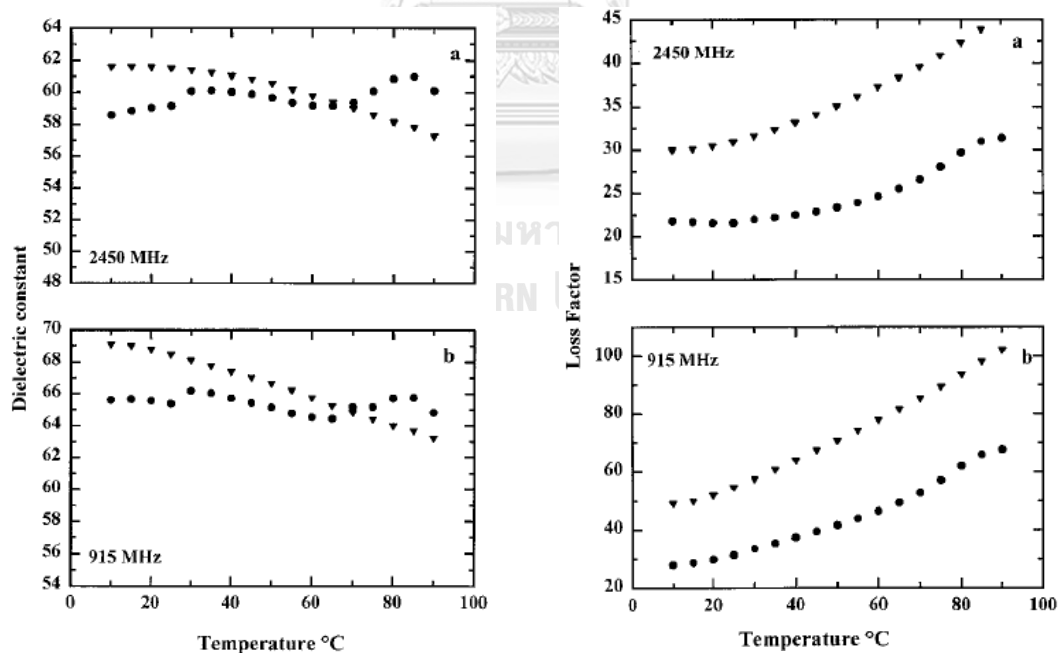
Figure 2.9 Dielectric properties of (▼) non-marinated shrimp and (●) marinated shrimp at 915 MHz and 2,450 MHz at different temperature

(Zheng et al., 1998)

Other ingredients, e.g. carbohydrates and fat have relatively low impact on heat generation from microwave except for very low moisture content samples; for instance, syrup and bakery (Venkatesh & Raghavan, 2004).

2.2.3.3 Material's thermal properties

During microwave heating, heat transfer also takes place and impacts temperature distribution. Two main variables involve with this are thermal conductivity (k), which describes the ability of a material to allow the heat transfer through, and specific heat (C_p), which explains how much energy needed to increase the temperature (Holdsworth & Simpson, 2007). These parameters become the essential factors with low dielectric properties food (Venkatesh & Raghavan, 2004).

2.2.3.4 Size and shape

Size of the product is another factor affecting temperature distribution within a material. Processing a material with low penetration depth compared to the size of the material leads to surface overheating. On the other hand, if the penetration is much larger than the material's dimension, center overheating could occur (Remmen, Ponne, Nijhuis, Bartels, & Kerkhof, 1996).

Different shape impacts microwave heating uniformity as well. The main cautions of shape effect for microwave heating are edge and corner overheating and center overheating. Food with sharp edges and/or corners could face overheating at these areas because microwave enters the material at these regions more than 1 direction. Figure 2.10 shows the simulated edge overheating of a rectangular food block.
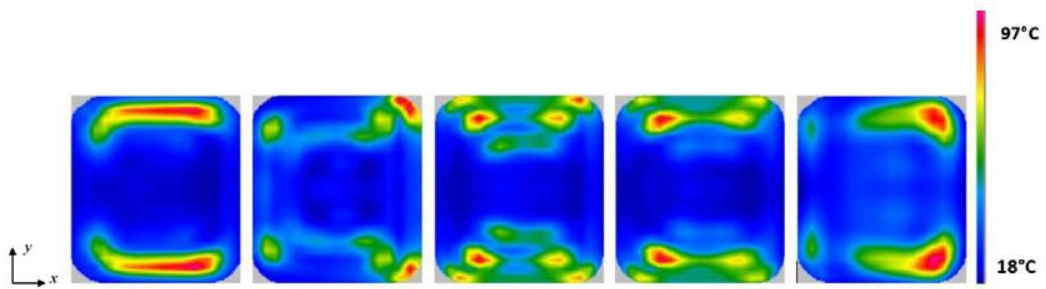
Figure 2.10 Simulated temperature distribution of a rectangular food block (50 mm ×

60 mm × 60 mm) with rounded corners. From left to right is the heating pattern from a

lower plane to an upper plane

(Wäppling Raaholt & Isaksson, 2017).

In addition, center overheating can occur in rounded shape objects due to refraction and reflection. As a result, power distribution at the center is higher (Figure 2.11) (Wäppling Raaholt & Isaksson, 2017).
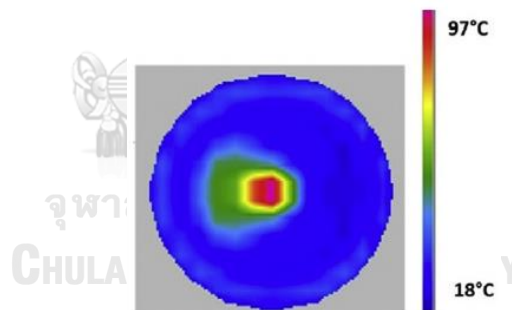
Figure 2.11 Simulated center overheating of a 20 mm-radius cylindrically shaped meat loaf at the middle plane

(Wäppling Raaholt & Isaksson, 2017).

2.3 Numerical simulation in microwave heating

Numerical simulation can be one method that potentially enhances the efficiency in studying microwave heating. Since there are several factors impacting heating pattern, simulation techniques allow researchers to investigate factor's effects on microwave heating with less experiments. It solves the problem by a numerical method, e.g. Finite Element Method (FEM), Finite-Difference-Time-Domain (FDTD), Method of Moment (MOM) (Birla & Pitchai, 2017). However, this thesis focused on using COMSOL® with FEM. The procedure to be discussed further is, thus, only for FEM.

2.3.1 Steps in numerical simulation

There are 5 main steps in numerical simulation: 1) geometry drawing, 2) defining conditions and initial value, 3) meshing, 4) solving, and 5) post-processing.

The system needed to be solved is drew by either COMSOL® or other drawing programs such as AutoCAD. It is not necessary to be a detailed scheme because it could lead to superfluous solving time without any importance. For instance, Hamoud-Agha, Curet, Simonin, and Boillereaux (2013) picked only ¼ of the system to be solved since the symmetry planar was found in their system.

The boundary condition and initial value of each part in the solving system needs to be defined. Either thermal insulation or heat flux boundary can be assigned at the heated surface and the walls of microwave oven are set as perfect electric conductor. The initial condition can be assigned to match what is observed.

For meshing, the geometry is divided into smaller pieces or meshed. Mesh size has a significant effect on solving time and results (Ehlers & Metaxas, 2005). Especially, in problems involving microwave with a narrow wavelength, the maximum mesh size is inversely proportional to the dielectric constant of each material (Pitchai et al., 2014). Other works found the appropriate mesh size by increasing the value until the result was independent from mesh size; for example, the study by Geedipalli, Rakesh, and Datta (2007).

The last two steps are solving and post-processing. Generally, solving microwave heating problems gives electric field distribution in the chamber and temperature distribution in the products. Additionally, other parameters can be calculated; for example, absorbed microwave power, sterilization value, and microbial inactivation. Figure 2.12 illustrates some steps of numerical simulation strategies.

(a)   (b)   (c)
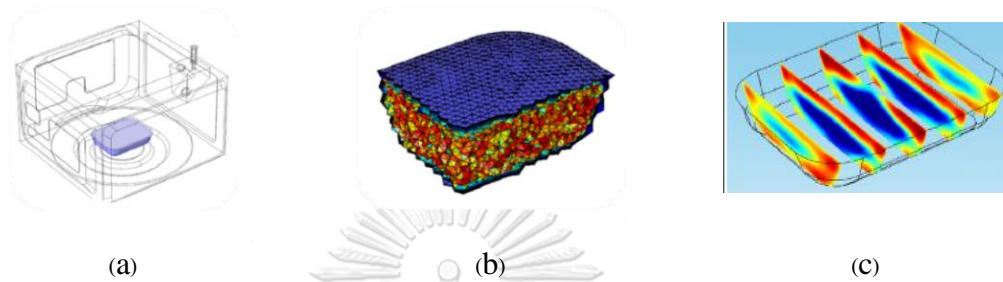
Figure 2.12 Steps in microwave heating simulation (a) geometry drawing, (b) meshing, and (c) post-processing showing temperature distribution inside the product (Chen et al., 2016)

2.3.2 Literature review on microwave pasteurization and sterilization using numerical simulation technique

Burfoot, Railton, Foster, and Reavell (1996) used simulation techniques to study microwave pasteurization of prepared meal. They found that numerical model could predict temperature distribution well. However, there were large differences between experimental data and predicted temperature due to meshing scheme. Boillereaux, Curet, Hamoud-Agha, and Simonin (2013) studied the effect of microwave power and conveyor belt's velocity in pasteurization of minced beef by conveyorized microwave oven. It was pointed out that heterogeneity was the main problem in microwave heating. Hamoud-Agha et al. (2013) and Hamoud-Agha, Curet, Simonin, and Boillereaux (2014) compared the efficiency of *E*.coli K12 inactivation by microwave and water bath heating. They found that numerical simulation techniques could calculate temperature profile for each heating condition well but it could not predict the inactivation of *E*.coli K12 because of the input model parameters for microbial inactivation.

Furthermore, the utilization of numerical model for improving microwave heating system is also investigated. Chen, Tang, and Liu (2008) reported the effect of microwave power and distance between each package on a continuous microwave heating system equipped with 2 microwave generators studied by numerical simulation techniques. It was pointed out that using the same power for each microwave generator and more distance between each package could increase temperature homogeneity. Additionally, the experimental data and predicted value from numerical simulation were in a good agreement. Luan, Tang, Pedrow, Liu, and Tang (2013) studied the effect of using a mobile metallic probe in continuous microwave assisted sterilization (MATS) system. It was reported that placing a probe perpendicular with electric field can decrease singularity and impact on temperature distribution of measuring materials. In addition, Resurreccion et al. (2015) investigated the effect of microwave frequency and types of circulating medium on products heated by MATS system. They reported that microwave frequency did not affect the temperature distribution, but it impacted the temperature profile. In addition, it was found out that using tap water with higher ionic substances as circulating medium notably reduced product's temperature compared with using deionized water.

2.4 Iconographic Correlation

Iconographic Correlation (IC) is one kind of data analysis using CORICO program. This method can be used to analyze the relationship between variables, develop models containing logical interactions between response and factors, and optimize the factors to get the target condition. CORICO determines the correlation between two tested variables if it does not confound with another variable and the value is greater than the set threshold. Then, it shows the significant links in the form of sphere (Figure 2.13).
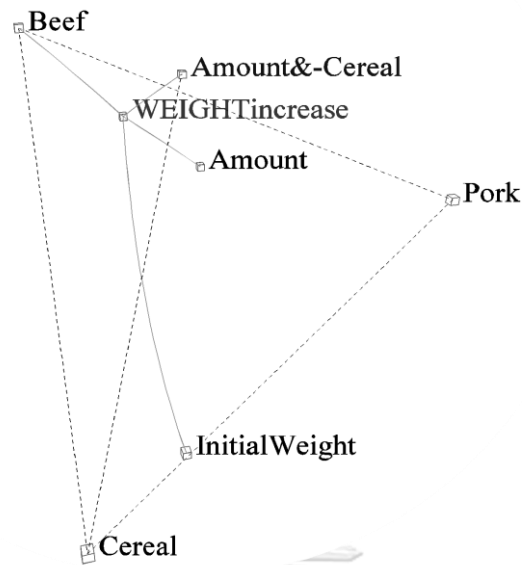
Figure 2.13 An example of iconography of correlation

(Lesty, 1999)

From Figure 2.13, there are 2 kinds of correlation between variables illustrating in 2 kinds of lines. The solid lines represent positive correlations while the dotted lines indicate negative correlations.

2.4.1 Models from Iconographic Correlation

IC proposes models that consist of logical interactions as exemplified in Equation 2.4.

Response = 11 + 2(A&-B) + 8.7(C-D) + 4.9(A]-E) + 2.9(A*C) + 1.9(C&D)   (2.4)

The symbols for CORICO models are displayed in Table 2.1 and Table 2.2.

Table 2.1 Table of symbols used on CORICO models

f(A,B)	Significance	The pattern of response (Y)
A*B	A or exclusive B	Y is strong when A is strong, and B is weak, or A is weak, and B is strong
A^B	A or B	Y is strong when A is strong, or B is strong
A^-B	A or not B	Y is strong when A is strong, or B is weak
A&B	A and B	Y is strong when A and B are strong
A&-B	A and not B	Y is strong when A is strong, and B is weak
A]B	A modulated by B	Y correlates with A when B is strong
A]-B	A modulated by not B	Y correlates with A when B is weak
A}B	A modulated by B mean	Y correlates with A when B is at average
A'B	Neither A nor B (gentle)	Y is strong when neither A nor B are extreme
A!B	Neither A nor B (strong)	Y is strong only A and B are at its average
A#B	A as B	Y is strong when A varies as B
A#-B	A as not B	Y is strong when A does not vary as B
A+B	A plus B	Y is strong when sum of A and B (centered – reduced) is strong
A-B	A minus B	Y is strong when difference of A and B (centered – reduced) is strong
A{B	A mean if B	Y is strong when A is at average and B is high
A{-B	A mean if not B	Y is strong when A is at average and B is low

Table 2.2 Effect of logical interaction with itself

f(A,B)	Significance	The pattern of response (Y)
A*A	A or exclusive A	The parabolic influence on Y
A]-A	A modulated by not A	Y correlates on A if A is weak
A!A	Not A (strong)	Y is high if A is strictly average
A}A	A if A mean	Y correlates on if A is average

Figure 2.14 shows some examples of response surfaces of logical interactions between A and B. Moreover, there are some plots showing interactions with itself shown in Figure 2.15.
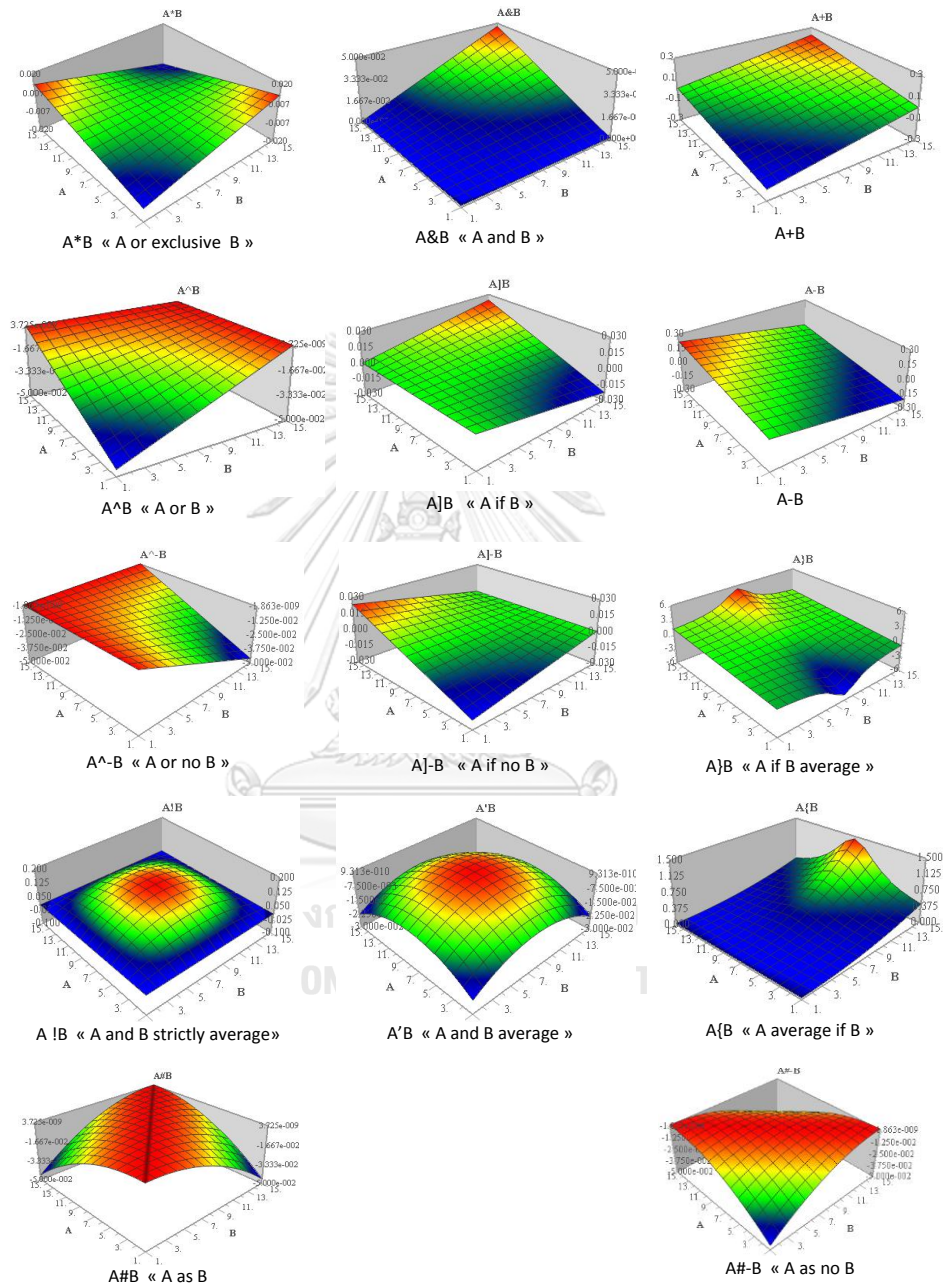
Figure 2.14 Some examples of response surfaces of logical interactions between A (the abscissa) and B (y-axis)

(Lesty, 1999)
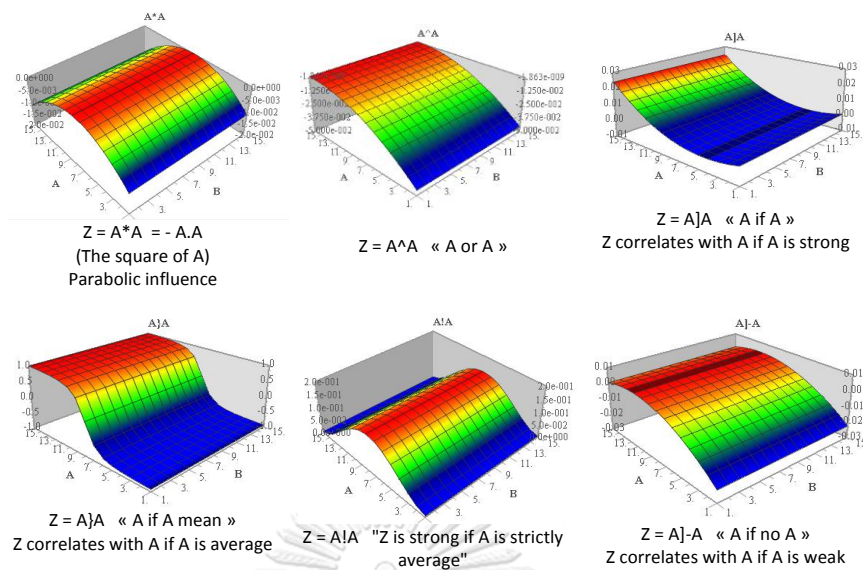
Figure 2.15 Some examples of response surfaces of logical interactions with itself

(Lesty, 1999)

2.4.2 Studies involving optimization using Iconographic Correlation

One advantage of optimization using the IC method over the classical response surface methodology (RSM) is that it can describe response in more alternative ways than the RSM does (Figures 2.15 and 2.16). A research work on optimization for fish cooking by microwave (Laguerre et al., 2013) showed the advantage of using the IC method for optimization. Another strength of IC lies in that it can optimize experimental parameters involving several factors with remarkably fewer number of experiments. Since the factors considering in food processing are normally numerous, IC could be a helpful tool. Laguerre, Ratovoarisoa, Vivant, Gadonna, and Jouquand (2017) studied the optimization of combined microwave/hot air drying of apples with 5 factors for physical and organoleptic properties using IC. They found that IC gave good accuracy for most responses. Jouquand et al. (2015) compared the trials necessary for microwave cooking of beef burgundy with 4 factors. They found that RSM with Doehlert matrix required 21 trials; whereas, IC needed only 12 observations.

Chapter 3 Materials and Methods

3.1 Ingredients

Maltodextrin, which has the dextrose equivalent (DE) 10-12 from corn starch, was purchased from Nutrition SC Co., Ltd. Soy protein isolate (SPI), which has 93 %(db) protein was obtained from Mighty international Co., Ltd. Whey protein isolate (WPI), which has 93 %(db) protein and Whey protein concentrate (WPC) containing 81 %(db) protein were from Vicchi Enterprise Co., Ltd. Hydrolyzed whey protein (without flavor), which has 85 %(db) protein was purchased from Myprotein®. Soy lecithin, malic acid, citric acid, and HFCS42 were obtained from Chemipan Cooperation Co., Ltd. Coconut cooking oil 100% (CCO) by P.O. CARE (Thailand) Co., Ltd. and King rice bran oil (RBO) by Thai Edible Oil Co., Ltd. were purchased from local supermarkets in Thailand.

3.2 Sample preparation

Samples were prepared using the recipe as per the formula specified for each experiment. After adding all ingredients, tube-feeding formula with caloric density either 1 kcal/mL or 2.5 kcal/mL were homogenized for 9 minutes by a portable mixer (VMI model V2004 Turbotest, Saint-Hilaire-de-Loulay, France) at 1500, and 3000 rpm, for 1 kcal/mL formula and 2.5 kcal/mL formula, respectively. The formulas with high caloric density (higher than 3.5 kcal/g) were mixed by a hand mixer (Moulinex®) at the lowest speed for 5 minutes.

3.3 Formulation for high caloric density enteral nutrition products

3.3.1 Experimental design

3.3.1.1 Factors

There were 9 factors to be optimized in this section, which were type of oil, lecithin concentration in % (w/w), caloric density [caldens] in kcal/g,

amount of solid in HFCS to acid ratio [FStoAcid], percentage of hydrolyzed whey protein to total protein [Hydrolyzed], percentage of calorie from fat to total calorie [Calfat], percentage of calorie from HFCS to total calorie [CalFS], complex whey protein concentration [WPconc] in % (w/w), and percentage of whey protein isolate to total complex whey protein [WPItoWP]. Table 3.1 shows the level of each factor used in the study.

Two kinds of design were established to compare the number of trials needed for optimization i.e. response surface methodology (RSM) with Doehlert matrix (DM), and IC using CORICO or CORICO design (CD).

Table 3.1 Definition, range and levels of 9 influencing factors used in the study

Variable	Definition	Range	Levels
Oil	Oil type (coconut oil or rice bran oil)	-	2 levels (defining CCO as 1, and RBO as 2)
Lecithin (% (w/w))	Lecithin concentration	0.5 to 1	5
Caldens (kcal/g)	Caloric density	3.5 to 4	5
FStoAcid	Ratio of solid in HFCS and acid (1:1 citric acid and malic acid)	10 to 30	5
Hydrolyzed (%)	Percentage of hydrolyzed whey protein to total protein	0 to 25	6
CalFat (%)	Percentage of calorie from fat to total calorie	50 to 60	7
CalFS (%)	Percentage of calorie from HFCS to total calorie	5 to 15	7
WPconc (% (w/w))	Complex whey protein concentration	1 to 8	7
WPItoWP (%)	Percentage of whey protein concentrate to total complex whey protein	0 to 100	7
LogVis	Log of viscosity in cP	(Response)	
Emul_Sep (%)	Percentage of emulsion separation	(Response)	

The calculation for the number of trials was conducted following Equation 3.1 for DM according to Ferreira et al. (2017). CD was set to fit economic occupation of corners and economic space filling. The number of trials required for DM was 524 trials while CD proposed only 17 experiments. Therefore, CD was selected as the means for experimental design.

$$N = 2^k + k + Co \qquad (3.1)$$

Where, N is the number of experiments.

k is the number of factors.

Co is the number of central points developed.

Indeed, CORICO designs are more efficient than classical ones from 4 studied factors. For example, Jouquand et al. (2015) found out that using a 4-factors CD for the optimization of microwave cooking of beef burgundy needed only 12 experiments while a Doehlert design required 21 experiments.

3.3.1.2 Responses measurement

Two responses, which were percentage of emulsion separation and viscosity, were needed to be optimized. After the preparation, the percentage of emulsion separation was determined following the method described by Antes et al. (2017) with some modifications by using an ultrasonic bath (Bandelin Sonorex, Berlin, Germany) that was operated at 35 kHz. The sample was filled in a 15-mL plastic tube before it was tempered at 60 °C for 1 hour and sonicated at 35 kHz and 60 °C for 2 hours. The height of the separated oil was recorded, and emulsion separation was calculated following Equation 3.2.

$$\text{Emul Sep} = \frac{H_o}{H_t} \times 100 \qquad (3.2)$$

Where, H_o and H_t is the height of oil separated from the emulsion and the height of the sample, respectively.

The sample's viscosity was measured at 50 Hz and 25 °C using a rheometer (Anton Paar, Austria, model MCR-92) with a 50-millimeter parallel plate geometry. The linear viscoelastic range (LVR) was determined by an amplitude sweep test. The sample's viscosity was determined using the deformation in the LVR from 5 Hz to 100 Hz.

3.3.2 Data analysis

Correlation analysis, model regression, optimization, and response surfaces drawing were carried out by CORICO ($p < 0.01$). Model regression was set to find the model with the least standard error.

The model from CORICO contains logical interactions such as that shown in Equation 3.3.

$$Y = a_0 + a_1 X_1 \& X_2 + a_2 X_1 \wedge X_2 + a_3 X_1 \& -X_2 + \dots \tag{3.3}$$

Where X_1, X_2 are factors and Y is a response.

With $X_1 \& X_2$ means that Y is high when the value of both X_1 and X_2 are high.

$X_1 \wedge X_2$ means that Y is high when the value either or both X_1 and X_2 are high.

$X_1 \& -X_2$ means that Y is high when the value of X_1 is high and X_2 is low.

3.3.3 Determination of optimal conditions and model validation

CORICO facilitates the optimization to find the condition that gives responses closest to the targeted value or range. In this research, CORICO was employed to optimize emulsion separation and viscosity of the enteral nutrition. For percentage of emulsion separation, it was not noticeable when the value was lower than 1%, consequently the optimal value was set from 0 to 1. According to Gallegos et al. (2017), the viscosity of oral-feeding enteral nutrition formula should be around 1,750 cP (or 3.24 log value) at 50 Hz and 25 °C, thus the optimal value range was set to 3.2 to 3.3 log value. Validation of the optimal formulas yielding the desirable responses was carried out. The predicted responses were compared to those obtained by the measurements detailed in section 3.3.1.2.

3.4 Optimization of microwave heating for tube-feeding enteral nutrition products

3.4.1 Tube-feeding enteral nutrition products

The formula used in this section was that having 1 kcal/mL caloric density with the ratio of calorie from carbohydrate: fat: protein equaled 50: 30: 20. Corn maltodextrin DE 10-12 and rice bran oil was used as the carbohydrate source and the fat source, respectively. Soy protein isolate, whey protein isolate, and whey protein concentrate at the 12: 3: 1 ratio were used as the protein source. Soy lecithin (0.75 %w/v) was added as an emulsifier. The preparation was proceeded according to section 3.2.

3.4.2 Microwave heating

150 mL of the enteral nutrition sample was filled in a clear retortable pouch (110 mm × 160 mm), then sealed with a hand-pressure hot heat-sealing machine. The pouch was placed in an in-house Teflon block. The block was fastened to tightly so that it could be able to withstand an increase in pressure that was generated inside the food load during heating. The system sample was then heated in a laboratory 2.45 GHz microwave oven (Minilabotron 2000, Neyron Cedex, France). Specific power (W/mL) and heating time (s) were assigned according to the Doehlert matrix with 3 replicates at the center points by inputting the specific power which was varied at 3 specific power values (W/mL) levels (3 W/mL, 5 W/mL, and 7 W/mL), and the microwave heating time which was varied at 5 different heating times levels (35 s, 41 s, 48 s, 54 s, and 60 s) as shown in Table 4.5. Doehlert design gave 9 experiments that included 3 replicates at the center point. The heated sample was cooled down by tap water at ambient temperature, then was kept refrigerated before further analyses.

3.4.3 Responses measurement

The average of surface temperature, the relative tryptophan loss, and the FAST index were determined for each sample.

After microwave heating, the pressure in the sample was slowly reduced within 2 minutes. The surface temperature of the sample was measured by using an FLIR® system AB (Danderyd, Sweden), which is a handheld thermal camera. The temperature of a total number varied from 16,227 to 22,160 points on the surface of the sample (110 mm × 160 mm area) were recorded.

Relative tryptophan loss and FAST index were determined by fluorometric spectroscopy as described in Birlouez-Aragon, Sabat, and Gouti (2002) with some modifications. First, dilute 500 mg sample with 4.5 mL of 0.1 M sodium acetate buffer, pH 4.6, then shake in a tube rotating shaker. Next, centrifuge at 4000 rpm for 10 minutes, filter the supernatant through 0.45 μ pore nylon filter. For relative tryptophan loss, the filtered sample either before or after heating was diluted 10 times

before measuring to get the reliable response. The relative tryptophan loss was calculated by Equation 3.4.

$$\text{Relative tryptophan loss (\%)} = \frac{(F_{Trp, \text{ before heating}} - F_{Trp, \text{after heating}})}{F_{Trp, \text{ before heating}}} \times 100 \quad (3.4)$$

Where, F_{Trp} was tryptophan fluorescene which was the counts of emitted photon per second measuring at 290/340 nm of 10-time diluted filtered samples.

The FAST index of samples was calculated by Equation 3.5.

$$\text{FAST index} = \frac{F_{AMP}}{F_{Trp}} \times 100 \quad (3.5)$$

Where, F_{AMP} was the advanced mailard products fluorescene which was the counts of emitted photon per second measuring at 330/420 nm for undiluted filtered samples.

3.4.4 Statistical analysis

3.4.4.1 Response surface methodology (RSM)

Input factors (specific power and time) were coded by using Equation 3.6.

$$x = \frac{X_i - X_0}{\Delta X} \quad (3.6)$$

Where X_i was the actual value, X_0 was the value at the center of the domain, and ΔX was the increment for 1 unit of x. For heating time, -1, 0, and 1 were coded for 35 s, 47.5 s, and 60 s, respectively. For specific power, 2.67 W/mL, 5 W/mL, and 7.33 W/mL were coded to -1, 0, and 1, respectively.

The quadratic model between coded time and coded specific power was described as Equation 3.7.

$$Y = a_0 + a_1 X_1 + a_2 X_2 + a_{12} X_1 X_2 + a_{11} X_1^2 + a_{22} X_2^2 \quad (3.7)$$

Where Y was the response, X_1, and X_2 was coded time and coded specific power, respectively. a_0, a_1, a_2, a_{12}, a_{11}, and a_{22} were coefficients.

Model regression and optimization were analyzed by regression module and solver module in Microsoft Excel 2016. Then, the response surface plot was developed by MATLAB R2018a.

3.4.4.2 Iconographic correlation (IC)

According to the data obtained from Doehlert design for microwave heating in section 3.4.2, correlation analysis, model regression, optimization, and response surface plots were analyzed and developed by CORICO ($p < 0.01$). Model regression was set to find the model with the least standard error.

3.4.4.3 Optimization of microwave heating

Optimal conditions were obtained from both methods; the RSM and the IC, with an aim to maximize average surface temperature and minimize relative tryptophan loss and FAST index. The conditions were validated through an experiment.

3.5 Numerical simulation of commercial sterilization of liquid enteral nutrition products using batch microwave oven

3.5.1 Liquid enteral nutrition samples

The samples with 3 different caloric density, which were 1 kcal/mL, 2.5 kcal/mL, and 3.78 kcal/g, were prepared using the recipe shown in Table 3.2. Then, it was prepared as per section 3.2.

Table 3.2 Liquid enteral nutrition sample's composition

Formula	1 kcal/mL	2.5 kcal/mL	3.78 kcal/g
Maltodextrin (g)	133.58	333.94	66.72
Soy protein isolate (g)	42.33	105.83	118.31
Whey protein isolate (g)	10.68	26.70	9.47
Whey protein concentrate (g)	3.43	8.58	53.03
Hydrolyzed whey protein (g)	-	-	42.16
Rice bran oil	32.79	81.99	236.10
HFCS42 (g)	-	-	201.92
Lecithin (g)	7.50	7.50	5.6
Malic acid (g)	-	-	0.30
Citric acid (g)	-	-	0.30
Water (g)	813.31*	542.68*	266.10
Total weight (g)	1044*	1107*	1000

*By calculation

3.5.2 Properties determination

3.5.2.1 Proximate composition

The measurement as following except for crude fiber and ash was carried out in 4 replications.

3.5.2.1.1 Moisture content

Moisture content was determined by the hot air oven method (AOAC, 2000).

3.5.2.1.2 Protein content

Protein content was measured by a modified Dumas method using Leco® FP528. 50 mg of dried sample was analysed and all combusted nitrogen was assumed to be initiated from protein. The conversion factor 6.25 was used to calculate protein content in the sample which comprised of several protein sources (AOAC, 2000).

3.5.2.1.3 Fat content

Fat was obtained by batch extraction using hexane. Firstly, 0.2 mg of dried sample was mixed with 1 mL of hexane, then centrifuged at 4,000 rpm for 15 minutes. The supernatant was collected. The extraction was repeated 2 times. The supernatant from each extraction was combined before it was evaporated under N_2 gas flush.

3.5.2.1.4 Carbohydrates

Carbohydrate was calculated by difference (AOAC, 2000).

3.5.2.2 Density

Density of the samples was carried out following the method of Rahman, Perera, Chen, Driscoll, and Potluri (1996) with using a volumetric cylinder instead of a pycnometer. A 25-mL volumetric cylinder was used to measure the volume of the known weighed sample at ambient temperature (about 25 °C). The measurement was done in triplicate for powder ingredients and 4 replicates for the final products.

3.5.2.3 Thermal properties

Volumetric specific heat and thermal conductivity of each powdered ingredient were determined using CT meter (SA TELEPH, Meylan, France) at ambient temperature that ranged from 22 °C to 24 °C with triplicate. Then, specific heat was calculated following Equation 3.8. The formula's specific heat and thermal conductivity were calculated following Equation 3.9 and 3.10.

$$\text{Volumetric specific heat } \left(^{J}/_{m^3 \cdot K} \right) = \rho C_p \tag{3.8}$$

$$C_p = \sum_i C_{p,i} x_i \tag{3.9}$$

$$k = \sum_i k_i x_i \tag{3.10}$$

3.5.2.4 Rheological properties

The rheological properties of the samples were determined by a steady shear test at the probe rotation range from 5 to 500 rpm, which equals to 2.2 1/s or 2.2 Hz to 220 Hz. The test temperature was varied from 30 °C to 60 °C. The tests were conducted using HAAKE Viscotester VT 550 (Thermo Electron, Karlsruhe, Germany) with a coaxial cylinder consisted with a stainless steel 18/8 rotor cup with top and bottom surfaces recession (MV3) sensor system connected with Thermo Fischer Scientific heating circulator using water as the media for temperature control. The measurement was carried out in duplicate. Only the downward flow curve was selected for model regression to assess the rheological behavior of the sample. Bingham model (Equation 3.11) was used to describe flow behavior of the samples.

$$\tau = \tau_0 + K\dot{\gamma} \tag{3.11}$$

For 1 kcal/mL formula, the rheological property was assumed to be temperature-independent and equal as being reported by Xiang, Simpson, Ngadi, and Simpson (2011) for skimmed milk (Table 4.12).

For 2.5 kcal/mL and 3.78 kcal/g formulas, the rheological property was presumed to be temperature dependent. The temperature dependency of the consistency

index (K) and yield stress (τ_0) could be explained by the Arrhenius equation as illustrated in Equation 3.12.

$$A = A_0 e^{\frac{-E_a}{RT}}$$ (3.12)

3.5.2.5 Dielectric properties

The dielectric properties of each formula were obtained from previous studies. The work by Muñoz et al. (2018) on dielectric properties of raw milk and concentrated non-fat milk were used to interpolate the properties for 1 kcal/mL and 2.5 kcal/mL formula, respectively. The dielectric properties of 3.78 kcal/g were assumed to be similar to those of low moisture to fat ratio processed cheese from Everard, Fagan, O'Donnell, O'Callaghan, and Lyng (2006). The dielectric properties as a function of temperature in °C was modeled by a quadratic model as shown in Equation 3.13 and 3.14.

$$\varepsilon' = a_1 + b_1 T + c_1 T^2$$ (3.13)

$$\varepsilon'' = a_2 + b_2 T + c_2 T^2$$ (3.14)

3.5.3 Microwave heating

150 mL or g of sample was filled in a clear retortable pouch, then sealed with a heat-sealing machine as explained in section 3.4.2. The pouch was placed in a Teflon block (Figure 3.1a) and the block was fastened. The sample was heated in a laboratory microwave oven at 2.45 GHz (Minilabotron 2000, Neyron Cedex, France) using the TE_{10} mode waveguide without a stirrer mode and a rotating plate. The setting is shown in Figure 3.1b. This system ensures its reliability on microwave power by controlling reflected power. As a result, real input power for a magnetron consists of the incident power and the reflected power.

(a)   (b)

Figure 3.1 (a) product with a Teflon block, and (b) microwave heating system

3.5.3.1 Continuous heating

The microwave power was set at 450 W for 105 s, 75 s, and 60 s for 1 kcal/mL, 2.5 kcal/mL, and 3.78 kcal/g formula, respectively. The input power was 640 W, 480 W, and 450 W for 1 kcal/mL, 2.5 kcal/mL, and 3.78 kcal/g formula, respectively.

3.5.3.2 Intermittent heating

The sample with 2.5 kcal/mL formula was also heated under intermittent heating at the same microwave power for 150 s. The magnetron was turn on and off every 25 s, which resulted in 3 cycles of 1:1 heating and tempering time. The input power during heating is shown in Figure 4.15a.

3.5.3.3 Sterilization value (F_0), Cooking value (C_{100}), and FAST index determination

The sample with 1 kcal/mL calories was processed at 850 W microwave power that yielded 1230 W input power for 45 s. F_0, C_{100}, and FAST index were numerically calculated describing in section 3.5.4.5

3.5.4 Simulation strategy

3.5.4.1 Problem description

The enteral nutrition samples (150 mL in a clear retortable pouch) with different caloric density was heated in assigned conditions as described in 3.5.3 in order to obtain sterilization by microwave heating. However, to save computational time, only the waveguide, the oven chamber, and the product were sketched as shown in Figure 3.2.

3.5.4.2 Model assumptions

1) Dielectric loss factor of the surrounding air and the Teflon block was assumed to be zero; thus, heat transfer equations were not solved within these domains.

2) The product was homogeneous and isotropic.

3) Product's thermal properties were constant.

4) Density of the product was constant (incompressible flow).

5) Rheological properties of 1 kcal/mL sample were independent of temperature while those of 2.5 kcal/mL and 3.78 kcal/g samples were a function of temperature following the Arrhenius relationship (Equation 3.12).

6) Dielectric properties were temperature-dependent (Equation 3.13 and 3.14).

7) The initial temperature of the product was homogeneous and was set at 28.4 °C.

8) The boundary of the product was no-slip boundary.

9) There was no headspace in the product.

10) The product's expansion was negligible.

3.5.4.3 Governing equation

3.5.4.3.1 Microwave propagation

A time-harmonic form of fields, assuming sinusoidal excitation and linear media gives a time harmonic equation for electric fields as illustrated in Equation 3.15.

$$\nabla \times (\mu^{-1} \nabla \times \mathbf{E}) - \omega^2 \varepsilon_c E = 0 \qquad (3.15)$$

The wave number in vacuum (k_0), relative permittivity (μ_r), complex permittivity (ε_c), and relative permittivity (ε_r) are defined as in Equation 3.16 to 3.19.

$$k_0 = \omega\sqrt{\varepsilon_0 \mu_0} \qquad (3.16)$$

$$\mu_r = \frac{\mu}{\mu_0} \qquad (3.17)$$

$$\varepsilon_c = \varepsilon - \frac{j\sigma}{\omega} \qquad (3.18)$$

$$\text{And } \varepsilon_r = \frac{\varepsilon}{\varepsilon_0} \qquad (3.19)$$

Replacing Equation 3.16 to 3.19 in Equation 3.15 gives the equation solving electric fields in the system as shown in Equation 3.20.

$$\nabla \times \mu_r^{-1}(\nabla \times \mathbf{E}) - k_0^2 \left(\varepsilon_r - \frac{j\sigma}{\omega\varepsilon_0}\right) \mathbf{E} = 0 \qquad (3.20)$$

3.5.4.3.2 Convective heat transfer

Localized heat balance equation (Equation 3.21) in spatial frame is derived to solve convective heat transfer on the assumption that radiation heat transfer, work from pressure changes, and work from viscous dissipation are negligible.

$$\rho C_p \frac{\partial T}{\partial t} + \rho C_p \mathbf{u} \cdot \nabla T + \nabla \mathbf{q} = Q \qquad (3.21)$$

Where $\mathbf{q} = -h_c \nabla T$ \hfill (3.22)

Equation 3.23 shows the heat source (Q) during microwave heating caused by electromagnetic losses of electric field within the material on the assumption that magnetic losses is negligible.

$$Q = \frac{1}{2} Re(\mathbf{J} \cdot \mathbf{E}^*) \qquad (3.23)$$

3.5.4.3.3 Fluid flow

The continuity and momentum equations applied for incompressible liquid give the equations for solving fluid flow under gravity as shown in Equation 3.24 to 3.25.

$$\rho \nabla \cdot \mathbf{u} = 0 \qquad (3.24)$$

$$\rho \frac{\partial \mathbf{u}}{\partial t} + \rho (\mathbf{u} \cdot \nabla)\mathbf{u} = \nabla[-p\mathbf{I} + \eta(\nabla \mathbf{u} + (\nabla \mathbf{u})^T)] + \mathbf{F} + \rho \mathbf{g} \qquad (3.25)$$

Viscosity of the products is derived from its shear stress (Equation 3.11) as shown in Equation 3.26.

$$\eta = \frac{\tau}{\dot{\gamma}} \qquad (3.26)$$

3.5.4.4 Boundary conditions

The wall of the waveguide and the oven made of steel coated with epoxy resin was assumed to be a perfect electric conductor. The condition assigned to this material is defined in Equation 3.27.

$$n \times \mathbf{E} = 0 \qquad (3.27)$$

The pouch and the Teflon block were defined as thermal insulators. The condition assigned to these materials is shown in Equation 3.28.

$$-n \cdot \mathbf{q} = 0 \qquad (3.28)$$

The pouch was also assumed to be no-slip boundary condition. The condition assigned to this boundary is described in Equation 3.29.

$$\mathbf{u} = 0 \qquad (3.29)$$

3.5.4.5 Modeling safety and quality of heated product

Sterilization value concerning C. *botulinum* spore of the heated product was calculated by Equation 3.30.

$$F_0 = \int_0^t 10^{\frac{T-121.1}{10}} dt \qquad (3.30)$$

Cooking value considering thiamine of the product can be calculated using Equation 3.31 by assigning the z-value as 31.4 °C (Datta & Deeth, 2007) .

$$C_{100} = \int_0^t 10^{\frac{T-100}{31.4}} dt \qquad (3.31)$$

FAST index (Fluorescene of Advanced mailard products and Soluble Tryptophan) was assumed to follow the zeroth-order kinetic model (Roux et al., 2016) illustrated in Equation 3.32.

$$\frac{d[A]}{dt} = r \qquad (3.32)$$

The work by Roux et al. (2016) for ohmic heating indicated that the rate constant (r) was the function with temperature (K) as described in Equation 3.33.

$$r = r_{T_{ref}} \times \exp\left(\frac{-E_a}{R} \times \left(\frac{1}{T} - \frac{1}{T_{ref}}\right)\right) \qquad (3.33)$$

Where, r_{Tref} is rate constant at 130 °C (0.24 U/s)

E_a is the activation energy (49 kJ/mol)

T_{ref} is reference temperature (130 °C)

3.5.4.6 Numerical models of commercial sterilization of liquid enteral nutrition products

The numerical models for processing 2.5 kcal/mL formula and 3.78 kcal/g sample at 800 W for 1 minutes. Sterilization value and cooking value were determined for each scenario.

3.5.4.7 Development of the numerical models

The model to be simulated (Figure 3.2a) was drawn by AutoCAD 2019 before it was imported into COMSOL® Multiphysics 5.3a used for solving numerical model. Then, Finite Element Method by coupling with CAD import module, RF module, Heat transfer module and CFD module was used to solve the domain. The mesh of the geometry was generated on the basis that it conversely related to dielectric constant of the component (Ehlers & Metaxas, 2005). The minimum mesh quality was higher than 0.02 to give the faster convergence (Pitchai et al., 2014). Figure 3.2b shows the model to be simulated in full meshing. Personal laptops (hp® with Intel® Core i7-5500U 2.40 GHz CPU with 8GB of Ram) were used to compute the result.

(a)   (b)
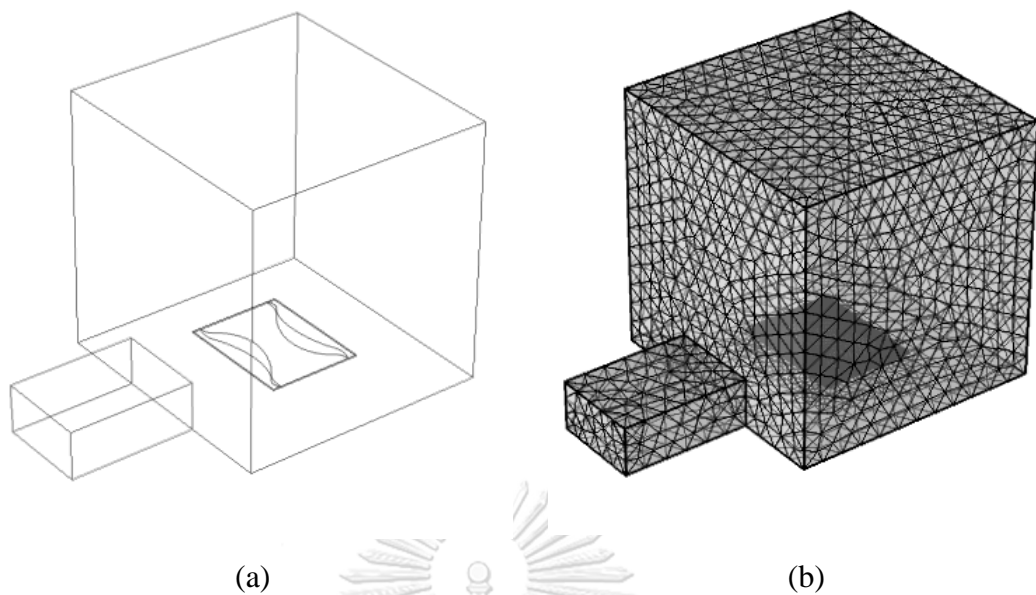
Figure 3.2 (a) microwave heating system geometry and (b) meshed geometry

3.5.5 Model validation

The surface temperature at different heating time was measured by using a handheld thermal camera by FLIR® system AB (Danderyd, Sweden). Moreover, The FAST index were determined by the fluorometric spectroscopy method described in Birlouez-Aragon et al. (2002) with some modifications as explained in section 3.4.3.

Chapter 4 Results and Discussions

4.1 Formulation for high caloric density enteral nutrition products

4.1.1 Experimental design and responses

Table 4.1 shows the design arrangement along with the responses from formula optimization using CORICO. The viscosity value ranged from 3.08 log value or 1,202 cP (trial 15) to 5.09 log value or 123,037 cP (trial 9). Caloric density (Caldens) and calorie from fat (CalFat) affected the viscosity. Higher caloric density tended to increase the viscosity value. On the other hand, more calorie from fat reduced it.

Percentage of emulsion separation was varied from "not detected" in trial 1 to 3, 5 to 7, 9 to 10, 13, and 15 to 16 to the highest separation obsreved in trial 12 with 3.86% separation. This response did not show a clear correlation with any influencing factors.

Table 4.1 Design arrangement from IC and responses

Trial	Oil*	Lecithin* (%(w/w))	Caldens* (kcal/g)	FStoAcid*	Hydrolyzed* (%)	CalFat* (%)	CalFS* (%)	WPconc* (%(w/w))	WPItoWP* (%)	LogVis*	Emul Sep* (%)
1	RBO	0.75	3.75	20	20	54	13	5.2	40	3.43 ± 0.07	ND
2	CCO	1	3.75	15	15	56	9	2.4	20	3.59 ± 0.33	ND
3	CCO	0.625	4	20	5	52	11	6.6	60	4.33 ± 0.77	ND
4	RBO	0.75	3.625	30	10	58	7	3.8	80	3.13 ± 0.16	1.72 ± 0.51
5	CCO	0.625	3.625	15	5	52	7	2.4	20	3.58 ± 0.12	ND
6	CCO	1	4	30	20	58	13	6.6	80	3.51 ± 0.03	ND
7	RBO	0.75	3.75	20	15	55	10	4.5	50	3.57 ± 0.03	ND
8	RBO	1	4	10	0	50	15	8	100	4.66 ± 0.01	3.57 ± 0.28
9	RBO	0.5	4	30	0	50	5	8	100	5.09 ± 0.84	ND
10	CCO	1	3.5	30	25	50	5	1	100	3.96 ± 0.05	ND
11	RBO	1	4	10	25	60	5	1	0	3.60 ± 0.03	2.08 ± 0.70
12	CCO	0.875	3.875	30	0	60	15	1	0	4.43 ± 0.19	3.87 ± 0.35
13	RBO	0.5	3.875	25	25	50	15	8	0	4.37 ± 0.14	ND
14	CCO	0.5	3.5	25	25	60	5	8	100	3.17 ± 0.05	1.11 ± 0.08
15	RBO	0.5	3.5	10	25	60	15	1	100	3.08 ± 0.25	ND
16	CCO	0.875	3.5	10	0	60	15	8	0	3.13 ± 0.04	ND
17	CCO	0.875	3.875	25	25	60	15	8	100	3.39 ± 0.18	1.43 ± 0.30

* See Table 3.1 for the meaning of the acronyms.

4.1.2 Correlation analysis

Figure 4.1a shows the result of correlation analysis by CORICO program in the form of sphere, only the significant links ($p < 0.01$) from each response are shown in Figures 4.1b and 4.1c.

(a)

(b)

(c)
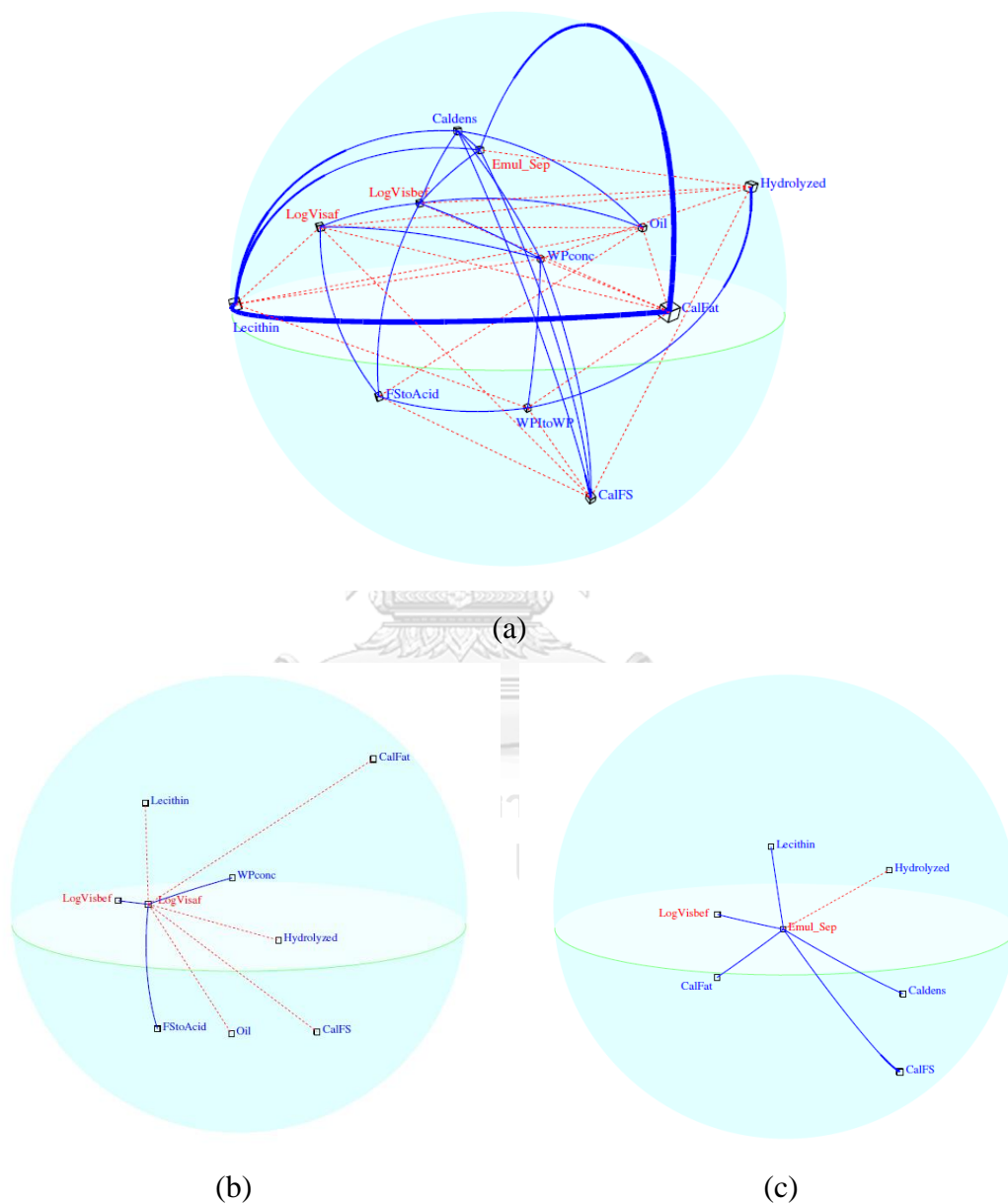
Figure 4.1 CORICO sphere (a) full sphere, (b) significant links ($p < 0.01$) with log viscosity (LogVisbef), and (c) significant links ($p < 0.01$) with percentage of emulsion separation (Emul_Sep)

According to Figure 4.1, CORICO showed relationships between each variable by using blue solid lines for positive correlation ($r > 0$), and red dotted lines for negative correlation ($r < 0$).

The pearson correlation coefficients are displayed in Table 4.2 for significant links from each response ($p < 0.01$).

Table 4.2 Pearson correlation coefficients of significant links ($p < 0.01$) from correlation analysis

Variable 1	Variable 2	Pearson correlation coefficients ($p < 0.01$)
LogVisbef	Caldens	0.64
LogVisbef	FStoAcid	0.25
LogVisbef	Emul_Sep	0.25
LogVisbef	WPconc	0.21
LogVisbef	Oil	0.16
LogVisbef	CalFat	-0.69
LogVisbef	Hydrolyzed	-0.47
Emul_Sep	Lecithin	0.36
Emul_Sep	LogVisbef	0.25
Emul_Sep	CalFat	0.25
Emul_Sep	Caldens	0.17
Emul_Sep	CalFS	0.17
Emul_Sep	Hydrolyzed	-0.28

From Table 4.2, viscosity appeared to positively relate with caloric density, and negatively correlate to calorie from fat ($|r| > 0.5$). As a result, reducing caloric density and increasing calorie from fat lowered viscosity due to the dilution effect by either reducing caloric density or adding more fat. Since fat has a higher caloric value (9 kcal/g) compared with other macronutrients. Therefore, when adding more fat, other compositions could be reduced and water could be added which yielded

in lower product's viscosity (Yanniotis, Skaltsi, & Karaburnioti, 2006). The work from Yanniotis et al. (2006) reported that the viscosity of honey with higher moisture content was lower.

The other links where correlation coeffcient was in the range between -0.5 and 0.5 had weak correlations. Thus, it could be drawn that there was no clear trend for factor-response of each link.

4.1.3 Model and response surface of logarithm of viscosity

CORICO proposed the model for logarithm of viscosity (ModelLogVis) with 9 terms, which comprised a constant and other 8 factors that showed logical interactions. The model is shown in Equation (4.1) with $R^2_{adj} = 0.99$.

$$
\begin{aligned}
\text{ModelLogVis} = {} & 3.766 + 1.796\ \text{Caldens-CalFat} - 1.015\ \text{Hydrolyzed*Hydrolyzed} \\
& - 0.4357\ \text{WPconc]CalFS} + 0.4818\ \text{CalFS*WPItoWP} \\
& + 0.4038\ \text{Hydrolyzed\{-Hydrolyzed} + 0.1003\text{Caldens\textasciicircum FStoAcid} \\
& + 0.1308\text{Caldens\{-Oil} + 0.3515\text{Caldens\textasciicircum Hydrolyzed} \qquad (4.1)
\end{aligned}
$$

From regression analysis, the experimental values and the predicted values had a strong correlation with R value of 0.998, slope of 0.996 and Y-intercept of 0.0143.

According to Equation 4.1, the response mostly depended on the "Caldens-CalFat" term. This term is defined as Caldens "minus" CalFat, which means that LogVis value was high when the difference between Caldens and CalFat was high. Moreover, the term "Hydrolyzed*Hydrolyzed" also affected this response. This term is described as the square of the percentage of hydrolyzed whey protein with respect to the total amount of protein. The negative coefficient means that change in the percentage of hydrolyzed protein resulted in a decreasing log value of viscosity in the downward concave manner.

To develop a response surface, the most important interaction with the highest absolute value of coefficient was selected (Jouquand et al., 2015). In this study,

logarithm of viscosity values (Model logVis) was plotted with calorie from fat and caloric density as illustrated in Figure 4.2.
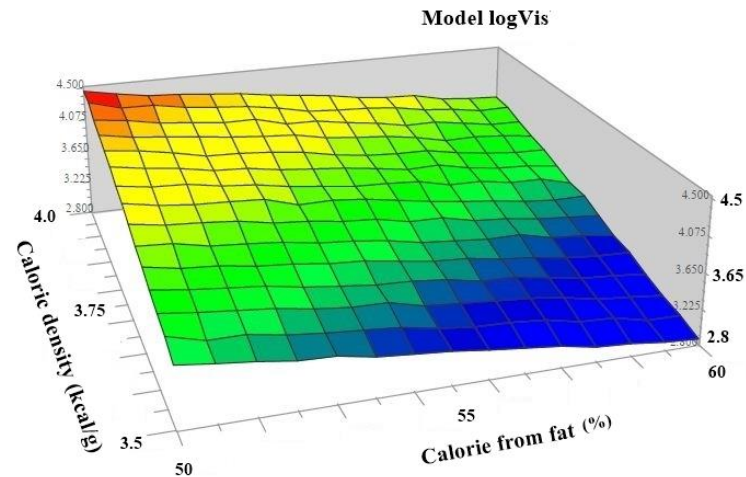
Figure 4.2 3D response surface for logarithm of viscosity (Model logVis) with caloric

density (kcal/g) and calorie from fat (%)

Figure 4.2 shows that the response relied on both the caloric density of the enteral nutrition formula and the calorie from fat as explained earlier by Equation 4.1. As shown in Figure 4.2, viscosity decreased with decreasing caloric density and increasing calorie from fat as discussed in section 4.1.2.

4.1.4 Model and response surface of percentage of emulsion separation

IC suggested the model for the percentage of emulsion separation with 7 terms which are displayed in Equation 4.2 with $R^2_{adj} = 0.93$.

$$\begin{aligned}
\text{Emul\_Sep} = \quad & 0.8106 - 3.681\,\text{FStoAcid\#-CalFat} + 2.128\text{Caldens\&-WPconc} \\
& - 1.803\text{CalFS\&-CalFS} + 0.9670\,\text{Lecithin\{CalFat} \\
& - 0.8741\,\text{WPconc\{-Oil} + 0.8154\,\text{FStoAcid\{Caldens} \qquad (4.2)
\end{aligned}$$

The experimental value and the predicted value had a strong correlation but a bit weaker than that for logarithm of viscosity with R value of 0.978, slope of 0.957 and Y-intercept of 0.0346. Because there were many observations with unnoticeable separation and was input as 0 or no separation even though separation would occur.

From Equation 4.2, "FStoAcid#-CalFat" had a strong effect on the percentage of emulsion separation but with a negative coefficient. This term is defined as FStoAcid "as not" CalFat, which means that the emulsion separation was high when the solid in HFCS to acid ratio did not vary in the same way as the calorie from fat. However, the response inversely depended on this interaction. Therefore, the value was transposed between high and low. In addition, the term "Caldens&-WPconc" also impacted the separation. This term is described as Caldens "and not" WPconc, which indicates that the response was high only when the caloric density was high, and the concentration of whey protein was low.

The percentage of emulsion separation (Model Emulsion separation) was plotted against the solid in HFCS to acid ratio and the calorie from fat. The resulted response surface is shown in Figure 4.3.
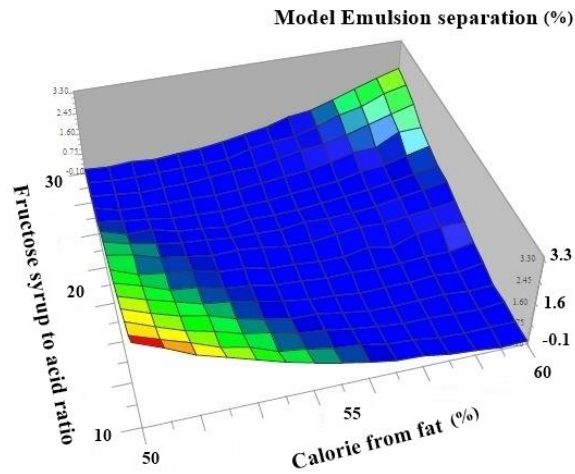
Figure 4.3 3D response surface for the percentage of emulsion separation (Model Emulsion separation) in (%) versus solid in HFCS to acid ratio and calorie from fat (%)

Figure 4.3 shows the relationship between the percentage of emulsion separation, the solid in HFCS to acid ratio, and the calorie from fat as mention earlier in Equation 4.2. A study on the emulsion's viscoelasticity (Figure 4.4) revealed that the emulsion separation was related with the sample's viscoelastic property. Dominating viscous behavior was found in the sample that showed high oil separation, while dominating elastic behavior at low frequencies was observed for stable, no oil separation, samples. Emulsion with viscous or fluid-like behavior allowed the oil droplet to accumulate and resulted in oil separation. On the other hand, elastic or solid-like emulsion could not flow well and obstruct coalescence that leads to emulsion's breakdown (Xiong et al., 2018). Tzoumaki, Moschakis, Kiosseoglou, and Biliaderis (2011) studied the effect of chitin-stabilized oil-in-water emulsion with various added chemical compounds. It was noted that the emulsion with lower stability had more viscous characteristic. Tadros (2015) collected the data on the relationship between emulsion stability and viscoelasticity of the system. It was indicated that the emulsion with lower volume fraction or lower stability tended to have more viscous behavior. Xiong et al. (2018) conducted a study on the emulsion with ovalbumin/chitosan complex. They reported that the emulsion with fluid-like pattern had lower stability.

(a)   (b)
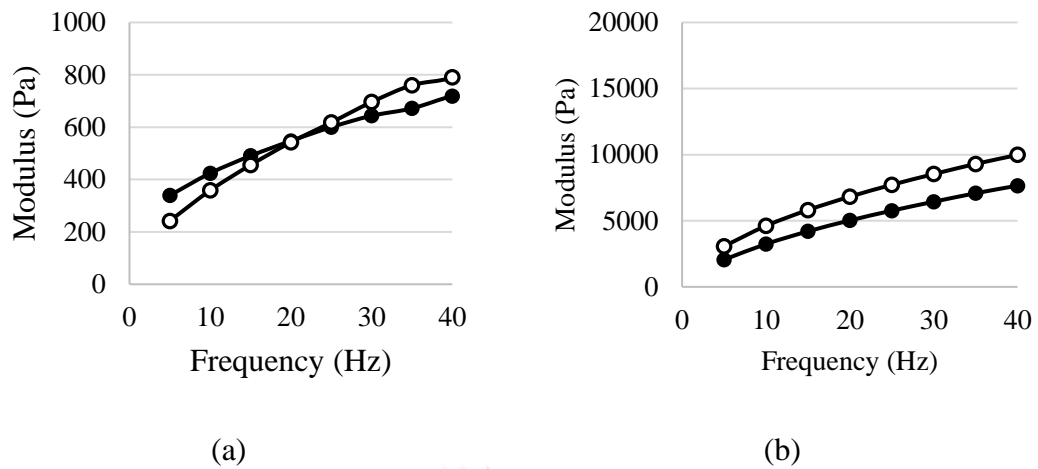
Figure 4.4 Storage modulus (G′) in black circle (●) and loss modulus (G″) in white circle (○) of samples (a) with unnoticable separation (trial 2), and (b) with 3.57% separation (trial 8)

Lecithin could be another reason that impacted the stability of the emulsion as the correlation analysis pointed out a slightly positive correlation between emulsion separation and lecithin concentration (Table 4.2). Adding too much lecithin into emulsion system can cause rapid coalescence that, in turn, yields an emulsion breakdown (Muhamad, Quin, & Selvakumaran, 2016). McCrae (1999) studied the efficiency of lecithin in stabilizing different kinds of milk products. They found that increasing lecithin in whole milk reduced its stability. Dammak and José do Amaral Sobral (2018) investigated the effect of lecithin addition on the stability of pickering emulsion for hesperidin encapsulation. They indicated that the increasing lecithin concentration in a low range can increase emulsion stability. However, adding too much lecithin could make the system unstable.

4.1.5 Optimal formulas amd validation

By setting the targeted response range for each response as detailed in section 3.3.3, the optimal conditions for each kind of oil were suggested as shown in Table 4.3. These formulas would yield the enteral nutrition products that have the viscosity in the 3.2-3.3 log value range with low oil separation.

Table 4.3 Optimal formulas calculated from IC

Factor*	Formula 1	Formula 2
Oil	Coconut oil	Rice bran oil
Lecithin (%w/w)	0.82	0.77
Caldens (kcal/g)	3.89	3.58
FstoAcid	12.88	29.10
Hydrolyzed (%)	17.09	20.15
CalFat (%)	59.51	53.17
CalFS (%)	14.46	11.80
WPconc (%w/w)	5.74	5.31
WPItoWP (%)	83.05	63.81

* See Table 3.1 for the meaning of the acronyms.

From Table 4.3, both conditions did not have high caloric density and low calorie from fat that resulted in too high viscosity. In addition, both formulas had solid in HFCS to acid ratio and calorie from fat in the range that gave low emulsion separation.

IC proposed the value of responses at each optimal formula as shown in Table 4.4.

Table 4.4 Predicted value using IC method compared with experimental data (n = 3)

of each response for formula for each oil

Response	Predicted value	Experimental data (n = 3)
Formula with Coconut oil		
Log value of viscosity	3.23	2.90 ± 0.01
Percentage of emulsion separation	0.15	Not detected
Formula with rice bran oil		
Log value of viscosity	3.30	3.33 ± 0.00
Percentage of emulsion separation	0.01	Not detected

From Table 4.4, IC calculated the viscosity value of the optimal formula obtained for rice bran oil in a close proximity with the experimental data. However, the predicted viscosity value of the optimal formula with coconut oil showed higher difference from the experimental data. On the other hand, values for percentage of emulsion separation were not much different since they were all unnoticeable; thus, they were noted as less than 1 or "not detected".

4.2 Optimization of microwave heating for tube-feeding enteral nutrition products

4.2.1 Experimental design and responses

Table 4.5 illustrates DM arrangement for microwave heating with 2 factors. It suggested 9 trials for 5 heating times and 3 specific powers, which included 3 replicates at the center point condition.

According to Table 4.5, microwave heating could increase surface temperature from 31.5 ℃ to at least 49.8 ℃ (trial 5) and to the maximum temperature of 80.5 ℃ (trial 2). Moreover, relative typtophan loss which represents overall protein denaturation (Birlouez-Aragon et al., 2002) ranged from 3.06% (trial 5) to 48.1% (trial 2). Furthermore, FAST index, which is the indicator for advanced Mailard products, e.g. imidazole and pyrrole derivatives (Birlouez-Aragon et al., 2002) slightly increased after heating from 2.29 to 2.87 (trial 4) and to 3.70 (trial 1 and 2). The FAST index of the samples was quite low compared with other studies since protein source and carbohydrate source were diluted. Birlouez-Aragon et al. (2002) reported that the FAST index of raw milk, thermized milk, pasteurized milk, and sterilized milk were 10.4, 11.8 to 13.1, 12.7 to 75.2, and 23.0 to 187.2, respectively. Moreover, Laguerre et al. (2011) investigated the impact of microwave heating of infant formula that contained whey protein. The FAST index of the infant formula varied from around 5 to less than 40.

Table 4.5 Microwave heating conditions with Doehert matrix arrangement and responses

Trial	Time (s)	Specific power (W/mL)	Average of bottom surface temperature (°C)	Relative tryptophan loss (%)	FAST index
Before heating	-	-	31.5	0	2.29
1	60	5	69.0 ± 1.0	40.6 ± 2.0	3.70 ± 0.52
2	54	7	80.5 ± 1.3	48.1 ± 0.7	3.70 ± 0.44
3	41	7	70.3 ± 0.7	30.6 ± 0.2	3.58 ± 0.23
4	35	5	56.8 ± 1.0	3.33 ± 0.32	2.87 ± 0.45
5	41	3	49.8 ± 0.9	3.06 ± 0.51	3.26 ± 0.78
6	54	3	54.2 ± 1.1	5.07 ± 0.22	3.43 ± 0.51
7	48	5	66.8 ± 0.7	12.5 ± 1.2	3.15 ± 0.23
8	48	5	64.2 ± 0.7	14.1 ± 2.2	3.38 ± 0.12
9	48	5	65.8 ± 0.3	13.4 ± 3.4	3.20 ± 0.32

Table 4.6 shows the regression analysis between experimental and calculated data of experimental designs for models proposed by RSM and IC. It can be seen that the predicted responses from RSM and IC correlated well with the experimental data for the average surface temperature and the relative tryptophan loss of the sample, with the slope tending toward 1 and an R from 0.986-0.997 for RSM result and 0.988-0.994 for IC result. The predicted FAST index from IC did not correlate well with the experimental data, with R equaled to 0.685. However, RSM failed to develop the model for this response ($p > 0.01$).

Table 4.6 Regression analysis

Response	RSM model			IC model		
	Slope	**Y-intercept**	**R**	**Slope**	**Y-intercept**	**R**
Average of bottom surface temperature (°C)	0.994	0.366	0.997	1.007	-0.472	0.988
Relative tryptophan loss (%)	0.973	0.514	0.986	1.01	-0.182	0.994
FAST index	N/A	N/A	N/A	0.882	0.399	0.685

4.2.2 Correlation analysis

Figure 4.5 shows the result of correlation analysis by CORICO program in the form of sphere, only the significant links ($p < 0.01$) were to be shown.
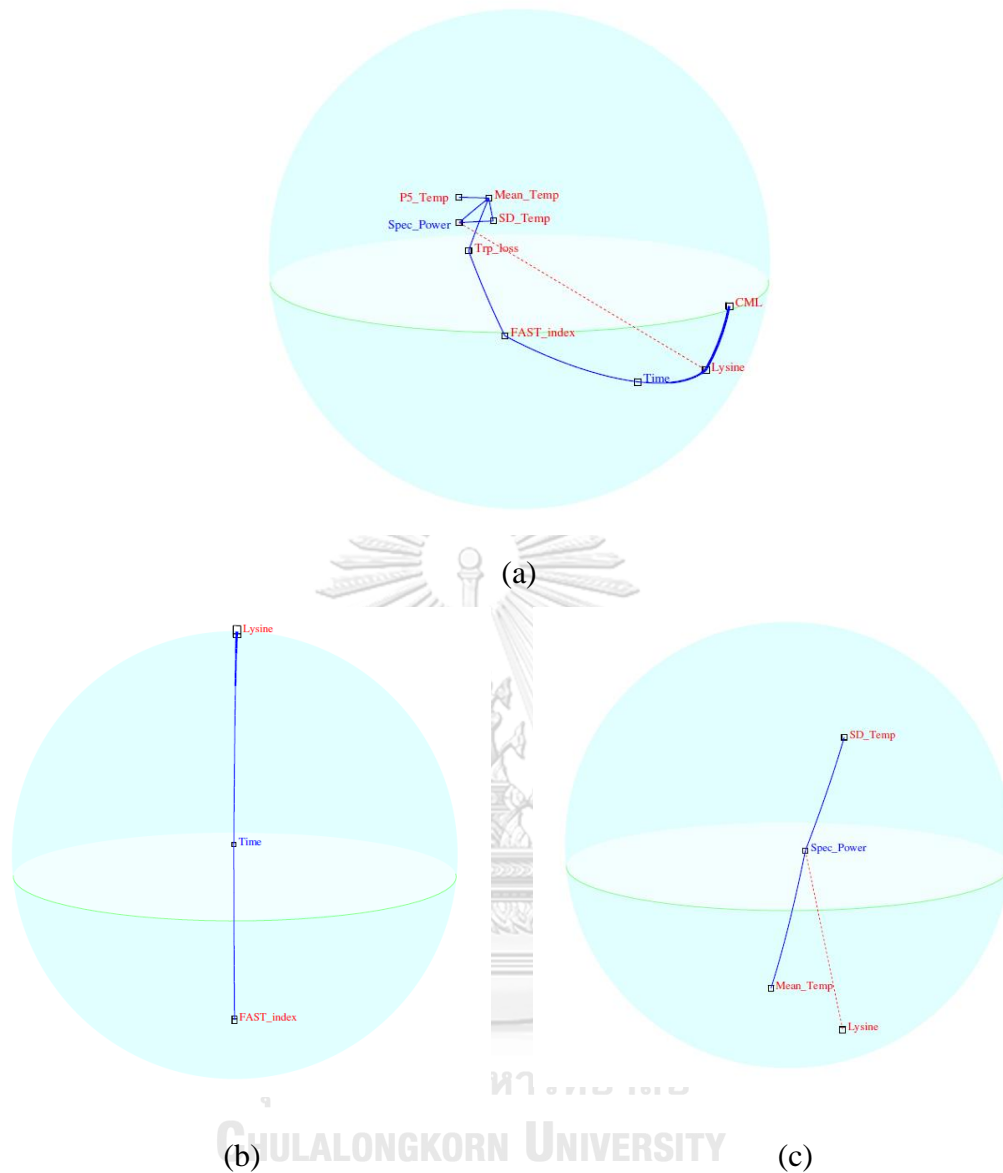
Figure 4.5 CORICO sphere (a) full sphere, (b) significant links (p < 0.01) with heating time (Time), and (c) significant links (p < 0.01) with microwave's specific power (Spec_Power)

According to Figure 4.5, CORICO showed relationships between each variable by using blue solid lines for positive correlation (r > 0), and red dotted lines for negative correlation (r < 0).

The pearson correlation coefficents were displayed in Table 4.7 for links from each factor.

Table 4.7 Pearson correlation coefficients from correlation analysis

Variable	Time	Spec_Power
Mean_Temp	0.43*	0.89
SD_Temp**	0.38*	0.89
Lysine**	0.64	-0.50
Trp_Loss	0.56*	0.75*
FAST_index	0.71	N/A
CML**	0.53*	N/A
P5_Temp**	0.44*	0.88*

**Correlations are not significant at $p = 0.01$

**Results are not being discussed in this chapter.

According to Table 4.7, heating time has good relationship with FAST index. Laguerre, Gadonna-Widehem, and Tessier (2006) reported that the FAST index of microwaved cow milk was impacted by heating time. Moreover, Birlouez-Aragon et al. (2002) pointed out that the FAST index of processed dairy products with the same process (thermization, pasteurization, and sterilization) was higher if it was processed for a longer period of time.

Moreover, microwave's specific power has strong correlation with average of bottom surface temperature. At a constant heating time, temperature was more elevated with higher specific power. The same finding was also reported by Lau and Tang (2002). They investigated the effect of different microwave heating power in pickled asparagus and found out that higher power caused higher temperature. This was also in accordance with a research work on egg pasteurization at different microwave powers (Dev et al., 2008) and infant formula sterilization (Laguerre et al., 2011).

4.2.3 Average surface temperature

RSM suggested the numerical model for average surface temperature as shown in Equation 4.3 with $R^2_{adj} = 0.98$.

Mean Temp = $65.4^* + 6.44X_1^* + 13.6X_2^* + 3.21X_1X_2 - 2.54X_1^2 - 1.32X_2^2$ (4.3)

(The terms with * were significant at $p = 0.01$)

From Equation 4.3, the temperature was mostly affected by X_2 term or specific power which was in agreement with the correlation analysis from IC and with a 3D surface plot in Figure 4.6a. Table 4.6 shows that the model could predict the response accurately.

IC proposed the model with lower correlation between predicted values and experimental values (Table 4.6) with 4 terms as shown in Equation 4.4 with $R^2_{adj} = 0.99$.

ModelMeanTemp = 64.1731 + 22.6103 Time+Spec_Power

- 8.5505 Time&-Spec_Power + 2.6112 Time!Time   (4.4)

According to Equation 4.4, the term "Time+Spec_Power" had the highest impact on the surface mean temperature. This term was defined as Time "plus" Spec_Power which meant that temperature value was high when the summation of coded time and coded specific power was high. The term "Time&-Spec_Power" had an impact on the surface mean temperature at a lower degree. It was descibed as Time "and not" Spec_Power. The negative coefficient meant that the temperature was low only when heating time was high and specific power was low. Figure 4.6b shows the response surface for the relationship explained earlier. From Figure 4.6, the 3D plot from both methods were similar.
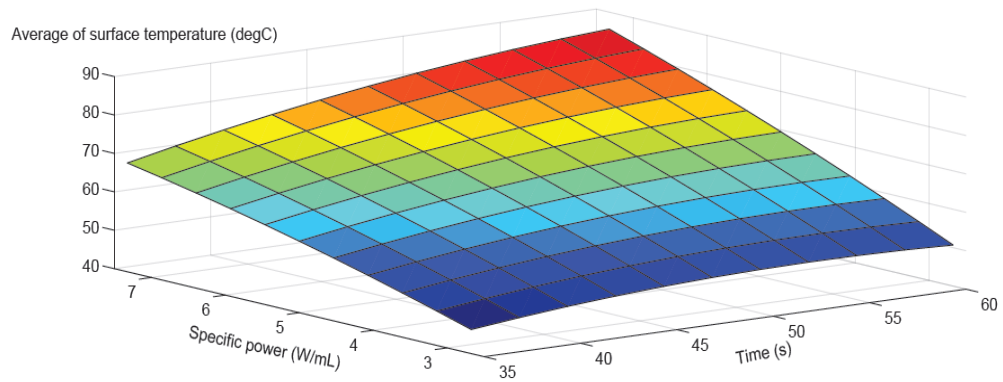
(a)
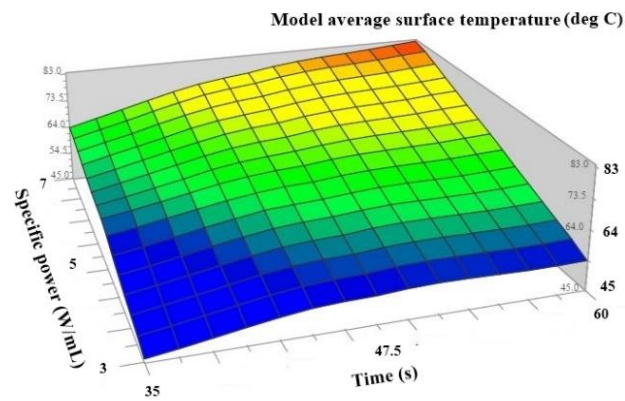
(b)

Figure 4.6 3D response surface calculated by RSM (a) and IC (b) for average surface temperature (°C) with heating time (s) and specific power (W/mL)

4.2.4 Relative tryptophan loss

The model that was proposed by the RSM for relative tryptophan loss is shown in Equation 4.5 with $R^2_{adj} = 0.93$.

$$\%\text{Trp loss} = 12.7^* + 15.4X_1^* + 20.5X_2^* + 8.71X_1X_2 + 9.25X_1^2 + 8.82X_2^2 \quad (4.5)$$

(The terms with * were significant at $p = 0.01$)

From Equation 4.5, The term X_2 or specific power had the strongest impact on relative tryptophan loss. Heating time (X_1) had a lower but notable effect since the coefficient was slightly lower. According to a regression analysis (Table 4.6), the model gave a predicted value in close proximity with the experimental data as shown by a slope that was close to 1.0 and high correlation coefficient.

The model that was obtained from the IC contained 3 terms as illustrated in Equation 4.6 with $R^2_{adj} = 0.95$.

$$ModelTrpLoss = 18.978 + 45.82Time\&Spec\_Power - 14.97Time\#Spec\_Power \quad (4.6)$$

From Equation 4.6, the term "Time&Spec_Power" was the main effect of relative tryptophan loss. It was Time "and" Spec_Power, so the loss was high only when both heating time and specific power were high. Figure 4.7b shows the 3D plot of this relationship. The term "Time#Spec_Power" was also important, but with a negative coefficient. The term was described as Time "as" Spec_Power which meant that the response was low when the heating time varied the same way as the specific power did, or the coded time was the same as the coded specific power. According to Figure 4.7, both surface plots are identical.

The models (Equation 4.5 and 4.6) and Figure 4.7 showed that both heating time and specific power or the extent of heating were the major contribution to tryptophan loss or milk protein denaturation. Laguerre et al. (2011) reported that infant formula with a higher degree of heating showed more tryptophan loss. Birlouez-Aragon et al. (1998) and Birlouez-Aragon et al. (2002) also pointed out that milk which experienced a high degree of heating, e.g. sterilization, had more tryptophan loss than those subjected to pasteurization.
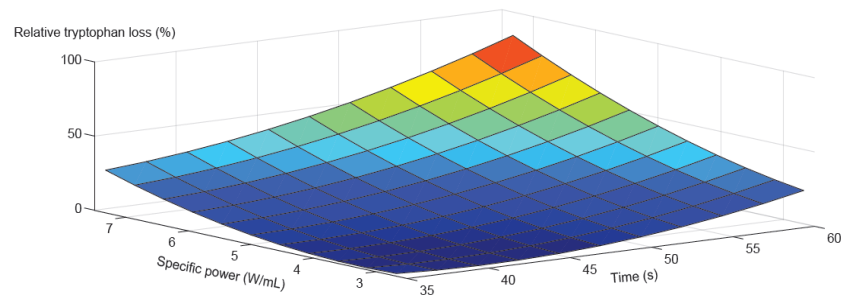
(a)
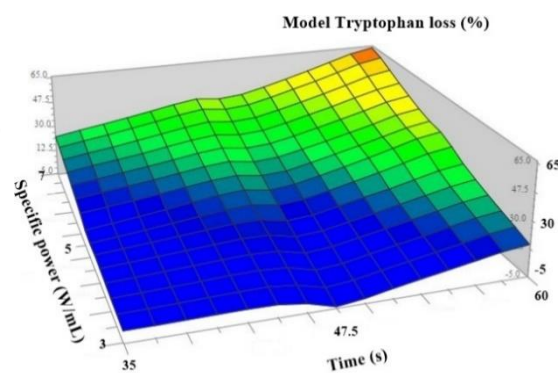
(b)

Figure 4.7 3D response surface caluculated by RSM (a) and IC (b) for relative tryptophan loss (%) with heating time (s) and specific power (W/mL)

4.2.5 FAST index

RSM could not develop the model for FAST index ($p > 0.01$) since the model was based on a quadratic model. Consequently, only the model from IC proposed the model consisting of 5 terms for the FAST index shown in Equation 4.7 with $R^2_{adj} =$ 0.90.

$$ModelFAST\_index = 3.3646 - 0.60Spec\_Power\{-Time - 0.34Time\{-Spec\_Power$$
$$+ 0.14Spec\_Power]-Spec\_Power + 0.15Time\}Time \quad (4.7)$$

The most important effect that caused the change in the FAST index was "Spec_Power{-Time" It was defined as Spec_Power "mean if not" Time. With a negative coefficient, this means that the FAST index was low for average value of

Spec_Power (5 W/mL) when Time was low. The other term, which was "Time{-Spec_Power", also impacted the FAST index. This term meant Time "mean if not" Spec_Power. As previously explained, at average time value (47.5 s), FAST index was low when Spec_Power was low. Figure 4.8 assures this explanation.
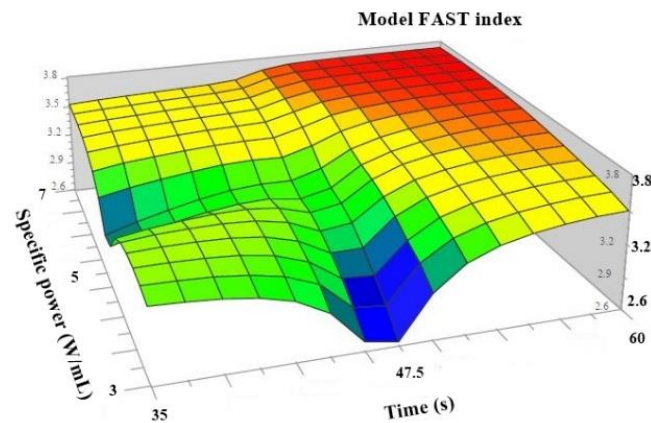
Figure 4.8 3D response surface calculated by IC for FAST index with Time (s) and Specific power (W/mL)

4.2.6 Optimal conditions and validation

The aim of the optimization was to find the condition which offered the highest average temperature, while maintaining the nutritional quality, or the lowest tryptophan loss and the lowest FAST index. Both RSM and IC were utilized to achieve these objectives and were compared for their efficiency. Two optimal conditions were obtained. Each was validated by experimental data and shown in Table 4.8.

Table 4.8 Predicted value compared with experimental data (n = 2) of each response

Response	Optimal condition proposed by RSM (heating at 5 W/mL for 45 s)			Optimal condition proposed by IC (heating at 5.67 W/mL for 45 s)		
	Data from experiment (n = 2)	Predicted value by RSM	Predicted value by IC	Data from experiment (n = 2)	Predicted value by RSM	Predicted value by IC
Average surface temperature (°C) [% deviation]	63.8 ± 1.3	64.0 [+0.3]	63.6 [-0.3]	65.8 ± 0.2	67.6 [+2.74]	67.3 [+2.28]
Relative tryptophan loss (%) [% deviation]	10.0 ± 1.3	10.0 [+0.4]	11.0 [+10]	11.0 ± 1.3	16.1 [+46.4]	17.0 [+54.5]
FAST index [% deviation]	2.58 ± 0.04	N/A	3.23 [+25.2]	2.69 ± 0.35	N/A	3.48 [+25.4]

The optimal conditions from either RSM or IC were roughly at the moderate heating time and specific power (Table 4.8). Because a higher degree of processing could give rise to higher temperature and increase tryptophan loss and FAST index.

According to Table 4.8, RSM predicted average temperature and relative tryptophan loss better than the IC did. However, IC could not predict the FAST index as it was not good enough to forecast the response.

4.3 Numerical simulation of commercial sterilization of liquid enteral nutrition products using batch microwave oven

4.3.1 Properties of ingredients and products

4.3.1.1 Ingredients' properties

Table 4.9 shows volumetric specific heat, true density, thermal conductivity, and calculated specific heat of each ingredient used in the formulation of the enteral nutrition formula.

Table 4.9 Physical and thermal properties of ingredients (n = 3)

Sample	Density (kg/m^3)	Thermal conductivity (W/m·K)	Volumetric heat capacity (kJ/m^3·K)	Specific heat (J/kg·K)	References
Maltodextrin	596 ± 9	0.139 ± 0.006	958.9 ± 4.3	1604 ± 32	Experiment
Hydrolyzed whey protein	371 ± 2	0.123 ± 0.009	704.9 ± 49.2	1902 ± 142	Experiment
Whey protein isolate	369 ± 10	0.124 ± 0.005	687.6 ± 7.9	1864 ± 69	Experiment
Whey protein concentrate	346 ± 18	0.131 ± 0.004	748.5 ± 31.5	2163 ± 208	Experiment
Soy protein isolate	426 ± 24	0.120 ± 0.006	788.4 ± 18.4	1849 ± 145	Experiment
Water	-	0.604	-	4176	Coupland and McClements (1997)
Rice bran oil	-	0.17	-	1800	Saravacos and Maroulis (2011)
HFCS42	-	0.353	-	2278	Giannandrea and Christensen (1993)

4.3.1.2 Product's proximate composition

Table 4.10 shows the product's proximate composition except for crude fiber and ash since there was no detectable fiber in any ingredients. Moreover, according to preliminary tests, ash content for all samples was less than 1 %(wb), it was, thus, assumed to be undetectable. Moisture content of formula decreased with increasing caloric density since more ingredients were applied. However, protein, fat and carbohydrates of 1 kcal/mL and 2.5 kcal/mL were not much different because they were formulated with the same caloric distribution with calorie from protein, fat, and carbohydrates at 20: 30: 50. On the contrary, the 3.78 kcal/g formula was clearly different for the reason that more fat was necessary to prepare high caloric density formula for reducing viscosity (Dautant, Simancas, Sandoval, & Müller, 2007).

Table 4.10 Proximate composition (no crude fiber and ash) of the products (n = 4)

Formula	1 kcal/mL	2.5 kcal/mL	3.78 kcal/g
Moisture content (%wb)	79.4 ± 0.3	50.2 ± 1.3	37.3 ± 0.1
Protein (%db)	21.1 ± 0.3	24.3 ± 0.3	30.2 ± 0.7
Fat (%db)	13.5 ± 0.6	5.98 ± 0.55	41.0 ± 0.4
Carbohydrate (%db)	65.4 ± 0.1	69.7 ± 0.8	28.9 ± 1.1

4.3.1.3 Density and thermal properties of products

According to Table 4.11, density of the product increased when the caloric density increased from 1 kcal/mL to 2.5 kcal/mL because of the increasing solid content (Wemmenhove, Wells-Bennik, Stara, van Hooijdonk, & Zwietering, 2016). The density of 3.78 kcal/g sample was dropped from that of 2.5 kcal/mL because oil, which had low density comparing with other ingredients (ASHRAE, 2006), substituted maltodextrin.

Increasing caloric density lowered the specific heat and thermal conductivity of the sample because of lower moisture content. Water is the material that possesses higher specific heat and thermal conductivity compared with other ingredients (Table 4.9).

Table 4.11 Physical and thermal properties of the products

Formula	1 kcal/mL	2.5 kcal/mL	3.78 kcal/g
Density (kg/m^3)	1043 ± 11	1107 ± 6	920 ± 0
Specific heat (J/kg·K)	3618 ± 45	2904 ± 45	2483 ± 45
Thermal conductivity (W/m·K)	0.50 ± 0.02	0.37 ± 0.02	0.30 ± 0.02

4.3.1.4 Rheological properties of products

Rheological data at each temperature were fitted with the Bingham model (Equation 3.11) with a good fitting for the 2.5 kcal/mL formula ($R^2 > 0.8$) and a fair fitting for the 3.78 kcal/g formula with the lowest correlation coefficient 0.69. From Table 4.12, the Arrhenius relationship (Equation 3.12) was established for temperature dependent properties with well fitting ($R^2 > 0.9$) except for the yield stress of the 2.5 kcal/mL formula with $R^2 = 0.34$. Since the coefficient of variation of the data was less than 10%, the average yield stress was used for describing its properties during the thermal treatment. Ahmed and Ramaswamy (2006) and Vandresen, Quadri, Souza, and Hotza (2009) also made this assumption for yield stress term in their works for sweet potato puree and carrot juice, respectively.

Table 4.12 Rheological model parameters for each formula (n = 2)

Formula	1 kcal/mL	2.5 kcal/mL	3.78 kcal/g
Yield stress (mPa)	53.2*	7314	Not applicable
A_0 (mPa)	Not applicable	Not applicable	0.145
E_a (kJ/mol)	Not applicable	Not applicable	-27.1
Consistency index (mPa·s)	1.34*	Not applicable	Not applicable
A_0 (mPa·s)	Not applicable	5.37×10^{-5}	0.255
E_a (kJ/mol)	Not applicable	-41.6	-21.5

*Data from Xiang et al. (2011)

4.3.1.5 Dielectric properties of products

Dielectric properties model parameters for the model presented in Equation 3.13 to 3.14 are illustrated in Table 4.13. The data from previous works was fitted in the quadratic equations for dielectric properties with good correlation ($R^2 > 0.8$). Dielectric constant seemed to decrease with increasing moisture content due to reduced water activity (Venkatesh & Raghavan, 2004). Moreover, higher temperature leads to lower ε' owing to lower orderliness of water molecule exposed to higher temperature (Wang et al., 2008). Unlike dielectric constant, the trend for dielectric loss factor by caloric density and temperature were not clear.

Table 4.13 Dielectric properties model parameters of each formula

Formula	1 kcal/mL	2.5 kcal/mL	3.78 kcal/g
Dielectric constant			
a_1	74.571	54.622	24.343
b_1 (1/°C)	-0.1974	-0.0855	-0.2067
c_1 (1/°C^2)	Not determined	Not determined	0.0017
Dielectric loss factor			
a_2	16.723	18.597	27.087
b_2 (1/°C)	-0.0969	-0.0106	-0.6029
c_2 (1/°C^2)	0.0007	0.0009	0.0061

4.3.2 Simulation of heat transfer during microwave heating

Figure 4.9 to Figure 4.11 illustrate the simulated and experimental temperature distribution of different products by continuous heating and Figure 4.12 shows the temperature profile of simulated and experiment data of different conditions.

From Figure 4.9 to Figure 4.11, hot spots were mainly at the left side of the product which directly exposed to the waveguide; thus, electric field intensity was more on this region. This observation was also found by Hamoud-Agha et al. (2014) and Tuta and Palazoğlu (2017) for microbial inactivation in gel and heating of model liquid, respectively. Moreover, hot spots were also noted at the corners on the other side due to reflected microwave field. Cold spots seemed to be around the middle of the formula due to inferior electric field distribution.

Change of maximum temperature appeared to be lower with more heating time or higher sample's temperature due to lower dielectric constant (Table 4.13); hence, heating rate was lower. Dev et al. (2008) and Llave et al. (2016) noticed this phenomenon as well in egg pasteurization and tylose water pastes thawing and heating, respectively.

However, temperature distribution of simulated heated product was significantly different from the experiment. Since there was a single mode microwave cavity and no rotating plate in the heating system, heat transfer coefficient was an important factor on temperature homogeneity (Tuta & Palazoğlu, 2017). Moreover, product's expansion due to boiling and its movement prior to temperature measurement were inevitable. Consequently, the temperature distribution was not identical. Nevertheless, predicted average temperature was in accordance with experimental data which indicated that absorbed power of simulated data agreed with the experiment (Hamoud-Agha et al., 2013).
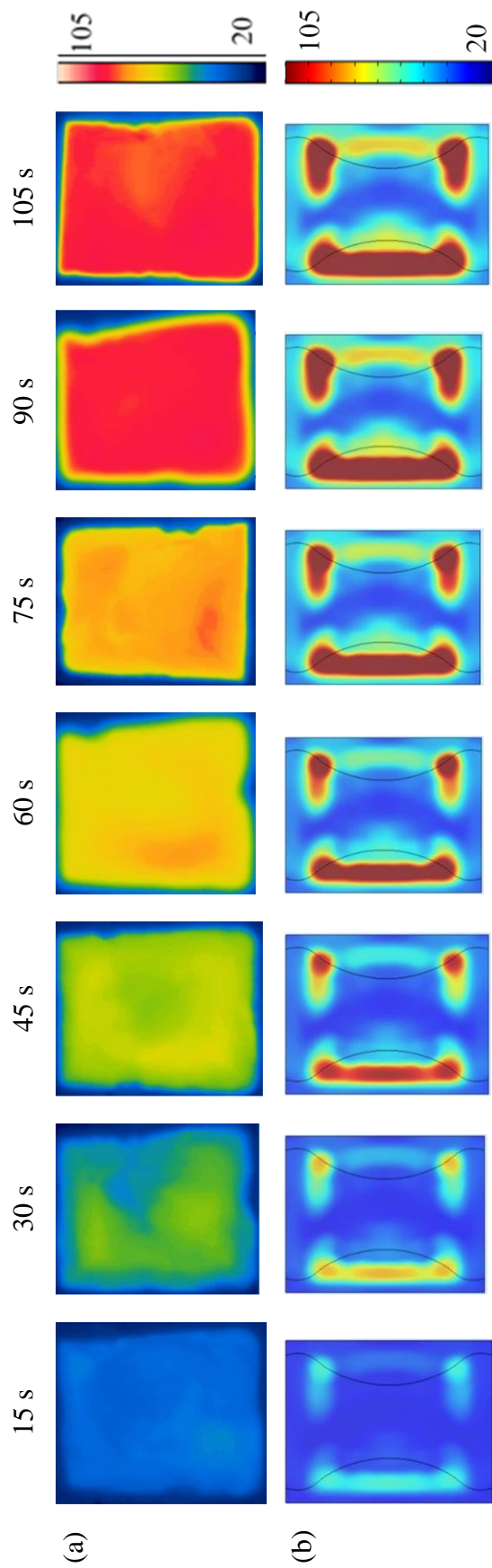
Figure 4.9 Top surface temperature of products by experiment (a) and simulation (b) of 1 kcal/mL formula with continuous heating at 450 W
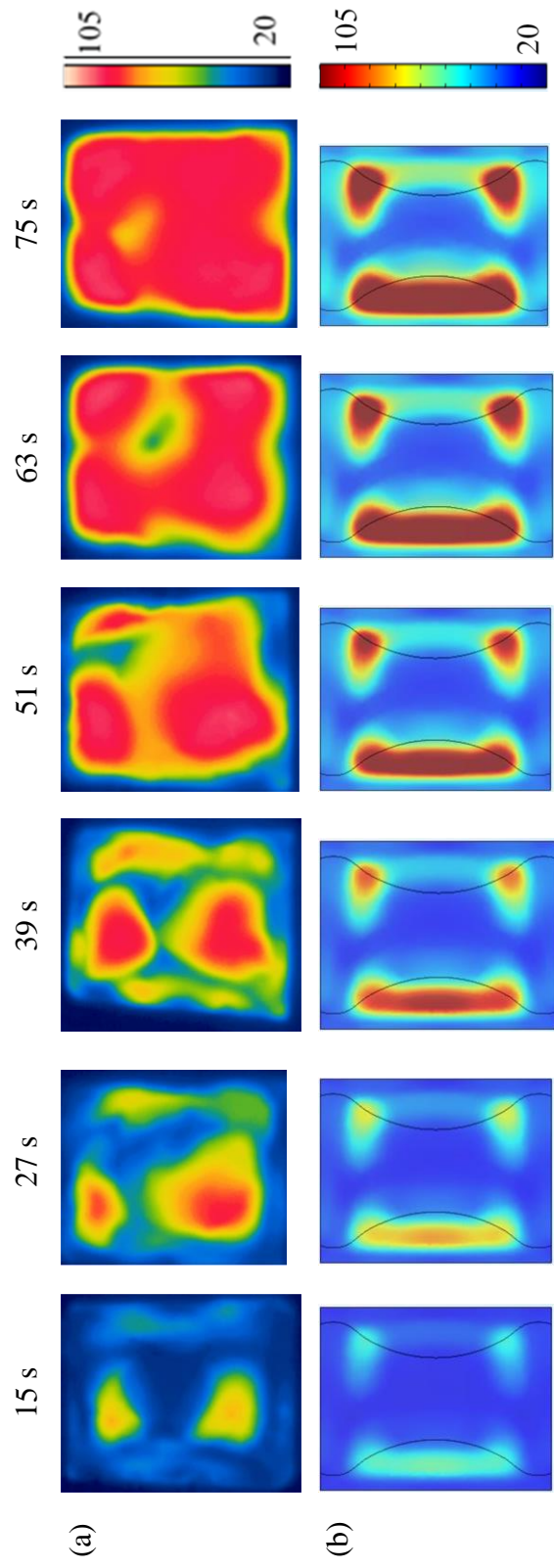
Figure 4.10 Top surface temperature of products by experiment (a) and simulation (b) of 2.5 kcal/mL formula with continuous heating at 450 W
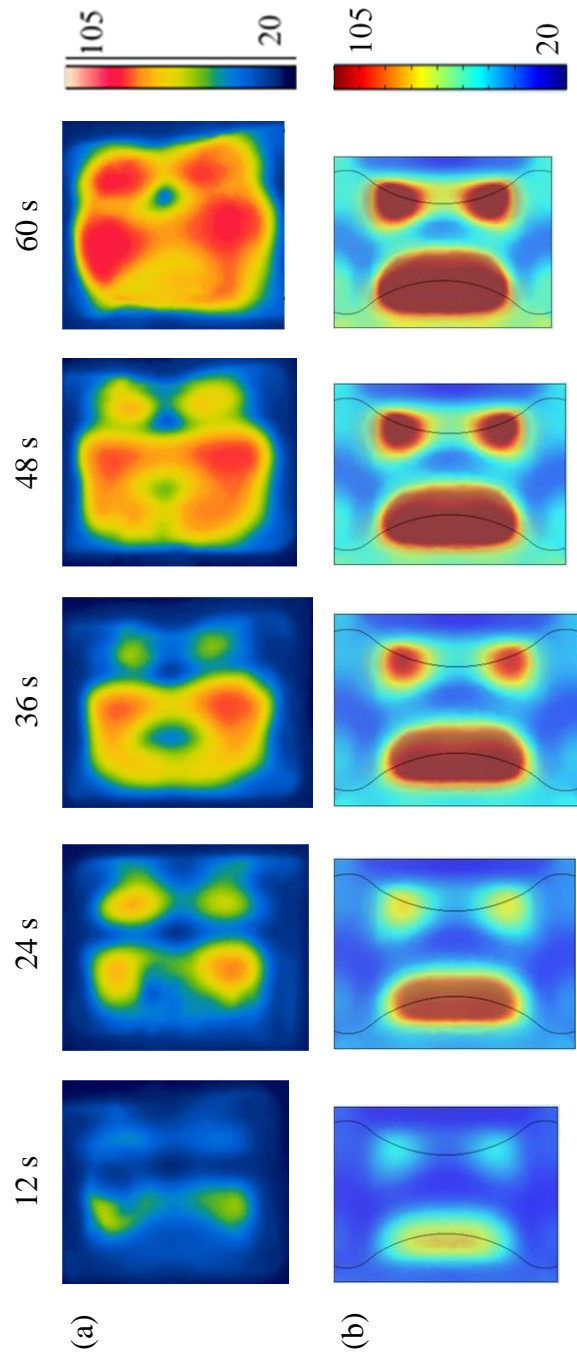
Figure 4.11 Top surface temperature of products by experiment (a) and simulation (b) of 3.78 kcal/g formula with continuous heating at 450 W
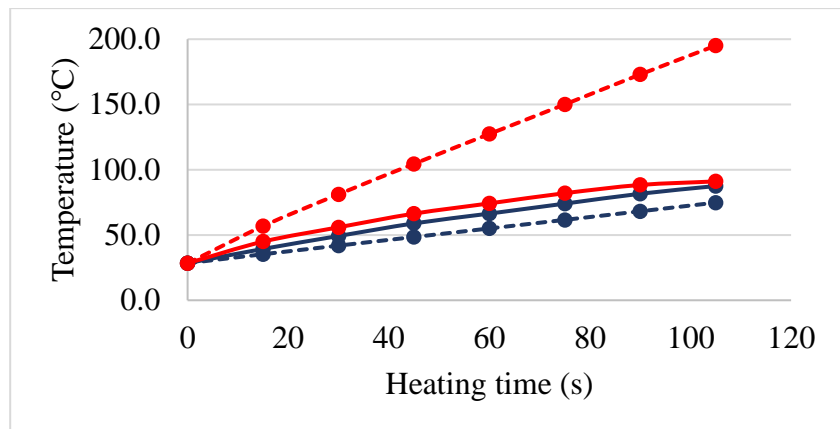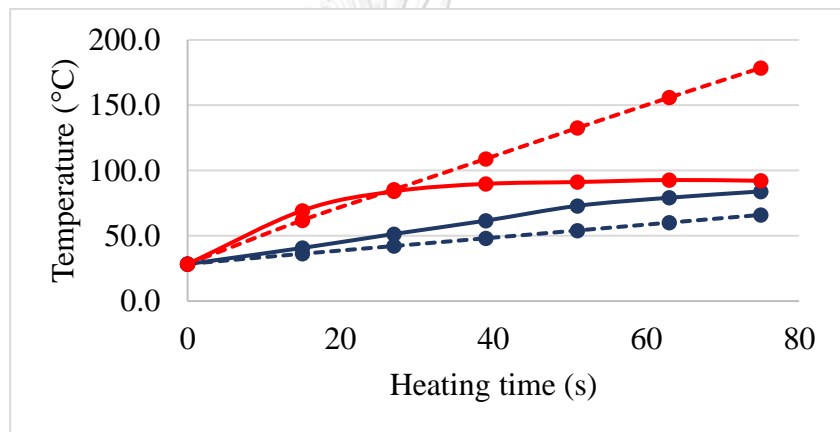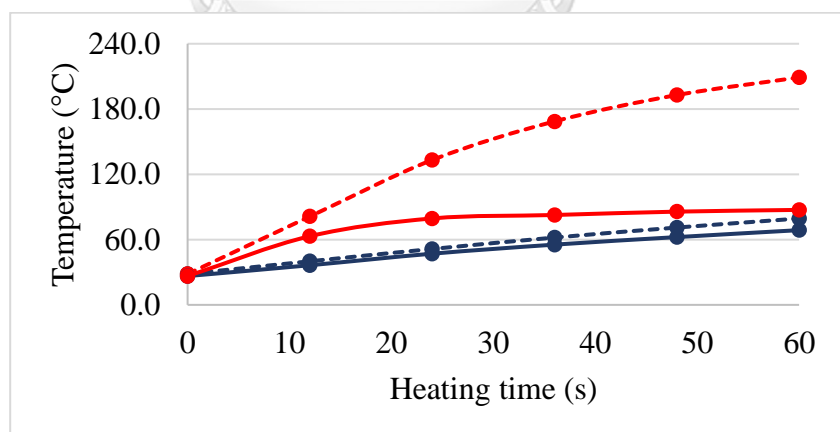
Figure 4.12 Average (blue) and maximum (red) of top surface temperature of products heated by continuous microwave heating at 450 W by experiment (solid line) and integration from simulation (dashed line) of (a) 1 kcal/mL formula, (b) 2.5 kcal/mL formula, and (c) 3.78 kcal/g formula

4.3.2.1 Effect of caloric density

Increasing caloric density seemed to increase heating rate owing to lower specific heat (Equation 3.21). Overall heating rate of 1 kcal/mL formula, 2.5 kcal/mL formula, and 3.78 kcal/g formula was 0.56 °C/s, 0.74 °C/s, and 0.70 °C/s, respectively. Increasing caloric density from 1 kcal/mL to 2.5 kcal/mL required less water, the highest specific heat material, so heating rate was higher. On the other hand, changing the formula from 2.5 kcal/mL to 3.78 kcal/g did not affect heating rate since oil substitution was necessary; hence, specific heat and dielectric properties decreased (Venkatesh & Raghavan, 2004). Effect of composition on dielectric properties and heating rate by microwave was investigated in the work from Dev et al. (2008) and Koskiniemi et al. (2011).

Caloric density also affected homogeneity. Standard deviation of top surface temperature was ranged from 2.54 °C to 5.66 °C, 8.34 °C to 14.3 °C, and 7.53 °C to 13.8 °C for 1 kcal/mL formula, 2.5 kcal/mL formula, and 3.78 kcal/g formula, respectively. Heat transfer coefficient is the main consideration for this effect. This term consists of several properties. However, thermal conductivity and viscosity are being discussed. Since thermal conductivity of 1 kcal/mL formula was higher than the rest because of higher water with high thermal conductivity in the recipe (Coupland & McClements, 1997); furthermore, this formula had significantly lower viscosity; hence, heat transfer was more pronounced, and heterogeneity was reduced (Holdsworth & Simpson, 2007). This point was also indicated in starch-based food sterilization by Llave, Hagiwara, and Sakiyama (2012) and model fluid food microwave heating by Tuta and Palazoğlu (2017).

4.3.2.2 Effect of intermittent heating

Figure 4.13 shows the simulated and experimental temperature distribution of 2.5 kcal/mL formula heated by intermittent heating and Figure 4.14 compares the temperature profile of simulated and experimental data of different conditions.

Intermittent heating could reduce heterogeneity during microwave process by lowering standard deviation of top surface temperature from 13.4 °C to 10.0 °C after the first heating period, and the first tempering period, respectively, from 14.6 °C to 12.8 °C, and from 11.0 °C to 10.3 °C during the second cycle and the last cycle, respectively. However, the maximum temperature and the average temperature slightly decreased during tempering owing to heat loss and heat transfer (Figure 4.14).

Intermittent microwave heating is useful for processing food with low heat transfer coefficient for improving heating uniformity which is challenging for microwave heating (Kumar, Joardder, Karim, Millar, & Amin, 2014). It has been proved by Soysal, Ayhan, Eştürk, and Arıkan (2009), Kumar, Joardder, Farrell, and Karim (2016), and Swamy and Muthukumarappan (2017) for drying red peppers, drying apples, and pectin extraction, respectively.

However, the calculated temperature data was different from experiment. Inconsistent absorbed microwave power could be one reason since the input power for simulation was a stepwise function as shown in Equation 4.8. The simulated microwave power pattern did not agree with either Equation 4.8 or the experimental data (Figure 4.15).

$$P = \begin{cases} 480 \text{ W} & \text{if } 25n \leq t < 25(n+1) \\ 10 \text{ W} & \text{if } 25(n+1) \leq t < 25(n+2) \end{cases} \quad \text{when } n = 2m \text{ and } m = 0, 1, \text{ and } 2 \quad (4.8)$$
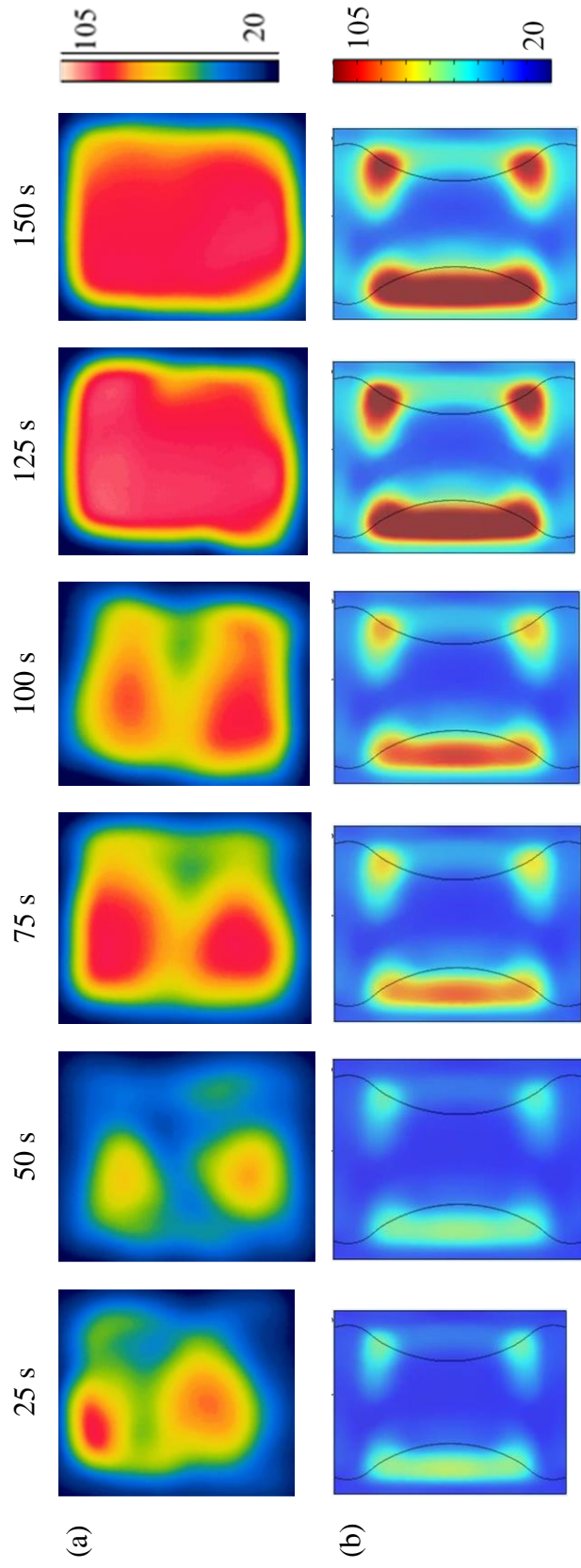
Figure 4.13 Top surface temperature of products by experiment (a) and simulation (b) of 2.5 kcal/mL formula with intermittent heating at 3W/mL by 3 cycles of 1:1 heating and tempering time.
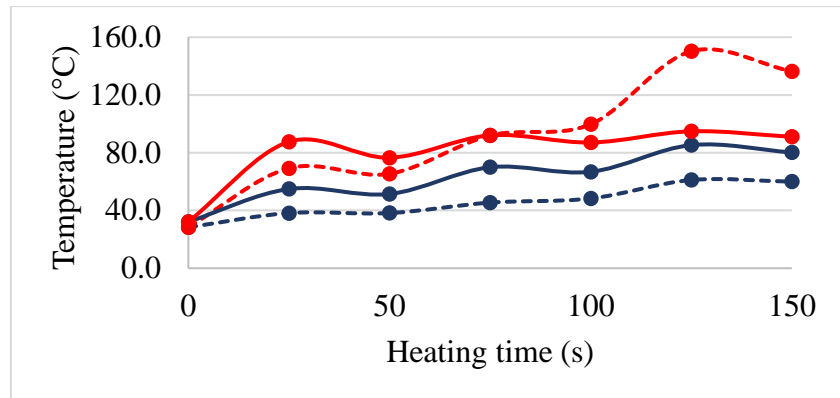
Figure 4.14 Average (blue) and maximum (red) of top surface temperature of heated products by experiment (solid line) and integration from simulation (dashed line) of 2.5 kcal/mL formula by intermittent heating at 450 W for 150 s
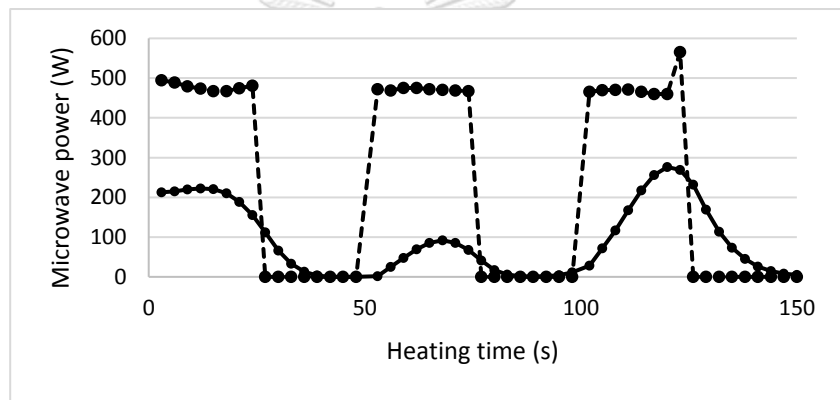
(a)
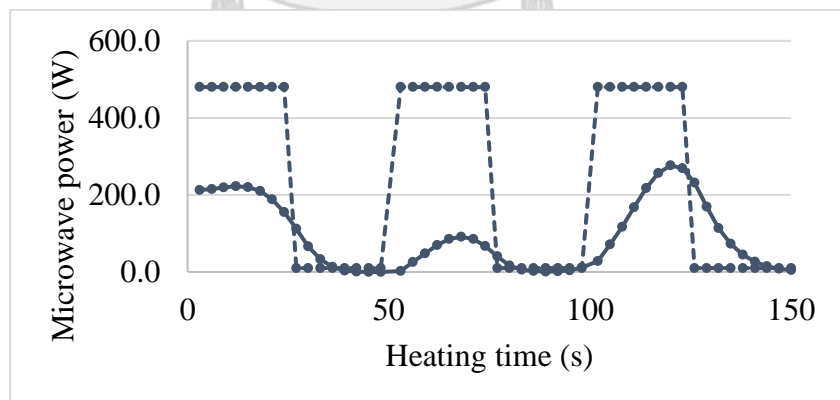
(b)

Figure 4.15 Microwave power for heating 2.5 kcal/mL products with intermittent heating at 450 W for 150 s (a) experiment microwave power (dashed line), and simulated absorbed microwave power (solid line), and (b) input microwave power by Equation 4.8 (dashed line), and simulated absorbed microwave power (solid line)

4.3.3 Safety, quality and FAST index

Table 4.14 shows sterilization value (F_0), cooking value (C_{100}), and FAST index of the heated sample obtained from simulation and experimental data.

Table 4.14 F_0, C_{100}, and FAST index of 1 kcal/mL formula before and after heating (simulation and experiment) at 850 W for 45 s

	Before heating	After heating (Simulation)	After heating (Experiment) (n = 2)
F_0	-	0.28	ND
C_{100}	-	0.35	ND
FAST index	2.25	2.27	2.33 ± 0.15

Sterilization value (F_0) relates to the safety parameter of product applied in thermal processing. The value did not reach commercial sterilization of dairy products which was 3 minutes for ensuring safety and 8 minutes for preventing spoilage by microorganism (Lewis & Deeth, 2009).

For cooking value, it is the indicator of nutrient loss, i.e. thiamine for dairy products. C_{100} was much lower than normal sterilization process, e.g. Tang et al. (2008) reported 20 minutes of C_{100} for beef in gravy sterilization with an F_0 of 3 minutes process. Nonetheless, the value was intended to be lower than traditional sterilization. Tang et al. (2008) reported that microwave heating could reduce 40% of cooking value.

FAST index is the indicator of heating extent for dairy products (Birlouez-Aragon et al., 2002). Birlouez-Aragon et al. (2002) found that the FAST index of raw milk, thermized milk, pasteurized milk, and sterilized milk were 10.4, 11.8 to 13.1, 12.7 to 75.2, and 23.0 to 187.2, respectively. Furthermore, Laguerre et al. (2011) reported the FAST index of microwave heated infant formula contained whey protein from around 5 to less than 40. However, the value of the enteral nutrition product found in this experiment as reported in Table 4.14 was 2.25 which is lower than

those reported in other works since protein and carbohydrate in the formula were diluted. Consequently, heating did not form much Maillard products and significantly denature tryptophan. The simulated value and the experimental data of FAST index agreed well thanks to temperature profile.

4.3.4 Numerical models of commercial sterilization

F_0 and C_{100} value of the conditions reaching commercial sterilization shown in Table 4.15.

Table 4.15 Input microwave power, F_0, and C_{100} value of products heating with conditions reaching commercial sterilization

Formula	Processing time (min)	Input microwave power (W)	F_0 (min)	C_{100} (min)
2.5 kcal/mL	3	870	3.0	3.4
3.78 kcal/g	3	800	3.2	3.7

All conditions gave F_0 value reached the minimum level for assuring safety and retained good quality since C_{100} value was quite low.

Chapter 5 Conclusions

The result from enteral nutrition products formulations by varying ingredients and their application levels showed that viscosity primarily affected by caloric density and calorie from fat. Further, emulsion separation was mainly depended on the solid in HFCS to acid ratio and calorie from fat. Moreover, according to microwave heating optimization at various specific powers and heating times, specific power affected temperature while the FAST index was mostly impacted by heating time.

Comparing optimization methods between Iconographic Correlation (IC) and response surface methodology (RSM), IC method using CORICO software was applicable for optimization with 9 factors. The method offers a more economical but efficient way for optimization that involves many factors. The models proposed by IC gave a good correlation between the experimental data and the predicted value. Furthermore, it could describe unusual behavior of a response pattern e.g. FAST index. However, RSM was a more reliable method for optimization for a few factors.

Lastly, numerical models were developed for commercial steriliation of liquid enteral nutrition formula at different caloric density. Samples were heated in a 2,450-MHz laboratory microwave oven. Hot spots and cold spots were found at the side directly exposed to the waveguide and the middle of the product, respectively. Increasing caloric density resulted in higher heating rate but lower homogeneity. Intermittent heating was able to reduce heterogeneity during microwave heating. Numerical simulation showed the possibility of using microwave oven for commercial sterilization with good agreement for surface average temperature for continuous heating and FAST index comparing to experimental data. However, it could not predict the temperature distribution in the product and the temperature profile for intermittent heating.

5.1 Suggestion

- Emulsion stability by means of other techniques e.g. oil droplet size, volume fraction analysis could improve the data.

- Sensory evaluation for viscosity acceptance should be compared to the rheological data.

- Temperature measurements during thermal treatment without loosen the in-house block could be considered for ensuring commercial sterilization process.

- Further numerical model set up e.g. temperature dependent of physical and thermal properties, heat loss to the Teflon block would enhance the model's accuracy.

- Model parameters for dielectric properties could be optimized for better input variables for numerical simulation.

จุฬาลงกรณ์มหาวิทยาลัย
CHULALONGKORN UNIVERSITY

REFERENCES

Ahmed, J., & Ramaswamy, H. S. (2006). Viscoelastic properties of sweet potato puree infant food. *Journal of Food Engineering, 74*(3), 376-382. doi:https://doi.org/10.1016/j.jfoodeng.2005.03.010

Ahmed, J., Ramaswamy, H. S., & Raghavan, V. G. S. (2007). Dielectric properties of Indian Basmati rice flour slurry. *Journal of Food Engineering, 80*(4), 1125-1133. doi:https://doi.org/10.1016/j.jfoodeng.2006.09.004

Al-Holy, M., Wang, Y., Tang, J., & Rasco, B. (2005). Dielectric properties of salmon (*Oncorhynchus keta*) and sturgeon (*Acipenser transmontanus*) caviar at radio frequency (RF) and microwave (MW) pasteurization frequencies. *Journal of Food Engineering, 70*(4), 564-570. doi:http://dx.doi.org/10.1016/j.jfoodeng.2004.08.046

Antes, F. G., Diehl, L. O., Pereira, J. S. F., Guimarães, R. C. L., Guarnieri, R. A., Ferreira, B. M. S., & Flores, E. M. M. (2017). Effect of ultrasonic frequency on separation of water from heavy crude oil emulsion using ultrasonic baths. *Ultrasonics Sonochemistry, 35*, 541-546. doi:https://doi.org/10.1016/j.ultsonch.2016.03.031

AOAC. (2000). *Official methods of analysis of AOAC International*. Gaithersburg, Md.: AOAC International.

ASHRAE. (2006). *2006 ASHRAE Handbook: Refrigeration*: American Society of Heating, Refrigeration and Air-Conditioning Engineers.

Auksornsri, T., Tang, J., Tang, Z., Lin, H., & Songsermpong, S. (2018). Dielectric properties of rice model food systems relevant to microwave sterilization process. *Innovative Food Science & Emerging Technologies, 45*, 98-105. doi:https://doi.org/10.1016/j.ifset.2017.09.002

Birla, S. L., & Pitchai, K. (2017). 18 - Simulation of microwave processes. In M. Regier, K. Knoerzer, & H. Schubert (Eds.), *The Microwave Processing of Foods (Second Edition)* (pp. 407-431): Woodhead Publishing.

Birlouez-Aragon, I., Nicolas, M., Metais, A., Marchond, N., Grenier, J., & Calvo, D. (1998). A Rapid Fluorimetric Method to Estimate the Heat Treatment of Liquid Milk. *International Dairy Journal, 8*(9), 771-777. doi:https://doi.org/10.1016/S0958-6946(98)00119-8

Birlouez-Aragon, I., Sabat, P., & Gouti, N. (2002). A new method for discriminating milk heat treatment. *International Dairy Journal, 12*(1), 59-67. doi:https://doi.org/10.1016/S0958-6946(01)00131-5

Boillereaux, L., Curet, S., Hamoud-Agha, M. M., & Simonin, H. (2013). Model-Based Settings of a Conveyorized Microwave Oven for Minced Beef Simultaneous

Cooking and Pasteurization. *IFAC Proceedings Volumes, 46*(31), 193-198. doi:https://doi.org/10.3182/20131216-3-IN-2044.00014

Burfoot, D., Railton, C. J., Foster, A. M., & Reavell, S. R. (1996). Modelling the pasteurisation of prepared meals with microwaves at 896 MHz. *Journal of Food Engineering, 30*(1), 117-133. doi:https://doi.org/10.1016/S0260-8774(96)00039-8

Chandrasekaran, S., Ramanathan, S., & Basak, T. (2013). Microwave food processing— A review. *Food Research International, 52*(1), 243-261. doi:http://dx.doi.org/10.1016/j.foodres.2013.02.033

Chen, H., Tang, J., & Liu, F. (2008). Simulation model for moving food packages in microwave heating processes using conformal FDTD method. *Journal of Food Engineering, 88*(3), 294-305. doi:https://doi.org/10.1016/j.jfoodeng.2008.02.020

Chen, J., Pitchai, K., Birla, S., Jones, D., Negahban, M., & Subbiah, J. (2016). Modeling heat and mass transport during microwave heating of frozen food rotating on a turntable. *Food and Bioproducts Processing, 99*, 116-127. doi:http://dx.doi.org/10.1016/j.fbp.2016.04.009

Coupland, J. N., & McClements, D. J. (1997). Physical properties of liquid edible oils. *Journal of the American Oil Chemists, 74*(12), 1559-1564. doi:10.1007/s11746-997-0077-1

Dammak, I., & José do Amaral Sobral, P. (2018). Formulation optimization of lecithin-enhanced pickering emulsions stabilized by chitosan nanoparticles for hesperidin encapsulation. *Journal of Food Engineering, 229*, 2-11. doi:https://doi.org/10.1016/j.jfoodeng.2017.11.001

Datta, N., & Deeth, H. (2007). *UHT and Aseptic Processing of Milk and Milk Products*.

Dautant, F. J., Simancas, K., Sandoval, A. J., & Müller, A. J. (2007). Effect of temperature, moisture and lipid content on the rheological properties of rice flour. *Journal of Food Engineering, 78*(4), 1159-1166. doi:https://doi.org/10.1016/j.jfoodeng.2005.12.028

Dev, S. R. S., Raghavan, G. S. V., & Gariepy, Y. (2008). Dielectric properties of egg components and microwave heating for in-shell pasteurization of eggs. *Journal of Food Engineering, 86*(2), 207-214. doi:10.1016/j.jfoodeng.2007.09.027

Ehlers, R. A., & Metaxas, R. A. C. (2005). An Investigation on the Effect of Varying the Load, Mesh and Simulation Parameters in Microwave Heating Applications. *Journal of Microwave Power and Electromagnetic Energy, 40*(4), 251-259. doi:10.1080/08327823.2005.11688545

Everard, C. D., Fagan, C. C., O'Donnell, C. P., O'Callaghan, D. J., & Lyng, J. G. (2006). Dielectric properties of process cheese from 0.3 to 3GHz. *Journal of*

Food Engineering, 75(3), 415-422.
doi:https://doi.org/10.1016/j.jfoodeng.2005.04.027

Fellows, P. J. (2009). 20 - Dielectric, ohmic and infrared heating. In *Food Processing Technology (Third edition)* (pp. 581-609): Woodhead Publishing.

Ferreira, S. L. C., Silva Junior, M. M., Felix, C. S. A., da Silva, D. L. F., Santos, A. S., Santos Neto, J. H., . . . Souza, A. S. (2017). Multivariate optimization techniques in food analysis – A review. *Food Chemistry*.
doi:https://doi.org/10.1016/j.foodchem.2017.11.114

Franco, A. P., Tadini, C. C., & Wilhelms Gut, J. A. (2017). Predicting the dielectric behavior of orange and other citrus fruit juices at 915 and 2450 MHz. *International Journal of Food Properties, 20*(sup2), 1468-1488.
doi:10.1080/10942912.2017.1347674

Gallegos, C., Brito-de la Fuente, E., Clavé, P., Costa, A., & Assegehegn, G. (2017). Nutritional Aspects of Dysphagia Management. *Advances in Food and Nutrition Research, 81*, 271-318. doi:http://dx.doi.org/10.1016/bs.afnr.2016.11.008

Geedipalli, S. S. R., Rakesh, V., & Datta, A. K. (2007). Modeling the heating uniformity contributed by a rotating turntable in microwave ovens. *Journal of Food Engineering, 82*(3), 359-368.
doi:http://dx.doi.org/10.1016/j.jfoodeng.2007.02.050

Giannandrea, E., & Christensen, U. (1993). Variable viscosity convection experiments with a stress-free upper boundary and implications for the heat transport in the Earth's mantle. *Physics of the Earth and Planetary Interiors, 78*(1), 139-152.
doi:https://doi.org/10.1016/0031-9201(93)90090-V

Gude, V. G., Patil, P., Martinez-Guerra, E., Deng, S., & Khandan, N. (2013). *Microwave energy potential for biodiesel production* (Vol. 1).

Hamoud-Agha, M. M., Curet, S., Simonin, H., & Boillereaux, L. (2013). Microwave inactivation of Escherichia coli K12 CIP 54.117 in a gel medium: Experimental and numerical study. *Journal of Food Engineering, 116*(2), 315-323.
doi:https://doi.org/10.1016/j.jfoodeng.2012.11.030

Hamoud-Agha, M. M., Curet, S., Simonin, H., & Boillereaux, L. (2014). Holding time effect on microwave inactivation of Escherichia coli K12: Experimental and numerical investigations. *Journal of Food Engineering, 143*(Supplement C), 102-113. doi:https://doi.org/10.1016/j.jfoodeng.2014.06.043

Hitchcock, R. T. (2004). I. Physical characteristics. In *Radio-frequency and microwave radiation* (pp. 1-4). Fairfax, Va.: American Industrial Hygiene Association.

Holdsworth, S. D., & Simpson, R. (2007). *Thermal Processing of Packaged Foods*: Springer US.

Hu, X., & Mallikarjunan, P. (2005). Thermal and dielectric properties of shucked oysters. *LWT - Food Science and Technology, 38*(5), 489-494. doi:http://dx.doi.org/10.1016/j.lwt.2004.07.016

Jouquand, C., Tessier, F. J., Bernard, J., Marier, D., Woodward, K., Jacolot, P., . . . Laguerre, J.-C. (2015). Optimization of microwave cooking of beef burgundy in terms of nutritional and organoleptic properties. *LWT - Food Science and Technology, 60*(1), 271-276. doi:https://doi.org/10.1016/j.lwt.2014.07.038

Koskiniemi, C. B., Truong, V.-D., Simunovic, J., & McFeeters, R. F. (2011). Improvement of heating uniformity in packaged acidified vegetables pasteurized with a 915MHz continuous microwave system. *Journal of Food Engineering, 105*(1), 149-160. doi:http://dx.doi.org/10.1016/j.jfoodeng.2011.02.019

Kumar, C., Joardder, M. U. H., Farrell, T. W., & Karim, M. A. (2016). Multiphase porous media model for intermittent microwave convective drying (IMCD) of food. *International Journal of Thermal Sciences, 104*, 304-314. doi:https://doi.org/10.1016/j.ijthermalsci.2016.01.018

Kumar, C., Joardder, M. U. H., Karim, A., Millar, G. J., & Amin, Z. (2014). Temperature Redistribution Modelling During Intermittent Microwave Convective Heating. *Procedia Engineering, 90*, 544-549. doi:https://doi.org/10.1016/j.proeng.2014.11.770

Laguerre, J.-C., Douiri-Bédoui, I., Chireux, C., David, M., Jacolot, P., Jouquand, C., . . . gadonna-Widehem, P. (2013, 13th - 15th, November). *The iconographic correlation (CORICO) method, a new approach for the optimization of microwave cooking processes: application for cooking fish.* Paper presented at the 2013 EFFOST Annual meeting, Bologna, Italy.

Laguerre, J.-C., Gadonna-Widehem, P., Marier, D., Onillon, E., Ait-Ameur, L., & Birlouez-Aragon, I. (2011). The impact of microwave heating of infant formula model on neo-formed contaminant formation, nutrient degradation and spore destruction. *Journal of Food Engineering, 107*(2), 208-213. doi:http://dx.doi.org/10.1016/j.jfoodeng.2011.06.021

Laguerre, J.-C., Gadonna-Widehem, P., & Tessier, F. J. (2006). *Optimisation of Microwave Pasteurisation of Raw Cow's Milk using a Centro-composite Design.* Paper presented at the IUFOST, 13th World Congress of Food Sciences Technology, Nantes, France.

Laguerre, J.-C., Ratovoarisoa, L. G., Vivant, A. C., Gadonna, J. P., & Jouquand, C. (2017, 23rd - 25th, October). *An iconographic correlation method for optimizing a combined microwave/hot air drying of apple Malus domestica Sp.* Paper presented at the 19th International Conference on Food Processing & Technology, Paris, France.

Lau, M. H., & Tang, J. (2002). Pasteurization of pickled asparagus using 915 MHz microwaves. *Journal of Food Engineering, 51*(4), 283-290. doi:http://dx.doi.org/10.1016/S0260-8774(01)00069-3

Lesty, M. (1999). *User's guide CORICO Release 4.0 For Windows Training Manual*.

Lewis, M. J., & Deeth, H. C. (2009). Heat Treatment of Milk. In A. Y. Tamime (Ed.), *Milk Processing and Quality Management*.

Liao, X., Raghavan, G. S. V., Dai, J., & Yaylayan, V. A. (2003). Dielectric properties of α-d-glucose aqueous solutions at 2450 MHz. *Food Research International, 36*(5), 485-490. doi:https://doi.org/10.1016/S0963-9969(02)00196-5

Llave, Y. A., Hagiwara, T., & Sakiyama, T. (2012). Artificial neural network model for prediction of cold spot temperature in retort sterilization of starch-based foods. *Journal of Food Engineering, 109*(3), 553-560. doi:https://doi.org/10.1016/j.jfoodeng.2011.10.024

Llave, Y. A., Mori, K., Kambayashi, D., Fukuoka, M., & Sakai, N. (2016). Dielectric properties and model food application of tylose water pastes during microwave thawing and heating. *Journal of Food Engineering, 178*, 20-30. doi:https://doi.org/10.1016/j.jfoodeng.2016.01.003

Luan, D., Tang, J., Pedrow, P. D., Liu, F., & Tang, Z. (2013). Using mobile metallic temperature sensors in continuous microwave assisted sterilization (MATS) systems. *Journal of Food Engineering, 119*(3), 552-560. doi:http://dx.doi.org/10.1016/j.jfoodeng.2013.06.003

Malheiro, R., Casal, S., Ramalhosa, E., & Pereira, J. (2011). *Microwave Heating: A Time Saving Technology or a Way to Induce Vegetable Oils Oxidation?*

Malone, A. (2005). Enteral formula selection: a review of selected product categories. *Practical Gastroenterology, 29*(6), 44.

McCrae, C. H. (1999). Heat stability of milk emulsions: phospholipid–protein interactions. *International Dairy Journal, 9*(3), 227-231. doi:https://doi.org/10.1016/S0958-6946(99)00065-5

Meda, V., Orsat, V., & Raghavan, V. (2017). 2 - Microwave heating and the dielectric properties of foods. In M. Regier, K. Knoerzer, & H. Schubert (Eds.), *The Microwave Processing of Foods (Second Edition)* (pp. 23-43): Woodhead Publishing.

Mishra, S. P., Nath, G., & Mishra, P. (2018). Ultrasonically Synthesized Dielectric Microwave Absorbing Material from Coconut Coir Dust. *Waste and Biomass Valorization*. doi:10.1007/s12649-018-0478-4

Muhamad, I. I., Quin, C. H., & Selvakumaran, S. (2016). Preparation and evaluation of water-in-soybean oil–in-water emulsions by repeated premix membrane

emulsification method using cellulose acetate membrane. *Journal of Food Science and Technology, 53*(4), 1845-1855. doi:10.1007/s13197-015-2107-6

Muñoz, I., Gou, P., Picouet, P. A., Barlabé, A., & Felipe, X. (2018). Dielectric properties of milk during ultra-heat treatment. *Journal of Food Engineering, 219*, 137-146. doi:https://doi.org/10.1016/j.jfoodeng.2017.09.025

Okiror, G. P., & Jones, C. L. (2012). Effect of temperature on the dielectric properties of low acyl gellan gel. *Journal of Food Engineering, 113*(1), 151-155. doi:https://doi.org/10.1016/j.jfoodeng.2012.04.011

Peng, J., Tang, J., Jiao, Y., Bohnet, S. G., & Barrett, D. M. (2013). Dielectric properties of tomatoes assisting in the development of microwave pasteurization and sterilization processes. *LWT - Food Science and Technology, 54*(2), 367-376. doi:http://dx.doi.org/10.1016/j.lwt.2013.07.006

Pitchai, K., Chen, J., Birla, S., Gonzalez, R., Jones, D., & Subbiah, J. (2014). A microwave heat transfer model for a rotating multi-component meal in a domestic oven: Development and validation. *Journal of Food Engineering, 128*, 60-71. doi:http://dx.doi.org/10.1016/j.jfoodeng.2013.12.015

Prakash, A., Nelson, S. O., Mangino, M. E., & Hansen, P. M. T. (1992). Variation of microwave dielectric properties of hydrocolloids with moisture content, temperature and stoichiometric charge. *Food Hydrocolloids, 6*(3), 315-322. doi:https://doi.org/10.1016/S0268-005X(09)80098-2

Rahman, M. S., Perera, C. O., Chen, X. D., Driscoll, R. H., & Potluri, P. L. (1996). Density, shrinkage and porosity of calamari mantle meat during air drying in a cabinet dryer as a function of water content. *Journal of Food Engineering, 30*(1), 135-145. doi:https://doi.org/10.1016/S0260-8774(96)00013-1

Regier, M., Knoerzer, K., & Schubert, H. (2017). 1 - Introducing microwave-assisted processing of food: Fundamentals of the technology. In M. Regier, K. Knoerzer, & H. Schubert (Eds.), *The Microwave Processing of Foods (Second Edition)* (pp. 1-22): Woodhead Publishing.

Remmen, H. H. J., Ponne, C. T., Nijhuis, H. H., Bartels, P. V., & Kerkhof, P. J. A. M. (1996). Microwave Heating Distributions in Slabs, Spheres and Cylinders with Relation to Food Processing. *Journal of food science, 61*(6), 1105-1114. doi:10.1111/j.1365-2621.1996.tb10941.x

Resurreccion, F. P., Luan, D., Tang, J., Liu, F., Tang, Z., Pedrow, P. D., & Cavalieri, R. (2015). Effect of changes in microwave frequency on heating patterns of foods in a microwave assisted thermal sterilization system. *Journal of Food Engineering, 150*, 99-105. doi:http://dx.doi.org/10.1016/j.jfoodeng.2014.10.002

Roux, S., Courel, M., Birlouez-Aragon, I., Municino, F., Massa, M., & Pain, J.-P. (2016). Comparative thermal impact of two UHT technologies, continuous ohmic heating and direct steam injection, on the nutritional properties of liquid

infant formula. *Journal of Food Engineering, 179*, 36-43.
doi:https://doi.org/10.1016/j.jfoodeng.2016.02.001

Rufián-Henares, J. Á., Guerra-Hernandez, E., & García-Villanova, B. (2006). Colour
measurement as indicator for controlling the manufacture and storage of enteral
formulas. *Food Control, 17*(6), 489-493.
doi:https://doi.org/10.1016/j.foodcont.2005.02.011

Sakai, N., Mao, W., Koshima, Y., & Watanabe, M. (2005). A method for developing
model food system in microwave heating studies. *Journal of Food Engineering,
66*(4), 525-531. doi:https://doi.org/10.1016/j.jfoodeng.2004.04.025

Saravacos, G. D., & Maroulis, Z. B. (2011). *Food Process Engineering Operation*. Boca
Raton, FL: CRC Press Taylor & Francis Group.

Sosa-Morales, M. E., Valerio-Junco, L., López-Malo, A., & García, H. S. (2010).
Dielectric properties of foods: Reported data in the 21st Century and their
potential applications. *LWT - Food Science and Technology, 43*(8), 1169-1179.
doi:https://doi.org/10.1016/j.lwt.2010.03.017

Soysal, Y., Ayhan, Z., Eştürk, O., & Arıkan, M. F. (2009). Intermittent microwave–
convective drying of red pepper: Drying kinetics, physical (colour and texture)
and sensory quality. *Biosystems Engineering, 103*(4), 455-463.
doi:https://doi.org/10.1016/j.biosystemseng.2009.05.010

Swamy, G. J., & Muthukumarappan, K. (2017). Optimization of continuous and
intermittent microwave extraction of pectin from banana peels. *Food Chemistry,
220*, 108-114. doi:https://doi.org/10.1016/j.foodchem.2016.09.197

Tadros, T. (2015). Viscoelastic properties of sterically stabilised emulsions and their
stability. *Advances in Colloid and Interface Science, 222*, 692-708.
doi:https://doi.org/10.1016/j.cis.2015.03.001

Tang, Z., Mikhaylenko, G., Liu, F., Mah, J.-H., Pandit, R., Younce, F., & Tang, J.
(2008). Microwave sterilization of sliced beef in gravy in 7-oz trays. *Journal of
Food Engineering, 89*(4), 375-383.
doi:http://dx.doi.org/10.1016/j.jfoodeng.2008.04.025

Tuta, S., & Palazoğlu, T. K. (2017). Finite element modeling of continuous-flow
microwave heating of fluid foods and experimental validation. *Journal of Food
Engineering, 192*, 79-92. doi:https://doi.org/10.1016/j.jfoodeng.2016.08.003

Tzoumaki, M. V., Moschakis, T., Kiosseoglou, V., & Biliaderis, C. G. (2011). Oil-in-
water emulsions stabilized by chitin nanocrystal particles. *Food Hydrocolloids,
25*(6), 1521-1529. doi:https://doi.org/10.1016/j.foodhyd.2011.02.008

Vandresen, S., Quadri, M. G. N., Souza, J. A. R. d., & Hotza, D. (2009). Temperature effect on the rheological behavior of carrot juices. *Journal of Food Engineering, 92*(3), 269-274. doi:https://doi.org/10.1016/j.jfoodeng.2008.11.010

Venkatesh, M. S., & Raghavan, G. S. V. (2004). An Overview of Microwave Processing and Dielectric Properties of Agri-food Materials. *Biosystems Engineering, 88*(1), 1-18. doi:https://doi.org/10.1016/j.biosystemseng.2004.01.007

Wang, Y., Tang, J., Rasco, B., Kong, F., & Wang, S. (2008). Dielectric properties of salmon fillets as a function of temperature and composition. *Journal of Food Engineering, 87*(2), 236-246. doi:http://dx.doi.org/10.1016/j.jfoodeng.2007.11.034

Wang, Y., Tang, J., Rasco, B., Wang, S., Alshami, A. A., & Kong, F. (2009). Using whey protein gel as a model food to study dielectric heating properties of salmon (*Oncorhynchus gorbuscha*) fillets. *LWT - Food Science and Technology, 42*(6), 1174-1178. doi:http://dx.doi.org/10.1016/j.lwt.2009.01.005

Wäppling Raaholt, B., & Isaksson, S. (2017). 17 - Improving the heating uniformity in microwave processing. In M. Regier, K. Knoerzer, & H. Schubert (Eds.), *The Microwave Processing of Foods (Second Edition)* (pp. 381-406): Woodhead Publishing.

Wemmenhove, E., Wells-Bennik, M. H. J., Stara, A., van Hooijdonk, A. C. M., & Zwietering, M. H. (2016). How NaCl and water content determine water activity during ripening of Gouda cheese, and the predicted effect on inhibition of Listeria monocytogenes. *Journal of Dairy Science, 99*(7), 5192-5201. doi:https://doi.org/10.3168/jds.2015-10523

Xiang, B. Y., Simpson, M. V., Ngadi, M. O., & Simpson, B. K. (2011). Flow behaviour and viscosity of reconstituted skimmed milk treated with pulsed electric field. *Biosystems Engineering, 109*(3), 228-234. doi:https://doi.org/10.1016/j.biosystemseng.2011.04.004

Xiong, W., Ren, C., Tian, M., Yang, X., Li, J., & Li, B. (2018). Emulsion stability and dilatational viscoelasticity of ovalbumin/chitosan complexes at the oil-in-water interface. *Food Chemistry, 252*, 181-188. doi:https://doi.org/10.1016/j.foodchem.2018.01.067

Yanniotis, S., Skaltsi, S., & Karaburnioti, S. (2006). Effect of moisture content on the viscosity of honey at different temperatures. *Journal of Food Engineering, 72*(4), 372-377. doi:https://doi.org/10.1016/j.jfoodeng.2004.12.017

Zhang, W., Liu, F., Nindo, C., & Tang, J. (2013). Physical properties of egg whites and whole eggs relevant to microwave pasteurization. *Journal of Food Engineering, 118*(1), 62-69. doi:https://doi.org/10.1016/j.jfoodeng.2013.03.003

Zhang, W., Luan, D., Tang, J., Sablani, S. S., Rasco, B., Lin, H., & Liu, F. (2015). Dielectric properties and other physical properties of low-acyl gellan gel as

relevant to microwave assisted pasteurization process. *Journal of Food Engineering, 149*, 195-203. doi:https://doi.org/10.1016/j.jfoodeng.2014.10.014

Zheng, M., Huang, Y., Nelson, S., Bartley, P., & Gates, K. (1998). Dielectric properties and thermal conductivity of marinated shrimp and channel catfish. *Journal of food science, 63*(4), 668-672.

Appendix A Supplementary data

A.1 Chemical composition (%wb) of ingredients used in the products needed for formulation

Table A.1 Chemical composition (%wb) of ingredients

	Carbohydrates	**Protein**	**Fat**	**References**
Maltodextrin (n = 4)	92.8 ± 0.1	-	-	Experiment
Whey protein concentrate	7.39	79	5.49	Manufacturer
Whey protein isolate	0.6	89	1.3	Manufacturer
Hydrolyzed whey protein	3.2	80	1.6	Manufacturer
Coconut oil	-	-	100	Approximation
Rice bran oil	-	-	100	Approximation
Inulin	8	-	-	Manufacturer
HFCS42	70.2	-	-	Manufacturer
Soy protein isolate	0.5	86	0.5	Manufacturer

A.2 Equations for tube feeding product formulation

Nomenclature: X_1 is amount of maltodextrin (g)

X_2 is amount of soy protein isolate (g)

X_3 is amount of whey protein isolate (g)

X_4 is amount of whey protein concentrate (g)

X_5 is amount of hydrolyzed whey protein (g)

X_6 is amount of oil (g)

X_7 is amount of soy lecithin (g)

$X_{a, i}$ is weight fraction of component i in

ingredient a

(Refer to table A.1)

Where CHO is carbohydrates

Pro is protein

Fat is fat

C is caloric density (1 kcal/mL or 2.5 kcal/mL)

A.2.1 Tube feeding formula using soy protein isolate, whey protein concentrate, and whey protein isolate as protein source

Condition

1) Caloric distribution from carbohydrates: fat: protein is 50: 30: 20
2) Ratio between soy protein isolate: whey protein isolate: whey protein concentrate is 12: 3: 1
3) Concentration of lecithin is 0.75 %(w/v)

Assumption

1) Carbohydrates and protein give 4 kilocalories of energy per gram while fat gives 9 kilocalories of energy per gram
2) There is no protein and fat in maltodextrin
3) There is no carbohydrates and protein in oil
4) Lecithin gives no calories

Equations for formulation (basis: 1000 mL)

Carbohydrates: $\quad X_{1,CHO} + X_{2,CHO} + X_{3,CHO} + X_{4,CHO} = \frac{0.5C}{4}$ (A.1)

Protein: $\quad X_{2,Pro} + X_{3,Pro} + X_{4,Pro} = \frac{0.2C}{4}$ (A.2)

Fat: $\quad X_{2,Fat} + X_{3,Fat} + X_{4,Fat} + X_{6,Fat} = \frac{0.3C}{4}$ (A.3)

Protein source (1): $\quad \frac{X_2}{X_3 + X_4} = 3$ (A.4)

Protein source (2): $\quad \frac{X_3}{X_4} = 3$ (A.5)

Lecithin: $\quad X_7 = 7.5$ (A.6)

A.2.2 Tube feeding formula using soy protein isolate and hydrolyzed whey protein as protein source

Condition

1) Caloric distribution from carbohydrates: fat: protein is 50: 30: 20
2) Ratio between soy protein isolate and hydrolyzed whey protein is 3:1
3) Concentration of lecithin is 0.75 %(w/v)

Assumption

1) Carbohydrates and protein give 4 kilocalories of energy per gram while fat gives 9 kilocalories of energy per gram
2) There is no protein and fat in maltodextrin
3) There is no carbohydrates and protein in oil
4) Lecithin gives no calorie

Equations for formulation (basis: 1000 mL)

Carbohydrates: $X_{1,\,CHO} + X_{2,CHO} + X_{5,CHO} = \dfrac{0.5C}{4}$ (A.7)

Protein: $X_{2,Pro} + X_{5,Pro} = \dfrac{0.2C}{4}$ (A.8)

Fat: $X_{2,Fat} + X_{5,Fat} + X_{6,Fat} = \dfrac{0.3C}{4}$ (A.9)

Protein source: $\dfrac{X_2}{X_5} = 3$ (A.10)

Lecithin $X_7 = 7.5$ (A.11)

A.3 Equations for spoon feeding product formulation

    Nomenclature: X_1 is amount of maltodextrin (g)

    X_2 is amount of soy protein isolate (g)

    X_3 is amount of whey protein isolate (g)

    X_4 is amount of whey protein concentrate (g)

    X_5 is amount of hydrolyzed whey protein (g)

    X_6 is amount of oil (g)

    X_7 is amount of soy lecithin (g)

    X_8 is amount of HFCS42 (g)

    X_9 is amount of citric acid (g)

    X_{10} is amount of malic acid (g)

    X_{11} is amount of water (g)

    $X_{a,\,i}$ is weight fraction of component i in

    ingredient a

    (Refer to table A.1)

    Where CHO is carbohydrates

    Pro is protein

    Fat is fat

The rest variables are referred to Table 3.1 in chapter 3

Condition

    1) Acid consists of citric acid and malic acid with 1:1 by weight

Assumption

1) Carbohydrates and protein give 4 kilocalories of energy per gram while fat gives 9 kilocalories of energy per gram

2) There is no protein and fat in maltodextrin and high fructose syrup

3) There is no carbohydrates and protein in oil

4) Lecithin, malic acid, citric acid and water give no calories

Equations for formulation (basis: 1000 g)

Carbohydrates: $X_{1,CHO} + X_{2,CHO} + X_{3,CHO} + X_{4,CHO} + X_{5,CHO} + X_{8,CHO}$

$$= 2.5 \times Caldens \times (80\text{-}CalFat) \qquad (A.12)$$

Protein: $X_{2,Pro} + X_{3,Pro} + X_{4,Pro} + X_{5,Pro} = 50 \times Caldens \qquad (A.13)$

Fat : $X_{2,Fat} + X_{3,Fat} + X_{4,Fat} + X_{5,Fat} + X_{6,Fat}$

$$= \frac{10}{9} \times Caldens \times CalFat \qquad (A.14)$$

High fructose syrup: $X_{8,CHO} = 2.5 \times Caldens \times CalFS \qquad (A.15)$

Whey protein: $X_3 + X_4 = 10 \times WPconc \qquad (A.16)$

Complex whey protein: $\dfrac{X_3}{X_4} = \dfrac{WPItoWP}{(100\text{-}WPItoWP)} \qquad (A.17)$

Total protein: $\dfrac{X_3 + X_4}{X_5} = \dfrac{Hydrolyzed}{100\text{-}Hydrolyzed} \qquad (A.18)$

Lecithin: $X_7 = 10Lecithin \qquad (A.19)$

Acid (1): $X_9 + X_{10} = \dfrac{X_{8,CHO}}{FStoAcid} \qquad (A.20)$

Acid (2): $X_9 = X_{10} \qquad (A.21)$

Water: $X_{11} = 1000 - \sum_1^{10} X_i \qquad (A.22)$

A.4 Rheological data of formula proposed by IC for optimization

Table A.2 Linear Viscoelastic Range (LVR), and log value of complex viscosity at 50 Hz and 25 °C in cP of product formulated by formula proposed by IC for optimization

Trial	Before heating		After heating	
	LVR	Log viscosity	LVR	Log viscosity
1	0.5	3.43 ± 0.07	0.1	3.27 ± 0.14
2	0.05	3.59 ± 0.33	0.01	4.76 ± 0.17
3	0.1	4.33 ± 0.77	0.01	4.85 ± 0.55
4	0.5	3.13 ± 0.16	0.01	3.51 ± 0.14
5	0.1	3.58 ± 0.12	0.01	4.48 ± 0.11
6	1	3.51 ± 0.03	0.01	4.09 ± 0.01
7	0.01	3.57 ± 0.03	0.01	3.44 ± 0.04
8	0.5	4.66 ± 0.01	1	4.57 ± 0.06
9	0.5	5.09 ± 0.84	0.01	5.03 ± 1.00
10	0.05	3.96 ± 0.05	0.01	4.06 ± 0.05
11	0.01	3.60 ± 0.03	0.1	3.60 ± 0.06
12	0.05	4.43 ± 0.19	0.05	4.54 ± 0.17
13	0.01	4.37 ± 0.14	0.1	4.26 ± 0.00
14	0.01	3.17 ± 0.05	0.01	5.19 ± 0.74
15	0.01	3.08 ± 0.25	0.01	2.94 ± 0.20
16	0.01	3.13 ± 0.04	0.1	3.06 ± 0.31
17	0.01	3.39 ± 0.18	0.01	3.05 ± 0.16

A.5 Correlation analysis for log viscosity after heating
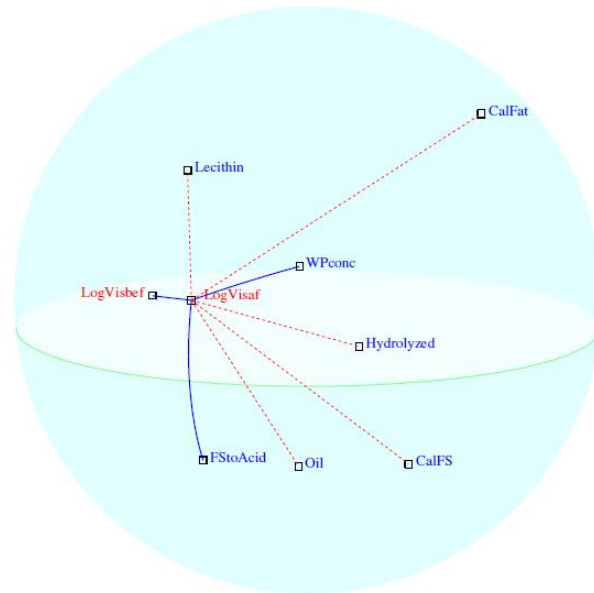
Figure A.1 CORICO sphere showing significant link (p < 0.01) with log value of
viscosity after heating (LogVisaf)

Table A.3 Pearson correlation coefficient of significant links (p < 0.01) from
correlation analysis

Variable 1	Variable 2	Pearson correlation (p < 0.01)
LogVisaf	LogVisbef	0.61
LogVisaf	FStoAcid	0.28
LogVisaf	WPconc	0.17
LogVisaf	CalFat	-0.44
LogVisaf	CalFS	-0.39
LogVisaf	Hydrolyzed	-0.32
LogVisaf	Lecithin	-0.32
LogVisaf	Oil	-0.28

A.6 Full logical models and surface plot of log viscosity after heating for high caloric density formula optimization

LogVisaf = 4.042 - 1.866 CalFS&-Caldens - 1.343 Lecithin{Lecithin

+ 1.101 Caldens{-Hydrolyzed - 0.4715 Caldens]CalFat

− 0.4651 Oil}Hydrolyzed + 0.7777 CalFS#-WPItoWP

+ 0.5464 CalFat*CalFS + 0.1349E-02 Lecithin^WPconc

- 0.4379 Lecithin{WPItoWP + 0.4287 Lecithin^WPItoWP

R^2_{adj} = 0.99   (A.23)
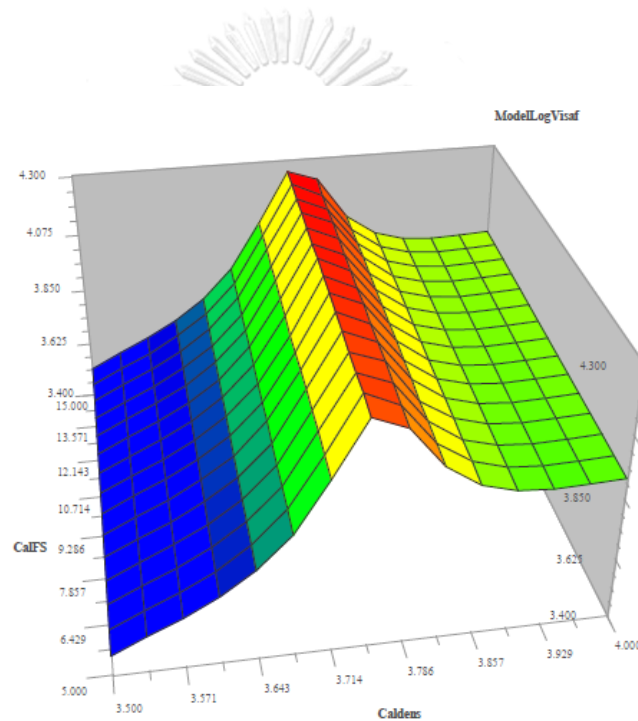
Figure A.2 3D response surface for logarithm of viscosity after heating (ModelLogvisaf) with caloric density (Caldens) in kcal/g and calorie from high fructose syrup (CalFS) in %

A.7 Validation of optimized formula including data from log viscosity after heating

Table A.4 Predicted value using IC method compared with experimental data (n = 3) of each response for formula for each oil

Response*	Predicted value	Experimental data (n = 3)
Formula with Coconut oil		
Logvisbef	3.23	2.90 ± 0.01
Logvisaf	3.18	3.10 ± 0.08
Emul_Sep	0.15	Not detected
Formula with rice bran oil		
Logvisbef	3.30	3.33 ± 0.00
Logvisaf	3.24	3.22 ± 0.04
Emul_Sep	0.01	Not detected

*Logvisbef and Logvisaf is log value of viscosity before and after heating, respectively.

A.8 Recipe for all formula selected for further investigation

Table A.5 Condition for each tube feeding formula

Formula	Protein*	Oil	Fiber addition	Caloric density (kcal/mL)
1	Hydrolyzed	Coconut	No	1
2	Hydrolyzed	Coconut	No	2.5
3	Hydrolyzed	Coconut	Yes	1
4	Hydrolyzed	Coconut	Yes	2.5
5	Hydrolyzed	Rice bran	No	1
6	Hydrolyzed	Rice bran	No	2.5
7	Hydrolyzed	Rice bran	Yes	1
8	Hydrolyzed	Rice bran	Yes	2.5
9	Whey	Coconut	No	1
10	Whey	Coconut	No	2.5
11	Whey	Coconut	Yes	1
12	Whey	Coconut	Yes	2.5
13	Whey	Rice bran	No	1
14	Whey	Rice bran	No	2.5
15	Whey	Rice bran	Yes	1
16	Whey	Rice bran	Yes	2.5

*Hydrolyzed and Whey means hydrolyzed whey protein and mixture of whey protein concentrate and whey protein isolate

Table A.6 Composition of each tube feeding formula (Basis: 1000 mL)

Formula	Amount of ingredients (g)								
	MD	**SPI**	**WPI**	**WPC**	**HP**	**CCO**	**RBO**	**Inulin**	**Lecithin**
1	133.20	54.32	-	-	18.11	32.21	-	-	7.50
2	332.99	135.80	-	-	45.27	80.53	-	-	7.50
3	132.33	54.32	-	-	18.11	32.21	-	10.00	7.50
4	332.13	135.80	-	-	45.27	80.53	-	10.00	7.50
5	133.20	54.32	-	-	18.11	-	32.21	-	7.50
6	332.99	135.80	-	-	45.27	-	80.53	-	7.50
7	132.33	54.32	-	-	18.11	-	32.21	10.00	7.50
8	332.13	135.80	-	-	45.27	-	80.53	10.00	7.50
9	133.58	42.33	10.68	3.43	-	32.79	-	-	7.50
10	333.94	105.83	26.70	8.58	-	81.99	-	-	7.50
11	132.71	42.33	10.68	3.43	-	32.79	-	10.00	7.50
12	333.08	105.83	26.70	8.58	-	81.99	-	10.00	7.50
13	133.58	42.33	10.68	3.43	-	-	32.79	-	7.50
14	333.94	105.83	26.70	8.58	-	-	81.99	-	7.50
15	132.71	42.33	10.68	3.43	-	-	32.79	10.00	7.50
16	333.08	105.83	26.70	8.58	-	-	81.99	10.00	7.50

*MD, SPI, WPI, WPC, HP, CCO, and RBO means maltodextrin, soy protein isolate, whey protein isolate, whey protein concentrate, hydrolyzed whey protein, coconut oil, and rice bran oil, respectively

Table A.7 Condition for each spoon-feeding formula

Formula	Oil	Fiber addition	Caloric density (kcal/g)
1	Coconut	No	3.89
2	Rice bran	No	3.58
3	Coconut	Yes	3.89
4	Rice bran	Yes	3.58

Table A.8 Composition of each spoon-feeding formula (Basis: 1000 g)

Formula	MD	SPI	WPI	WPC	HP	CCO	RBO	HFCS42	Inulin	Lecithin	Citric acid	Malic acid	Water
1	58.37	127.41	47.69	9.74	38.10	253.43	-	200.20	-	8.20	0.545	0.545	255.78
2	139.52	112.59	33.88	19.22	41.81	-	207.60	150.56	-	7.72	0.182	0.182	286.75
3	58.37	127.41	47.69	9.74	38.10	253.43	-	200.20	10.00	8.20	0.545	0.545	245.78
4	139.52	112.59	33.88	19.22	41.81	-	207.60	150.56	10.00	7.72	0.182	0.182	276.75

*MD, SPI, WPI, WPC, HP, CCO, and RBO means maltodextrin, soy protein isolate, whey protein isolate, whey protein concentrate, hydrolyzed whey protein, coconut oil, and rice bran oil, respectively.

A.9 Other responses of formula heated with different heating time and specific power assigned by Doehlert matrix

Table A.9 Microwave heating conditions with doehert matrix arrangement and other responses from Table 4.1

Trial	Time (s)	Specific power (W/mL)	5-Percentile of bottom surface temperature (°C)	Standard deviation of bottom surface temperature (°C)	Lysine (mg/g)	Carboxymethyllysine (µg/g)
Before heating	-	-	28.4	28.4	4.04 ± 0.22	7.61 ± 0.43
1	60	5	53.5 ± 1.3	6.25 ± 0.21	3.79 ± 0.11	7.61 ± 0.28
2	54	7	59.4 ± 1.6	8.80 ± 0.30	3.93 ± 0.24	7.88 ± 0.12
3	41	7	54.1 ± 1.1	6.65 ± 0.29	3.21 ± 0.10	7.04 ± 0.17
4	35	5	45.1 ± 1.1	4.92 ± 0.25	3.23 ± 0.20	7.12 ± 0.21
5	41	3	41.3 ± 1.2	3.62 ± 0.21	3.98 ± 0.09	7.81 ± 0.15
6	54	3	43.8 ± 1.6	4.36 ± 0.29	4.02 ± 0.08	7.43 ± 0.16
7	48	5	51.9 ± 0.6	6.27 ± 0.19	3.83 ± 0.09	7.56 ± 0.22
8	48	5	49.9 ± 1.1	6.06 ± 0.22	3.77 ± 0.07	7.43 ± 0.19
9	48	5	52.2 ± 0.6	5.63 ± 0.40	3.26 ± 0.04	7.18 ± 0.08

A.10 Model and its regression analysis from response surface methodology of other responses

Nomenclature: Refer to Equation 4.4

Table A.10 Coefficient of model proposed by response surface methodology for other responses

Response	a_0	a_1	a_2	a_{12}	a_{11}	a_{22}	R^2_{adj}
5-Percentile of bottom surface temperature (°C)	51.18	4.03	8.28	1.54	-1.90	-1.38	0.98
Standard deviation of bottom surface temperature (°C)	5.95	0.92	2.17	0.79	-0.36	0.01	0.91
Lysine (mg/g)	3.79	0.31	-0.25	0.38	-0.28	0.10	0.98
Carboxymethyllysine (µg/g)	7.49	0.24	-0.09	0.68	-0.12	0.12	0.96

Table A.11 Regression analysis for other responses

Response	RSM model			IC model		
	Slope	Y-intercept	R	Slope	Y-intercept	R
5-Percentile of bottom surface temperature (°C)	0.988	0.610	0.994	0.888	0.652	0.866
Standard deviation of bottom surface temperature (°C)	0.968	0.188	0.994	0.949	2.55	0.991
Lysine (mg/g)	0.991	0.033	0.996	-0.008	3.76	-0.011
Carboxymethyl-lysine (µg/g)	0.985	0.111	0.993	0.923	0.557	0.974

A.11 Full logical models of other responses in microwave heating optimization

A.11.1 Model for 5-percentile of bottom surface temperature

ModelP5_Temp = 50.1327 + 0.0276 Time*SpecPower - 0.3210 Time*Time

+ 1.1659 SpecPow]SpecPower + 14.056 Time+SpecPower

- 3.639 Time&-SpecPower + 3.0185 Time{-Time

R^2_{adj} = 0.95   (A.24)

A.11.2 Model for standard deviation of bottom surface temperature

ModelSD_Temp = 5.84 + 3.68 Time&SpecPower + 1.36 SpecPow&-Time

R^2_{adj} = 0.94   (A.25)

A.11.3 Model for Lysine content

ModelLysine = 3.7289 - 0.8179 SpecPow&-Time + 0.2890 Time*Time

+ 0.1948 SpecPow]SpecPower R^2_{adj} = 0.98   (A.26)

A.11.4 Model for carboxymethyllysine content

ModelCML = 7.4867 + 0.6299 Time]SpecPower - 0.2442 Time^SpecPower

- 0.1654 Time*SpecPower - 0.1248 SpecPow{-SpecPower

+ 0.1282 Time&-Time R^2_{adj} = 0.96   (A.27)

A.12 Surface plots of other responses

A.12.1 5-Percentile of bottom surface temperature

(a)

(b)
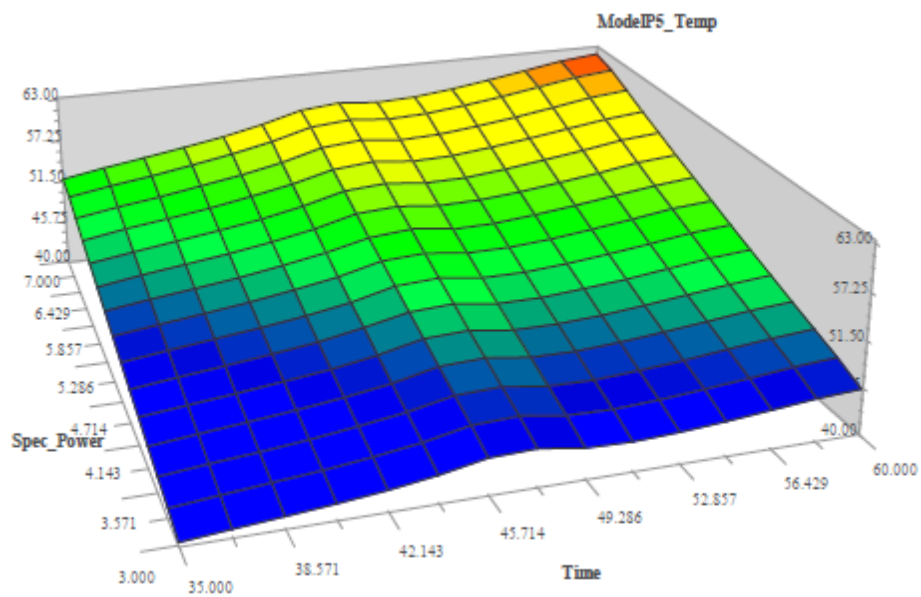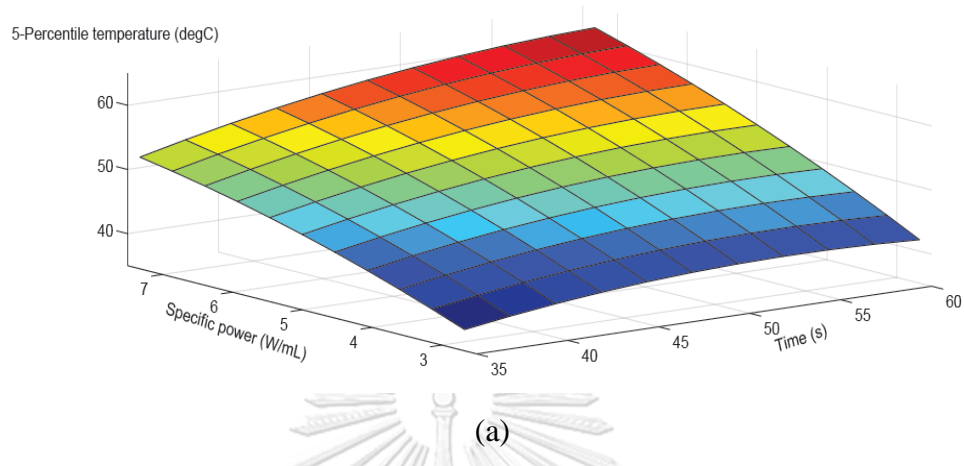
Figure A.3 3D response surface by RSM (a) and IC (b) for 5-Percentile of bottom surface temperature (°C) with heating time (s) and specific power (W/mL)

A.12.2 Standard deviation of bottom surface temperature

(a)
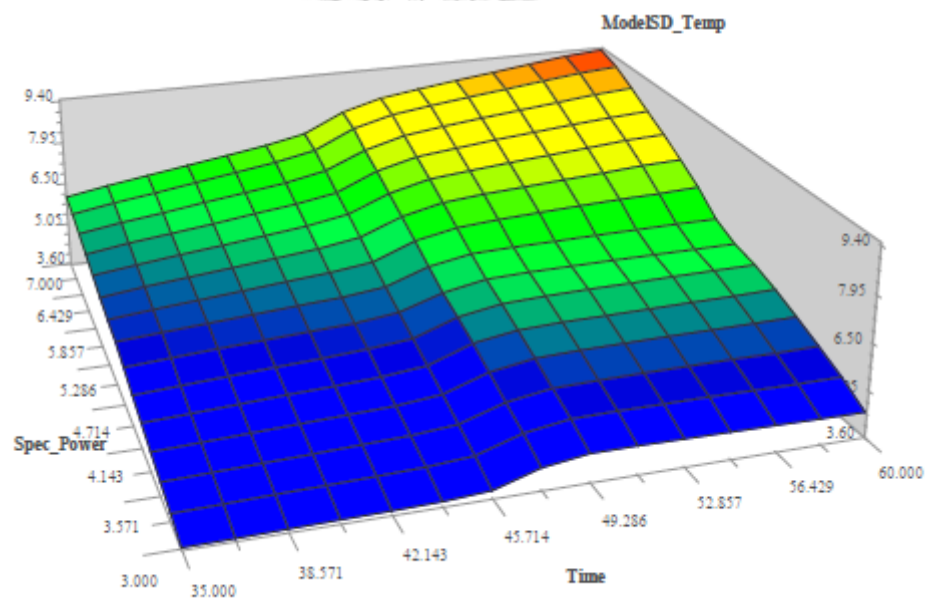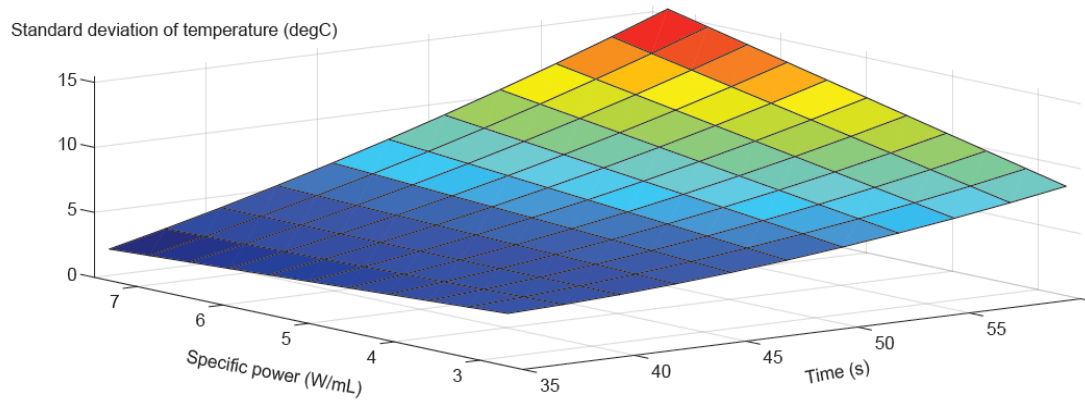
(b)

Figure A.4 3D response surface by RSM (a) and IC (b) for standard deviation of bottom surface temperature (°C) with heating time (s) and specific power (W/mL)

A.12.3 Lysine content

(a)

(b)
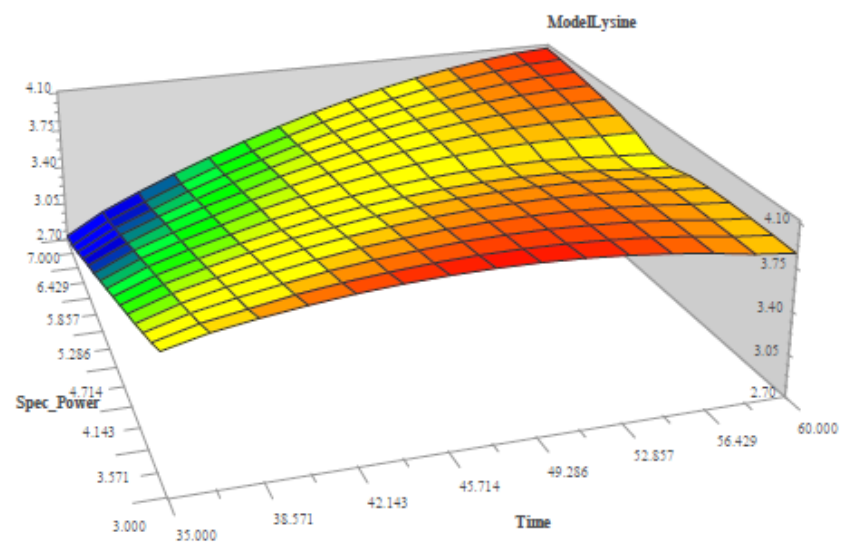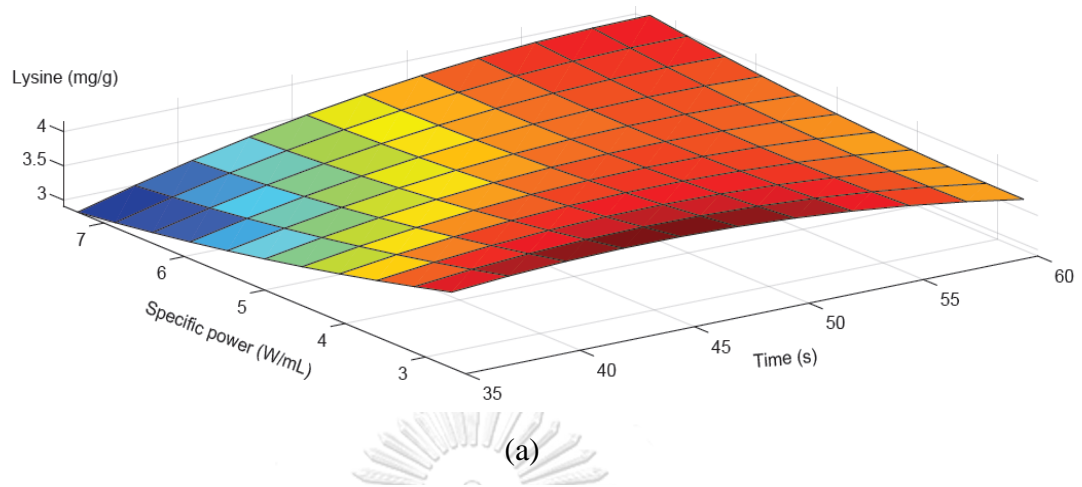
Figure A.5 3D response surface by RSM (a) and IC (b) for lysine content (mg/g) with heating time (s) and specific power (W/mL)

A.12.4 Carboxymethyllysine content

(a)
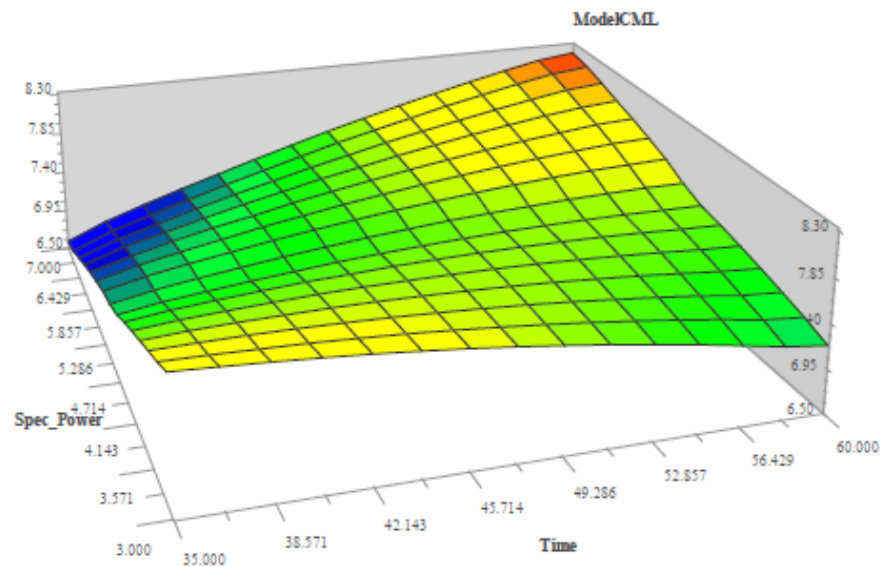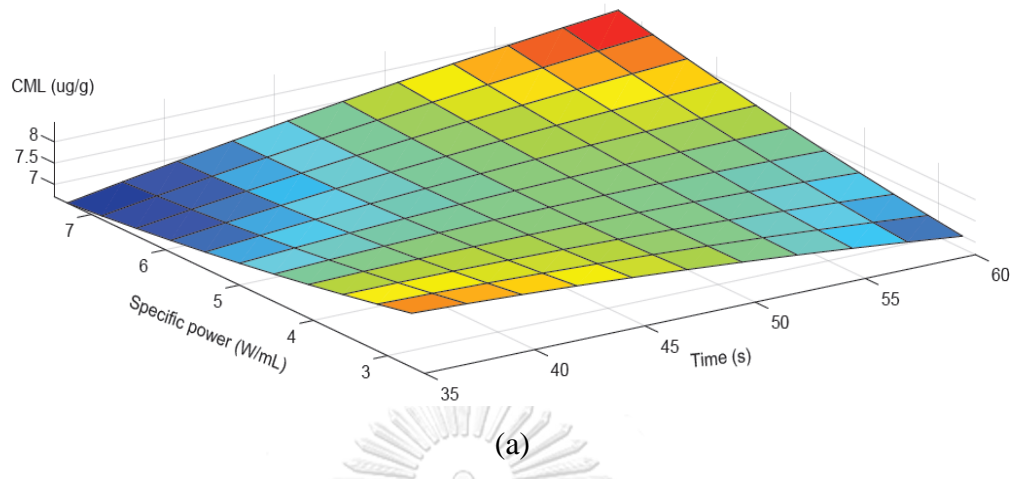
(b)

Figure A.6 3D response surface by RSM (a) and IC (b) for carboxymethyllysine content (µg/g) with heating time (s) and specific power (W/mL)

A.13 Validation of optimal heating condition including data from other responses

Table A.12 Predicted value compared with experimental data of other response

Response	Optimal condition proposed by RSM (heating at 5 W/mL for 45 s)			Optimal condition proposed by IC (heating at 5.67 W/mL for 45 s)		
	Experimental value (n = 3)	Predicted value by RSM	Predicted value by IC	Experimental value (n = 3)	Predicted value by RSM	Predicted value by IC
5-Percentile of bottom surface temperature (°C) [%deviation]	50.7 ± 1.0	50.3 [-0.79%]	49.6 [-2.17%]	52.1 ± 0.5	52.5 [+0.77%]	51.9 [-0.38%]
Standard deviation of bottom surface temperature (°C) [%deviation]	5.27 ± 0.17	5.75 [+9.1%]	5.66 [+7.4%]	5.67 ± 0.17	6.33 [+11.64]	6.22 [+9.7%]
Lysine (mg/g) [%deviation]	3.32 ± 0.12	3.71 [+11.7%]	3.71 [+11.7%]	3.56 ± 0.07	3.63 [+1.97%]	3.62 [+1.69%]
CML (µg/g) [%deviation]	8.41 ± 0.27	7.43 [-11.7%]	7.44 [-11.5%]	8.90 ± 0.22	7.38 [-17.1%]	7.46 [-16.2%]

A.14 Viscosity data of chosen formulas for microwave heating simulation

Table A.13 Viscosity (cP) of 2.5 kcal/mL formula chosen for microwave heating simulation at various temperature (°C) and shear rate (s⁻¹) (downward curve)

Temperature (°C)	Replicate	Shear rate (s^{-1})									
		220	130.9	79.02	47.43	28.42	19.93	10.2	6.116	3.652	2.2
30	1	1180	1280	1350	1300	1400	1730	1750	1360	3190	4790
	2	636	626	615	477	437	467	-	-	-	-
	3	1040	1110	1160	1120	1120	1370	1060	1270	2940	4030
37.5	1	924	999	1050	989	1050	1060	1120	1120	3060	4640
	2	478	466	474	315	285	285	-	-	-	-
	3	815	868	903	833	843	1050	663	762	2150	4030
45	1	724	764	814	760	835	1070	782	998	2880	4640
	2	354	345	358	191	164	167	-	-	-	-
	3	644	690	719	659	620	863	728	562	2090	3270
52.5	1	614	639	686	627	691	946	989	762	3000	4740
	2	288	279	294	117	82	200	-	-	-	-
	3	538	558	588	524	538	790	695	598	2000	3480
60	1	483	506	568	482	562	835	619	744	2300	3630
	2	233	228	247	77.2	72.4	172	-	-	273	403
	3	413	424	460	369	410	657	739	526	1610	3170

Table A.14 Viscosity (cP) of 3.78 kcal/g formula chosen for microwave heating simulation at various temperature (°C) and shear rate (s^{-1}) (downward curve)

Temperature (°C)	Replicate	Shear rate (s^{-1})									
		220	130.9	79.02	47.43	28.42	19.93	10.2	6.116	3.652	2.2
30	1	1220	1380	1520	1570	1550	1700	1310	1410	2580	3930
	2	1100	1280	1460	1530	1590	1770	1900	1920	3130	5550
37.5	1	1010	1120	1210	1150	1190	1450	869	725	1790	2420
	2	929	1060	1180	1190	1260	1440	1580	1320	3060	3780
45	1	831	921	983	910	976	1000	652	471	1850	2420
	2	703	790	879	861	825	1170	1080	1170	3000	5090
52.5	1	685	742	807	758	769	835	484	272	1480	1610
	2	608	677	751	744	792	963	989	1070	2120	3730
60	1	565	606	658	634	671	684	250	54.4	1300	1610
	2	516	579	650	624	718	907	859	871	2370	3730

A.15 Parameters for bingham model of each formula at each temperature and its correlation coefficient

Table A.15 Parameters for bingham model of 2.5 kcal/mL formula at each temperature and its correlation coefficient

Temperature (°C)	Yield stress (mPa)	Consistency index (mPa·s)	R^2
30	7561	802	0.85
37.5	7628	505	0.85
45	7317	359	0.84
52.5	7848	255	0.86
60	6468	199	0.90

Table A.16 Parameters for bingham model of 3.78 kcal/g formula at each temperature and its correlation coefficient

Temperature (°C)	Yield stress (mPa)	Consistency index (mPa·s)	R^2
30	7056	1261	0.90
37.5	4499	1068	0.79
45	4342	808	0.78
52.5	2758	717	0.77
60	3091	594	0.69

A.16 Experimental microwave power at maximum heating of each formula

Nomenclature: PI is incident microwave power

PR is reflected microwave power

Table A.17 Experimental microwave power for continuous heating of 1 kcal/mL
formula at 450 W for 105 s

Time (s)	Replicate 1		Replicate 2		Replicate 3	
	PI (W)	PR (W)	PI (W)	PR (W)	PI (W)	PR (W)
3	498	154	N/A	N/A	517	203
6	498	139	N/A	N/A	524	200
9	490	152	N/A	N/A	522	199
12	485	137	N/A	N/A	517	198
15	488	127	N/A	N/A	515	190
18	490	127	N/A	N/A	520	188
21	488	125	N/A	N/A	517	181
24	478	117	N/A	N/A	512	181
27	476	112	N/A	N/A	507	168
30	478	112	N/A	N/A	512	173
33	485	107	N/A	N/A	512	161
36	483	111	N/A	N/A	507	168
39	478	107	N/A	N/A	505	155
42	473	102	N/A	N/A	510	163
45	473	105	N/A	N/A	510	157
48	480	100	N/A	N/A	507	164
51	480	107	N/A	N/A	505	157
54	473	100	N/A	N/A	512	167
57	473	104	N/A	N/A	512	156
60	483	100	N/A	N/A	507	170
63	480	105	N/A	N/A	510	159
66	471	96	N/A	N/A	517	173
69	468	100	N/A	N/A	515	163
72	483	93	N/A	N/A	510	171
75	483	102	N/A	N/A	507	165
78	476	100	N/A	N/A	515	162
81	471	100	N/A	N/A	515	175
84	478	103	N/A	N/A	517	164
87	488	102	N/A	N/A	515	181
90	485	106	N/A	N/A	512	182
93	478	100	N/A	N/A	517	177
96	478	104	N/A	N/A	520	183
99	488	92	N/A	N/A	520	178
102	483	96	N/A	N/A	510	162
105	478	91	N/A	N/A	507	173

Table A.18 Experimental microwave power for continuous heating of 2.5 kcal/mL formula at 450 W for 75 s

Time (s)	Replicate 1		Replicate 2		Replicate 3	
	PI (W)	PR (W)	PI (W)	PR (W)	PI (W)	PR (W)
3	451	151	449	14	461	83
6	449	108	446	9	466	85
9	446	121	446	8	456	73
12	446	83	449	8	458	75
15	444	75	449	6	461	67
18	446	51	446	6	456	66
21	449	57	449	8	454	59
24	446	34	446	11	449	51
27	446	46	449	12	444	42
30	444	37	449	12	441	41
33	446	52	446	9	441	37
36	446	46	446	8	439	39
39	446	24	449	8	439	39
42	446	18	446	6	441	44
45	449	14	446	6	444	38
48	449	13	449	4	441	38
51	441	14	446	4	444	25
54	446	0	449	4	444	21
57	449	0	446	3	446	14
60	446	0	446	2	449	13
63	446	0	449	2	446	12
66	446	0	449	2	446	8
69	449	0	449	5	449	6
72	446	0	449	7	446	4
75	449	0	385	391	446	2

Table A.19 Experimental microwave power for continuous heating of 3.78 kcal/g
formula at 450 W for 60 s

Time (s)	Replicate 1		Replicate 2		Replicate 3	
	PI (W)	PR (W)	PI (W)	PR (W)	PI (W)	PR (W)
3	449	0	449	3	446	20
6	446	0	444	1	446	13
9	449	0	446	1	449	12
12	449	0	449	0	446	9
15	449	0	449	0	446	9
18	446	0	449	0	446	9
21	446	0	449	0	446	8
24	449	0	446	0	446	8
27	446	0	446	0	449	8
30	446	0	449	0	446	8
33	446	0	446	0	446	8
36	449	0	446	0	446	8
39	446	0	446	0	446	8
42	446	0	446	0	449	8
45	446	0	449	0	446	8
48	446	0	449	0	449	9
51	446	2	449	2	449	9
54	446	3	446	3	449	9
57	446	12	449	5	446	10
60	446	24	446	10	446	12

Table A.20 Experimental microwave power for continuous heating of 1 kcal/mL
formula at 850 W for 45 s

Time (s)	Replicate 1		Replicate 2	
	PI (W)	PR (W)	PI (W)	PR (W)
3	935	300	932	342
6	937	318	939	344
9	937	318	942	347
12	935	310	942	347
15	937	321	944	335
18	939	309	939	338
21	935	323	935	313
24	935	319	937	319
27	932	308	925	288
30	932	301	913	291
33	920	276	925	287
36	903	260	935	293
39	900	237	925	273
42	913	239	905	246
45	910	222	935	250

Table A.21 Experimental microwave power for intermittent heating of 2.5 kcal/mL
formula at 450 W for 150 s with 3 cycles of 1:1 heating time and tempering time

Time (s)	Replicate 1		Replicate 2		Replicate 3		Replicate 4	
	PI (W)	PR (W)	PI (W)	PR (W)	PI (W)	PR (W)	PI (W)	PR (W)
3	449	33	446	43	454	46	449	59
6	449	30	446	40	449	38	449	56
9	444	21	449	35	446	30	444	48
12	449	20	449	33	446	23	444	32
15	446	14	449	31	444	18	446	21
18	449	13	446	36	446	18	444	18
21	449	12	449	45	449	22	446	26
24	449	11	458	51	446	25	446	36
27	0	0	0	0	0	0	0	0
48	0	0	0	0	0	0	0	0
53	449	13	449	28	446	16	446	41
56	449	6	451	41	446	17	449	15
59	446	6	451	46	449	23	446	33
62	449	7	451	44	446	22	446	36
65	449	7	446	38	446	18	446	39
68	449	10	449	31	446	17	446	34
71	449	12	446	31	449	13	446	29
74	449	12	449	31	449	9	446	25
77	0	0	0	0	0	0	0	0
98	0	0	0	0	0	0	0	0
102	446	6	446	31	449	13	446	24
105	446	14	446	41	446	17	446	21
108	446	13	444	52	446	12	446	24
111	446	13	444	56	446	8	449	22
114	446	9	446	36	446	8	446	24
117	446	6	446	20	446	8	449	20
120	446	4	449	17	444	17	449	14
123	446	4	520	370	446	18	446	13
126	0	0	0	0	0	0	0	0
150	0	0	0	0	0	0	0	0

Appendix B Statistical results

B.1 Correlation analysis and model regression by Iconographic Correlation for log viscosity before heating

Table B.1 Correlation analysis for log viscosity before heating (1)

1	1 Oil	LogVisbef	0.163
3	3 Caldens	LogVisbef	0.643
6	6 CalFat	LogVisbef	-0.687
13	13 Oil*WPconc	LogVisbef	-0.710 Oil*WPconc
13	13 CalFat]Oil	LogVisbef	-0.723 CalFat]Oil
13	13 CalFat]WPconc	LogVisbef	-0.813 CalFat]WPconc
13	13 Caldens&-Hydrolyzed	LogVisbef	0.813 Caldens&-Hydrolyzed
13	13 Caldens-CalFat	LogVisbef	0.841 Caldens-CalFat

   1 13 jmax = 13, comax = 0.84095 Caldens-CalFat

Table B.2 Correlation analysis for log viscosity before heating (2)

1	1 Oil	LogVisbef	-0.102
2	2 Lecithin	LogVisbef	-0.189
4	4 FStoAcid	LogVisbef	0.226
5	5 Hydrolyzed	LogVisbef	-0.432
14	14 Caldens*Hydrolyzed	LogVisbef	0.493 Caldens*Hydrolyzed
14	14 Hydroly*Hydrolyzed	LogVisbef	-0.756 Hydrolyzed*Hydrolyze

   2 14 jmax = 14, comax = -0.75567 Hydroly*Hydrolyzed

Table B.3 Correlation analysis for log viscosity before heating (3)

1	1 Oil	LogVisbef	-0.111
2	2 Lecithin	LogVisbef	-0.203
4	4 FStoAcid	LogVisbef	0.456
15	15 Caldens*Hydrolyzed	LogVisbef	0.480 Caldens*Hydrolyzed
15	15 FStoAci*Hydrolyzed	LogVisbef	0.489 FStoAcid*Hydrolyzed
15	15 CalFS*WPconc	LogVisbef	0.619 CalFS*WPconc
15	15 WPconc]CalFS	LogVisbef	-0.670 WPconc]CalFS

   3 15 jmax = 15, comax = -0.66999 WPconc]CalFS

Table B.4 Correlation analysis for log viscosity before heating (4)

1	1 Oil	LogVisbef	-0.182
4	4 FStoAcid	LogVisbef	0.572
16	16 Lecithi*WPconc	LogVisbef	0.583 Lecithin*WPconc
16	16 CalFS*WPItoWP	LogVisbef	0.747 CalFS*WPItoWP

   4 16 jmax = 16, comax = 0.74730 CalFS*WPItoWP

Table B.5 Correlation analysis for log viscosity before heating (5)

1	1 Oil	LogVisbef	-0.085
2	2 Lecithin	LogVisbef	0.146
3	3 Caldens	LogVisbef	0.357
17	17 Oil*WPconc	LogVisbef	-0.470 Oil*WPconc
17	17 FStoAci]-Lecithin	LogVisbef	0.483 FStoAcid]-Lecithin
17	17 Caldens{Lecithin	LogVisbef	0.491 Caldens{Lecithin
17	17 Hydroly{Lecithin	LogVisbef	0.503 Hydrolyzed{Lecithin
17	17 Hydroly{Caldens	LogVisbef	0.513 Hydrolyzed{Caldens
17	17 Caldens{-Hydrolyzed	LogVisbef	0.547 Caldens{-Hydrolyzed
17	17 Hydroly{-Hydrolyzed	LogVisbef	0.574 Hydrolyzed{-Hydrolyz

$\quad$ 5 17 jmax = 17, comax =   0.57379   Hydroly{-Hydrolyzed

Table B.6 Correlation analysis for log viscosity before heating (6)

1	1 Oil	LogVisbef	-0.099
2	2 Lecithin	LogVisbef	0.125
3	3 Caldens	LogVisbef	0.383
4	4 FStoAcid	LogVisbef	0.422
18	18 Lecithi*WPconc	LogVisbef	0.502 Lecithin*WPconc
18	18 Caldens]CalFS	LogVisbef	0.548 Caldens]CalFS
18	18 Caldens^FStoAcid	LogVisbef	0.601 Caldens^FStoAcid

$\quad$ 6 18 jmax = 18, comax =   0.60058   Caldens^FStoAcid

Table B.7 Correlation analysis for log viscosity before heating (7)

1	1 Oil	LogVisbef	-0.153
4	4 FStoAcid	LogVisbef	0.156
5	5 Hydrolyzed	LogVisbef	0.176
19	19 Oil*Lecithin	LogVisbef	0.311 Oil*Lecithin
19	19 Lecithi*Lecithin	LogVisbef	-0.331 Lecithin*Lecithin
19	19 Caldens*Hydrolyzed	LogVisbef	0.349 Caldens*Hydrolyzed
19	19 Hydroly]-Caldens	LogVisbef	0.378 Hydrolyzed]-Caldens
19	19 Caldens^Hydrolyzed	LogVisbef	0.390 Caldens^Hydrolyzed
19	19 Lecithi!WPconc	LogVisbef	-0.414 Lecithin!WPconc
19	19 Caldens#-Hydrolyzed	LogVisbef	0.422 Caldens#-Hydrolyzed
19	19 Lecithi}Caldens	LogVisbef	0.440 Lecithin}Caldens
19	19 WPconc}Hydrolyzed	LogVisbef	-0.449 WPconc}Hydrolyzed
19	19 WPconc}CalFat	LogVisbef	-0.463 WPconc}CalFat
19	19 Caldens{Lecithin	LogVisbef	0.474 Caldens{Lecithin
19	19 Caldens{CalFat	LogVisbef	0.476 Caldens{CalFat
19	19 Hydroly{Lecithin	LogVisbef	0.477 Hydrolyzed{Lecithin
19	19 Caldens{-Oil	LogVisbef	0.552 Caldens{-Oil

$\quad$ 7 19 jmax = 19, comax =   0.55214   Caldens{-Oil

Table B.8 Correlation analysis for log viscosity before heating (8)

1	1 Oil	LogVisbef	0.061
2	2 Lecithin	LogVisbef	-0.122
4	4 FStoAcid	LogVisbef	0.164
5	5 Hydrolyzed	LogVisbef	0.220
20	20 Oil*Lecithin	LogVisbef	0.306 Oil*Lecithin
20	20 Lecithi*Lecithin	LogVisbef	-0.407 Lecithin*Lecithin
20	20 Caldens*Hydrolyzed	LogVisbef	0.431 Caldens*Hydrolyzed
20	20 Hydroly]-Caldens	LogVisbef	0.469 Hydrolyzed]-Caldens
20	20 Caldens^Hydrolyzed	LogVisbef	0.485 Caldens^Hydrolyzed

8 20 jmax = 20, comax =   0.48479   Caldens^Hydrolyzed

Table B.9 Correlation analysis for log viscosity before heating (9)

1	1 Oil	LogVisbef	-0.024
2	2 Lecithin	LogVisbef	-0.106
21	21 Oil*Lecithin	LogVisbef	0.330 Oil*Lecithin
21	21 WPconc&-WPconc	LogVisbef	-0.337 WPconc&-WPconc
21	21 WPItoWP&-WPItoWP	LogVisbef	-0.338 WPItoWP&-WPItoWP
21	21 Lecithi!WPconc	LogVisbef	-0.344 Lecithin!WPconc
21	21 WPconc!WPconc	LogVisbef	-0.367 WPconc!WPconc
21	21 WPconc}Hydrolyzed	LogVisbef	-0.372 WPconc}Hydrolyzed
21	21 WPconc}CalFat	LogVisbef	-0.376 WPconc}CalFat
21	21 Caldens{CalFat	LogVisbef	0.425 Caldens{CalFat
21	21 Hydroly{-WPconc	LogVisbef	0.437 Hydrolyzed{-WPconc

9 21 jmax = 21, comax =   0.43717   Hydroly{-WPconc

Table B.10 Correlation analysis for log viscosity before heating (10)

1	1 Oil	LogVisbef	-0.036
2	2 Lecithin	LogVisbef	-0.167
22	22 Oil*Lecithin	LogVisbef	0.321 Oil*Lecithin
22	22 Oil*CalFat	LogVisbef	0.399 Oil*CalFat
22	22 WPconc&-Wpconc	LogVisbef	-0.431 WPconc&-WPconc

10 22 jmax = 22, comax = -0.43124   WPconc&-WPconc

Minimiser SEP

    10 régresseurs pour ModelLogVisbef modèle de LogVisbef   sur
    17 observations

Table B.11 Quality of models for log value of viscosity proposed by CORICO
program with different number of factors

1 regresseurs => F= 36.23	R^2_{adj} = 0.6877	Q^2 = 0.6798	SEP= 0.3524
2 regresseurs => F= 48.41	R^2_{adj} = 0.8556	Q^2 = 0.8295	SEP= 0.2662
3 regresseurs => F= 60.44	R^2_{adj} = 0.9177	Q^2 = 0.9002	SEP= 0.2113
4 regresseurs => F= 113.2	R^2_{adj} = 0.9656	Q^2 = 0.9605	SEP= 0.1385
5 regresseurs => F= 113.2	R^2_{adj} = 0.9723	Q^2 = 0.9532	SEP= 0.1574
6 regresseurs => F= 116.2	R^2_{adj} = 0.9774	Q^2 = 0.9588	SEP= 0.1548
7 regresseurs => F= 125.3	R^2_{adj} = 0.9819	Q^2 = 0.9568	SEP= 0.1671
8 regresseurs => F= 262.2	R^2_{adj} = 0.9924	Q^2 = 0.9875	SEP= 0.9548E-01
9 regresseurs => F= 243.3	R^2_{adj} = 0.9927	Q^2 = 0.9797	SEP= 0.1299
10 regresseurs => F= 387.9	R^2_{adj} = 0.9959	Q^2 = 0.9880	SEP= 0.1080

SEPmin 0.1384514 , pour 4 régresseurs
Coefficients de la régression de LogVisbef

Table B.12 Correlation of the model proposed by CORICO program for log value of
viscosity before heating

	Coefficient	Definition
0	3.765990913824	Constante
1	2.136904052078 Caldens-CalFat	Caldens – CalFat
2	-0.877740901948 Hydroly*Hydrolyzed	Hydrolyzed ou exclusif Hydrolyzed
3	-0.615837714447 WPconc]CalFS	WPconc si CalFS
4	0.493510300869 CalFS*WPItoWP	CalFS ou exclusif WPItoWP

LogVisbef = 3.766 + 2.137 Caldens-CalFat - 0.8777 Hydroly*Hydrolyzed
- 0.6158 WPconc]CalFS + 0.4935 CalFS*WPItoWP   (B.1)

ModelLogVisbef
TABLEAU D'ANALYSE DES COEFFICIENTS

Table B.13 Analysis of coefficient of model in Equation B.1

	Coefficient	Difference	t-value	Interaction
1	2.1369	0.1169	18.2754	Caldens-CalFat
2	-0.8777	0.1136	-7.7283	Hydroly*Hydrolyzed
3	-0.6158	0.1166	-5.2801	WPconc]CalFS
4	0.4935	0.1129	4.3703	CalFS*WPItoWP

16 a le + grand levier: 0.5365745
Coefficient de corrélation R : 0.9870090
Coefficient de détermination R^2 : 0.9741868
R^2 ajusté R^2_{adj} : 0.9655824
R^2 prédictif (1 à la fois) Q^2 : 0.9604530   Press 0.230025586338758

TABLEAU D'ANALYSE DE VARIANCE

Table B.14 Analysis of variance of regression for model proposed by CORICO program for log value of viscosity before heating

Source of variation	Sum of square	Df	Mean square	F	P
Régression	5.666	4	1.417	113.2	0.00
Résiduelle	0.1501	12	0.1251E-01		
Totale	5.817	16			

Erreur Standard d'estimation (SEE) = 0.1118564 , dans l'unité de LogVisbef
Erreur Standard de Prédiction (SEP) = 0.1384514 , dans l'unité de LogVisbef

F critique aux risques d'erreur 0.05, 0.025 et 0.01 :
$F_{0.05}$ = 3.260 ; $F_{0.025}$ = 4.120 ; $F_{0.01}$ = 5.410
Lorsque F est supérieur au F critique, on peut, avec un risque d'erreur inférieur au risque choisi, rejeter "l'hypothèse nulle H_0".

B.2 Correlation analysis and model regression by Iconographic Correlation for percentage of emulsion separation

!?! ESSAYER LE LOG DE LA REPONSE !?!

Table B.15 Correlation analysis for percentage of emulsion separation (1)

1	1 Oil	Emul_Sep	0.083
2	2 Lecithin	Emul_Sep	0.361
13	13 Oil*Lecithin	Emul_Sep	-0.445 Oil*Lecithin
13	13 FStoAci*CalFat	Emul_Sep	-0.558 FStoAcid*CalFat
13	13 WPconc*WPItoWP	Emul_Sep	-0.599 WPconc*WPItoWP
13	13 FStoAci#-CalFat	Emul_Sep	-0.782 FStoAcid#-CalFat

1   13 jmax = 13, comax = -0.78167   FStoAci#-CalFat

Table B.16 Correlation analysis for percentage of emulsion separation (2)

1	1 Oil	Emul_Sep	0.254
6	6 CalFat	Emul_Sep	0.390
14	14 Oil*CalFS	Emul_Sep	0.435 Oil*CalFS
14	14 Lecithi*WPItoWP	Emul_Sep	0.437 Lecithin*WPItoWP
14	14 Caldens*WPconc	Emul_Sep	0.455 Caldens*WPconc
14	14 FStoAci*Hydrolyzed	Emul_Sep	0.522 FStoAcid*Hydrolyzed
14	14 WPconc*WPconc	Emul_Sep	-0.530 WPconc*WPconc
14	14 WPconc]Caldens	Emul_Sep	-0.602 WPconc]Caldens
14	14 CalFat]-WPItoWP	Emul_Sep	0.644 CalFat]-WPItoWP
14	14 Caldens&-WPconc	Emul_Sep	0.671 Caldens&-WPconc

2   14 jmax = 14, comax = 0.67119   Caldens&-WPconc

Table B.17 Correlation analysis for percentage of emulsion separation (3)

1	1 Oil	Emul_Sep	0.339
15	15 FStoAci*FStoAcid	Emul_Sep	-0.339 FStoAcid*FStoAcid
15	15 Hydroly*Hydrolyzed	Emul_Sep	-0.543 Hydrolyzed*Hydrolyze
15	15 CalFS*CalFS	Emul_Sep	-0.641 CalFS*CalFS
15	15 CalFat&-CalFat	Emul_Sep	-0.655 CalFat&-CalFat
15	15 CalFS&-CalFS	Emul_Sep	-0.681 CalFS&-CalFS

3 15 jmax = 15, comax = -0.68105 CalFS&-CalFS

Table B.18 Correlation analysis for percentage of emulsion separation (4)

1	1 Oil	Emul_Sep	0.389
16	16 Oil]Lecithin	Emul_Sep	0.409 Oil]Lecithin
16	16 Oil]-CalFS	Emul_Sep	0.492 Oil]-CalFS
16	16 Lecithi{CalFat	Emul_Sep	0.525 Lecithin{CalFat

4 16 jmax = 16, comax = 0.52495 Lecithi{CalFat

Table B.19 Correlation analysis for percentage of emulsion separation (5)

1	1 Oil	Emul_Sep	0.397
17	17 Caldens*FStoAcid	Emul_Sep	0.451 Caldens*FStoAcid
17	17 WPconc{-Oil	Emul_Sep	-0.500 WPconc{-Oil

5 17 jmax = 17, comax = -0.50036 WPconc{-Oil

Table B.20 Correlation analysis for percentage of emulsion separation (6)

1	1 Oil	Emul_Sep	-0.010
2	2 Lecithin	Emul_Sep	0.071
3	3 Caldens	Emul_Sep	0.119
7	7 CalFS	Emul_Sep	-0.169
18	18 Oil*Lecithin	Emul_Sep	-0.221 Oil*Lecithin
18	18 Lecithi*Caldens	Emul_Sep	0.320 Lecithin*Caldens
18	18 Lecithi*WPconc	Emul_Sep	0.403 Lecithin*WPconc
18	18 Caldens*FStoAcid	Emul_Sep	0.406 Caldens*FStoAcid
18	18 Lecithi}WPItoWP	Emul_Sep	-0.414 Lecithin}WPItoWP
18	18 Caldens}FStoAcid	Emul_Sep	0.422 Caldens}FStoAcid
18	18 Hydroly}CalFS	Emul_Sep	-0.427 Hydrolyzed}CalFS
18	18 CalFat}CalFS	Emul_Sep	-0.457 CalFat}CalFS
18	18 CalFat}WPItoWP	Emul_Sep	-0.475 CalFat}WPItoWP
18	18 FStoAci{Caldens	Emul_Sep	0.506 FStoAcid{Caldens

6 18 jmax = 18, comax = 0.50587 FStoAci{Caldens

Table B.21 Correlation analysis for percentage of emulsion separation (7)

1	1 Oil	Emul_Sep	-0.041
2	2 Lecithin	Emul_Sep	0.103
4	4 FStoAcid	Emul_Sep	-0.125
7	7 CalFS	Emul_Sep	-0.232
19	19 Lecithi*Caldens	Emul_Sep	0.284 Lecithin*Caldens
19	19 Lecithi*FStoAcid	Emul_Sep	0.286 Lecithin*FStoAcid
19	19 Lecithi*WPconc	Emul_Sep	0.422 Lecithin*WPconc
19	19 Caldens*FStoAcid	Emul_Sep	0.426 Caldens*FStoAcid
19	19 CalFS{-CalFS	Emul_Sep	0.429 CalFS{-CalFS

   7 19 jmax = 19, comax = 0.42875   CalFS{-CalFS

Table B.22 Correlation analysis for percentage of emulsion separation (8)

1	1 Oil	Emul_Sep	-0.044
2	2 Lecithin	Emul_Sep	0.149
4	4 FStoAcid	Emul_Sep	-0.163
20	20 Oil*FStoAcid	Emul_Sep	0.191 Oil*FStoAcid
20	20 Lecithi*Caldens	Emul_Sep	0.224 Lecithin*Caldens
20	20 Lecithi*FStoAcid	Emul_Sep	0.251 Lecithin*FStoAcid
20	20 Lecithi*WPconc	Emul_Sep	0.307 Lecithin*WPconc
20	20 Lecithi*WPItoWP	Emul_Sep	0.312 Lecithin*WPItoWP
20	20 Caldens*FStoAcid	Emul_Sep	0.340 Caldens*FStoAcid
20	20 Caldens*Hydrolyzed	Emul_Sep	0.343 Caldens*Hydrolyzed
20	20 CalFS*Hydrolyzed	Emul_Sep	0.409 CalFS*Hydrolyzed
20	20 Hydroly#CalFS	Emul_Sep	-0.450 Hydrolyzed#CalFS

   8 20 jmax = 20, comax = -0.44991   Hydroly#CalFS

Table B.23 Correlation analysis for percentage of emulsion separation (9)

1	1 Oil	Emul_Sep	0.035
3	3 Caldens	Emul_Sep	0.050
4	4 FStoAcid	Emul_Sep	-0.115
21	21 Lecithi*Caldens	Emul_Sep	0.298 Lecithin*Caldens
21	21 Caldens*Hydrolyzed	Emul_Sep	0.339 Caldens*Hydrolyzed
21	21 FStoAci}Hydrolyzed	Emul_Sep	-0.351 FStoAcid}Hydrolyzed
21	21 FStoAci}CalFS	Emul_Sep	-0.351 FStoAcid}CalFS
21	21 Caldens{CalFat	Emul_Sep	0.364 Caldens{CalFat
21	21 FStoAci{WPItoWP	Emul_Sep	0.372 FStoAcid{WPItoWP

   9 21 jmax = 21, comax = 0.37247   FStoAci{WPItoWP

Table B.24 Correlation analysis for percentage of emulsion separation (10)

1	1 Oil	Emul_Sep	0.052
2	2 Lecithin	Emul_Sep	0.109
4	4 FStoAcid	Emul_Sep	-0.180
8	8 WPconc	Emul_Sep	-0.213
22	22 Lecithi*Caldens	Emul_Sep	0.324 Lecithin*Caldens
22	22 CalFS*Lecithin	Emul_Sep	0.336 CalFS*Lecithin
22	22 FStoAci]Hydrolyzed	Emul_Sep	-0.357 FStoAcid]Hydrolyzed
22	22 Lecithi}Caldens	Emul_Sep	0.374 Lecithin}Caldens
22	22 FStoAci}Hydrolyzed	Emul_Sep	-0.433 FStoAcid}Hydrolyzed
22	22 FStoAci}CalFat	Emul_Sep	-0.434 FStoAcid}CalFat

10 22 jmax = 22, comax = -0.43444   FStoAci}CalFat

10 régresseurs pour ModelEmul_Sep modèle de Emul_Sep   sur
17 observations

Table B.25 Quality of models for percentage of emulsion separation proposed by
CORICO program with different number of factors

1 regresseurs => F= 23.56	R^2_{adj} = 0.5851	Q^2 = 0.5621	SEP= 0.8896
2 regresseurs => F= 25.10	R^2_{adj} = 0.7508	Q^2 = 0.7075	SEP= 0.7526
3 regresseurs => F= 33.49	R^2_{adj} = 0.8590	Q^2 = 0.8557	SEP= 0.5486
4 regresseurs => F= 34.76	R^2_{adj} = 0.8941	Q^2 = 0.8517	SEP= 0.5789
5 regresseurs => F= 33.87	R^2_{adj} = 0.9113	Q^2 = 0.8729	SEP= 0.5598
6 regresseurs => F= 37.40	R^2_{adj} = 0.9317	Q^2 = 0.8902	SEP= 0.5456
7 regresseurs => F= 38.35	R^2_{adj} = 0.9423	Q^2 = 0.8993	SEP= 0.5507
8 regresseurs => F= 35.49	R^2_{adj} = 0.9452	Q^2 = 0.9101	SEP= 0.5519
9 regresseurs => F= 30.97	R^2_{adj} = 0.9440	Q^2 = 0.9084	SEP= 0.5957
10 regresseurs => F= 54.15	R^2_{adj} = 0.9708	Q^2 = 0.9274	SEP= 0.5729

SEPmin 0.5485676   , pour   3 régresseurs
Coefficients de la régression de Emul_Sep

Table B.26 Correlation of the model proposed by CORICO program for percentage
of emulsion separation

	Coefficient	Definition
0	0.810588235294	Constante
1	-3.652356536002 FStoAci#-CalFat	FStoAcid comme -CalFat
2	2.291369867480 Caldens&-WPconc	Caldens et non WPconc
3	-1.659107243384 CalFS&-CalFS	CalFS et non CalFS

Emul_Sep = 0.8106 - 3.652 FStoAci#-CalFat + 2.291 Caldens&-WPconc
- 1.659 CalFS&-CalFS   (B.2)

ModelEmul_Sep
 TABLEAU D'ANALYSE DES COEFFICIENTS

Table B.27 Analysis of coefficient of model in Equation B.2

	Coefficient	Difference	t-value	Interaction
1	-3.6524	0.4807	-7.5984	FStoAci#-CalFat
2	2.2914	0.4780	4.7940	Caldens&-WPconc
3	-1.6591	0.4841	-3.4270	CalFS&-CalFS

11 a le + grand levier: 0.6343487
Coefficient de corrélation   R : 0.9409705
Coefficient de détermination R^2 : 0.8854256
R^2 ajusté R^2_{adj}: 0.8589853
R^2 prédictif (1 à la fois) Q^2 : 0.8557171   Press 3.91204312602190

TABLEAU D'ANALYSE DE VARIANCE

Table B.28 Analysis of variance of regression for model proposed by CORICO
program for percentage of emulsion separation

Source of variation	Sum of square	Df	Mean square	F	P
Régression	24.01	3	8.002	33.49	0.00
Résiduelle	3.107	13	0.2390		
Totale	27.11	16			

Erreur Standard d'estimation (SEE) = 0.4888397 , dans l'unité de Emul_Sep
Erreur Standard de Prédiction (SEP) = 0.5485676   , dans l'unité de Emul_Sep

F critique aux risques d'erreur 0.05, 0.025 et 0.01 :
$F_{0.05}$ =   3.410 ; $F_{0.025}$ =   4.350 ; $F_{0.01}$ =   5.740
 Lorsque F est supérieur au F critique, on peut, avec un risque d'erreur inférieur au
risque choisi, rejeter "l'hypothèse nulle H_0".

B.3 Correlation analysis and model regression by Iconographic Correlation for average of bottom surface temperature

Table B.29 Correlation analysis for average of bottom surface temperature (1)

1	1 Time	MeanTemp	0.431
2	2 SpecPower	MeanTemp	0.886
10	10 Time&SpecPower	MeanTemp	0.925 Time&SpecPower
10	10 Time+SpecPower	MeanTemp	0.931 Time+SpecPower

1 10 jmax = 10, comax =   0.93137   Time+SpecPower

Table B.30 Correlation analysis for average of bottom surface temperature (2)

1	1 Time	MeanTemp	-0.614
2	2 SpecPower	MeanTemp	0.629
11	11 Time]Time	MeanTemp	-0.656 Time]Time
11	11 SpecPow]Time	MeanTemp	0.701 SpecPower]Time
11	11 Time&-SpecPower	MeanTemp	-0.931 Time&-SpecPower

2 11 jmax = 11, comax = -0.93050   Time&-SpecPower

Table B.31 Correlation analysis for average of bottom surface temperature (3)

1	1 Time	MeanTemp	-0.218
12	12 Time*Time	MeanTemp	0.689 Time*Time
12	12 Time&-Time	MeanTemp	0.699 Time&-Time
12	12 Time!Time	MeanTemp	0.757 Time!Time

3 12 jmax = 12, comax = 0.75669   Time!Time

Table B.32 Correlation analysis for average of bottom surface temperature (4)

1	1 Time	MeanTemp	-0.427
13	13 Time}SpecPower	MeanTemp	-0.659 Time}SpecPower

4 13 jmax = 13, comax = -0.65924   Time}SpecPower

Table B.33 Correlation analysis for average of bottom surface temperature (5)

1	1 Time	MeanTemp	-0.073
14	14 Time*Time	MeanTemp	0.081 Time*Time
14	14 SpecPow*SpecPower	MeanTemp	0.226 SpecPower*SpecPower
14	14 Time'SpecPower	MeanTemp	0.240 Time'SpecPower
14	14 SpecPow{-Time	MeanTemp	0.293 SpecPower{-Time

5 14 jmax = 14, comax = 0.29254   SpecPow{-Time

Table B.34 Correlation analysis for average of bottom surface temperature (6)

1	1 Time	MeanTemp	0.059
2	2 SpecPower	MeanTemp	0.068
15	15 Time*Time	MeanTemp	0.170 Time*Time
15	15 Time'SpecPower	MeanTemp	0.227 Time'SpecPower
15	15 Time{Time	MeanTemp	0.263 Time{Time

6 15 jmax = 15, comax = 0.26318   Time{Time

Table B.35 Correlation analysis for average of bottom surface temperature (7)

1	1 Time	MeanTemp	-0.006
2	2 SpecPower	MeanTemp	0.066
16	16 SpecPow]-Time	MeanTemp	0.076 SpecPower]-Time
16	16 Time}Time	MeanTemp	0.090 Time}Time
16	16 SpecPow{Time	MeanTemp	-0.125 SpecPower{Time

7 16 jmax = 16, comax = -0.12540   SpecPow{Time

Table B.36 Correlation analysis for average of bottom surface temperature (8)

1	1 Time	MeanTemp	0.002
2	2 SpecPower	MeanTemp	0.067
17	17 SpecPow]-Time	MeanTemp	0.078 SpecPower]-Time
17	17 SpecPow]-SpecPower	MeanTemp	0.079 SpecPower]-SpecPower
17	17 Time}Time	MeanTemp	0.106 Time}Time

8 17 jmax = 17, comax = 0.10637   Time}Time

Table B.37 Correlation analysis for average of bottom surface temperature (9)

1	1 Time	MeanTemp	-0.067
2	2 SpecPower	MeanTemp	0.075
18	18 Time]Time	MeanTemp	-0.076 Time]Time
18	18 Time]SpecPower	MeanTemp	-0.083 Time]SpecPower
18	18 SpecPow]-Time	MeanTemp	0.088 SpecPower]-Time
18	18 SpecPow&-Time	MeanTemp	0.111 SpecPower&-Time

9 18 jmax = 18, comax = 0.11082   SpecPow&-Time

9 régresseurs pour ModelMeanTemp modèle de MeanTemp   sur
9 observations

Table B.38 Quality of models for average of bottom surface temperature proposed by
CORICO program with different number of factors

1 regresseurs => F= 45.81	R^2_{adj} = 0.8485	Q^2 = 0.8344	SEP= 3.586
2 regresseurs => F= 167.1	R^2_{adj} = 0.9765	Q^2 = 0.9762	SEP= 1.361
3 regresseurs => F= 247.5	R^2_{adj} = 0.9893	Q^2 = 0.9875	SEP= 0.9839
4 regresseurs => F= 175.0	R^2_{adj} = 0.9886	Q^2 = 0.9859	SEP= 1.047
5 regresseurs => F= 123.2	R^2_{adj} = 0.9871	Q^2 = 0.9918	SEP= 0.7980
6 regresseurs => F= 69.05	R^2_{adj} = 0.9808	Q^2 = 0.9921	SEP= 0.7854

1 régresseur REDONDANT

SEPmin= 0.9838691   , pour   3 régresseurs
Coefficients de la régression de MeanTemp

Table B.39 Correlation of the model proposed by CORICO program for average of bottom surface temperature

	Coefficient	Definition
0	64.173125022222	Constante
1	22.610338382155 Time+SpecPower	Time + SpecPower
2	-8.550494789119 Time&-SpecPower	Time et non SpecPower
3	2.611215288996 Time!Time	Time strictement moyen et Time

MeanTemp = 64.17 + 22.61 Time+SpecPower - 8.550 Time&-SpecPower
+ 2.611 Time!Time   (B.3)

ModelMeanTemp
TABLEAU D'ANALYSE DES COEFFICIENTS
Table B.40 Analysis of coefficient of model in Equation B.3

	Coefficient	Difference	t-value	Interaction
1	22.6103	0.9141	24.7350	Time+SpecPower
2	-8.5505	0.9140	-9.3554	Time&-SpecPower
3	2.6112	0.9129	2.8605	Time!Time

Pas de grand levier.
Coefficient de corrélation   R : 0.9966494
Coefficient de détermination R^2 : 0.9933100
R^2 ajusté R^2_{adj}: 0.9892960
R^2 prédictif (1 à la fois) Q^2 : 0.9875376   Press   8.71198574085464

TABLEAU D'ANALYSE DE VARIANCE
Table B.41 Analysis of variance of regression for model proposed by CORICO program for average of bottom surface temperature

Source of variation	Sum of square	Df	Mean square	F	P
Régression	694.4	3	231.5	247.5	0.00
Résiduelle	4.677	5	0.9354		
Totale	699.1	8			

Erreur Standard d'estimation (SEE) = 0.7208603   , dans l'unité de MeanTemp
Erreur Standard de Prédiction (SEP) = 0.9838691   , dans l'unité de MeanTemp

F critique aux risques d'erreur 0.05, 0.025 et 0.01 :
$F_{0.05}$ =   5.410 ; $F_{0.025}$ =   7.760 ; $F_{0.01}$ =   12.060
Lorsque F est supérieur au F critique, on peut, avec un risque d'erreur inférieur au risque choisi, rejeter "l'hypothèse nulle H_0".

B.4 Correlation analysis and model regression by Iconographic Correlation for relative tryptophan loss

!?! ESSAYER LE LOG DE LA REPONSE !?!

Table B.42 Correlation analysis for relative tryptophan loss (1)

1	1 Time	TrpLoss	0.562
2	2 SpecPower	TrpLoss	0.746
10	10 Time&SpecPower	TrpLoss	0.927 Time&SpecPower

    1 10 jmax = 10, comax = 0.92732   Time&SpecPower

Table B.43 Correlation analysis for relative tryptophan loss (2)

1	1 Time	TrpLoss	-0.019
2	2 SpecPower	TrpLoss	0.223
11	11 Time*Time	TrpLoss	-0.494 Time*Time
11	11 Time&-Time	TrpLoss	-0.494 Time&-Time
11	11 Time'SpecPower	TrpLoss	-0.704 Time'SpecPower
11	11 Time#SpecPower	TrpLoss	-0.823 Time#SpecPower

    2 11 jmax = 11, comax = -0.82316   Time#SpecPower

Table B.44 Correlation analysis for relative tryptophan loss (3)

1	1 Time	TrpLoss	-0.036
2	2 SpecPower	TrpLoss	0.417
12	12 SpecPow]Time	TrpLoss	0.481 SpecPower]Time
12	12 Time{-SpecPower	TrpLoss	-0.515 Time{-SpecPower

    3 12 jmax = 12, comax = -0.51465   Time{-SpecPower

Table B.45 Correlation analysis for relative tryptophan loss (4)

1	1 Time	TrpLoss	-0.012
2	2 SpecPower	TrpLoss	0.229
13	13 Time*SpecPower	TrpLoss	-0.239 Time*SpecPower
13	13 SpecPow]Time	TrpLoss	0.316 SpecPower]Time
13	13 Time}SpecPower	TrpLoss	0.513 Time}SpecPower

    4 13 jmax = 13, comax = 0.51259   Time}SpecPower

Table B.46 Correlation analysis for relative tryptophan loss (5)

1	1 Time	TrpLoss	-0.367
14	14 Time]-SpecPower	TrpLoss	-0.456 Time]-SpecPower
14	14 Time&-SpecPower	TrpLoss	-0.511 Time&-SpecPower
14	14 Time}Time	TrpLoss	-0.576 Time}Time

    5 14 jmax = 14, comax = -0.57610   Time}Time

Table B.47 Correlation analysis for relative tryptophan loss (6)

1	1 Time	TrpLoss	0.093
2	2 SpecPower	TrpLoss	0.311
15	15 Time*SpecPower	TrpLoss	-0.327 Time*SpecPower
15	15 SpecPow]Time	TrpLoss	0.430 SpecPower]Time

6 15 jmax = 15, comax = 0.43001   SpecPow]Time

Table B.48 Correlation analysis for relative tryptophan loss (7)

1	1 Time	TrpLoss	-0.002
2	2 SpecPower	TrpLoss	0.064
16	16 Time*Time	TrpLoss	0.138 Time*Time
16	16 Time*SpecPower	TrpLoss	-0.219 Time*SpecPower
16	16 Time'SpecPower	TrpLoss	0.261 Time'SpecPower
16	16 Time!SpecPower	TrpLoss	0.275 Time!SpecPower
16	16 SpecPow{Time	TrpLoss	0.446 SpecPower{Time

7 16 jmax = 16, comax = 0.44626   SpecPow{Time

Table B.49 Correlation analysis for relative tryptophan loss (8)

1	1 Time	TrpLoss	-0.157
17	17 Time*Time	TrpLoss	0.208 Time*Time
17	17 Time*SpecPower	TrpLoss	-0.238 Time*SpecPower
17	17 Time]Time	TrpLoss	-0.251 Time]Time
17	17 Time]-SpecPower	TrpLoss	-0.256 Time]-SpecPower
17	17 Time{-Time	TrpLoss	0.360 Time{-Time

8 17 jmax = 17, comax = 0.35959   Time{-Time

Table B.50 Correlation analysis for relative tryptophan loss (9)

1	1 Time	TrpLoss	-0.097
18	18 Time*SpecPower	TrpLoss	-0.254 Time*SpecPower
18	18 SpecPow{-Time	TrpLoss	-0.372 SpecPower{-Time

9 18 jmax = 18, comax = -0.37244   SpecPow{-Time

9 régresseurs pour ModelTrpLoss   modèle de TrpLoss   sur
9 observations

Table B.51 Quality of models for relative tryptophan loss proposed by CORICO program with different number of factors

1 regresseurs => F= 42.97	R^2_{adj} = 0.8399	Q^2 = 0.8490	SEP= 6.135
2 regresseurs => F= 76.99	R^2_{adj} = 0.9500	Q^2 = 0.9261	SEP= 4.290
3 regresseurs => F= 59.77	R^2_{adj} = 0.9566	Q^2 = 0.9132	SEP= 4.651
4 regresseurs => F= 69.89	R^2_{adj}= 0.9718	Q^2 = 0.9480	SEP= 3.601
5 regresseurs => F= 1055.	R^2_{adj} = 0.9985	Q^2 = 0.9990	SEP= 0.4873
6 regresseurs => F= 594.1	R^2_{adj} = 0.9978	Q^2 = 0.9991	SEP= 0.4806

2 régresseurs REDONDANTS

SEPmin= 4.290400 , pour 2 régresseurs

Coefficients de la régression de TrpLoss

Table B.52 Correlation of the model proposed by CORICO program for relative tryptophan loss

	Coefficient	Definition
0	18.977990216111	Constante
1	45.824564567167 Time&SpecPower	Time et SpecPower
2	-14.967598253728 Time#SpecPower	Time comme SpecPower

TrpLoss = 18.98 + 45.82 Time&SpecPower - 14.97 Time#SpecPower   (B.4)

ModelTrpLoss

TABLEAU D'ANALYSE DES COEFFICIENTS

Table B.53 Analysis of coefficient of model in Equation B.4

	Coefficient	Difference	t-value	Interaction
1	45.8246	3.6950	12.4019	Time&SpecPower
2	-14.9676	3.6950	-4.0508	Time#SpecPower

2 a le + grand levier: 0.5036482

Coefficient de corrélation R : 0.9810675

Coefficient de détermination R^2 : 0.9624934

R^2 ajusté R^2_{adj} : 0.9499912

R^2 prédictif (1 à la fois) Q^2 : 0.9261364   Press 165.667778560061

TABLEAU D'ANALYSE DE VARIANCE

Table B.54 Analysis of variance of regression for model proposed by CORICO program for relative tryptophan loss

Source of variation	Sum of square	Df	Mean square	F	P
Régression	2159.	2	1079.	76.99	0.00
Résiduelle	84.12	6	14.02		
Totale	2243.	8			

Erreur Standard d'estimation (SEE) = 3.057288   , dans l'unité de TrpLoss
Erreur Standard de Prédiction (SEP) = 4.290400   , dans l'unité de TrpLoss

F critique aux risques d'erreur 0.05, 0.025 et 0.01 :
$F_{0.05} =$ 5.140 ; $F_{0.025} =$ 7.260 ; $F_{0.01} =$ 10.920
 Lorsque F est supérieur au F critique, on peut, avec un risque d'erreur inférieur au risque choisi, rejeter "l'hypothèse nulle H_0".

B.5 Correlation analysis and model regression by Iconographic Correlation for FAST index

Table B.55 Correlation analysis for FAST index (1)

1	1 Time	FAST_index	0.711
10	10 Time^SpecPower	FAST_index	0.717 Time^SpecPower
10	10 Time+SpecPower	FAST_index	0.771 Time+SpecPower
10	10 SpecPow{-Time	FAST_index	-0.815 SpecPower{-Time

1 10 jmax = 10, comax = -0.81518   SpecPow{-Time

Table B.56 Correlation analysis for FAST index (2)

1	1 Time	FAST_index	0.107
2	2 SpecPower	FAST_index	0.602
11	11 Time*Time	FAST_index	-0.670 Time*Time
11	11 Time&-Time	FAST_index	-0.676 Time&-Time
11	11 Time{-SpecPower	FAST_index	-0.801 Time{-SpecPower

2 11 jmax = 11, comax = -0.80146   Time{-SpecPower

Table B.57 Correlation analysis for FAST index (3)

1	1 Time	FAST_index	0.215
2	2 SpecPower	FAST_index	0.391
12	12 SpecPow*SpecPower	FAST_index	0.541 SpecPower*SpecPower
12	12 SpecPow]-SpecPower	FAST_index	0.637 SpecPower]-SpecPower

3 12 jmax = 12, comax = 0.63673   SpecPow]-SpecPower

Table B.58 Correlation analysis for FAST index (4)

1	1 Time	FAST_index	0.305
13	13 Time]Time	FAST_index	0.396 Time]Time
13	13 Time}Time	FAST_index	0.429 Time}Time

4 13 jmax = 13, comax = 0.42860   Time}Time

Table B.59 Correlation analysis for FAST index (5)

1	1 Time	FAST_index	-0.013
2	2 SpecPower	FAST_index	-0.050
14	14 Time*Time	FAST_index	-0.367 Time*Time
14	14 Time&-Time	FAST_index	-0.367 Time&-Time

5 14 jmax = 14, comax = -0.36682   Time&-Time

Table B.60 Correlation analysis for FAST index (6)

1	1 Time	FAST_index	-0.070
15	15 Time*Time	FAST_index	-0.157 Time*Time
15	15 Time*SpecPower	FAST_index	0.234 Time*SpecPower
15	15 SpecPow*SpecPower	FAST_index	0.237 SpecPower*SpecPower
15	15 Time}SpecPower	FAST_index	-0.339 Time}SpecPower

6 15 jmax = 15, comax = -0.33942   Time}SpecPower

Table B.61 Correlation analysis for FAST index (7)

1	1 Time	FAST_index	0.054
16	16 Time*Time	FAST_index	-0.287 Time*Time
16	16 SpecPow*SpecPower	FAST_index	0.311 SpecPower*SpecPower
16	16 SpecPow{-SpecPower	FAST_index	0.313 SpecPower{-SpecPower

7 16 jmax = 16, comax = 0.31313   SpecPow{-SpecPower

Table B.62 Correlation analysis for FAST index (8)

1	1 Time	FAST_index	0.054
17	17 Time*Time	FAST_index	-0.266 Time*Time
17	17 Time^-Time	FAST_index	0.268 Time^-Time

Time^-Time exactement corrélé à Time&-Time Tous les régresseurs sont trouvés.

Minimiser SEP
    7 régresseurs pour ModelFAST_inde modèle de FAST_index   sur
    9 observations

Table B.63 Quality of models for FAST index proposed by CORICO program with different number of factors

1 regresseurs => F= 13.87	$R^2_{adj} = 0.6166$	$Q^2 = 0.4526$	SEP= 0.2174
2 regresseurs => F= 19.31	$R^2_{adj} = 0.8207$	$Q^2 = 0.7947$	SEP= 0.1438
3 regresseurs => F= 19.83	$R^2_{adj} = 0.8759$	$Q^2 = 0.8455$	SEP= 0.1367
4 regresseurs => F= 18.66	$R^2_{adj} = 0.8983$	$Q^2 = 0.9091$	SEP= 0.1172
5 regresseurs => F= 11.22	$R^2_{adj} = 0.8646$	$Q^2 = 0.9037$	SEP= 0.1393
6 regresseurs => F= 6.510	$R^2_{adj} = 0.8052$	$Q^2 = 0.9195$	SEP= 0.1560
7 regresseurs => F= 2.790	$R^2_{adj} = 0.6103$	$Q^2 = 0.9186$	SEP= 0.2218

régresseur REDONDANT

SEPmin 0.1172070   , pour   4 régresseurs
Coefficients de la régression de FAST_index

Table B.64 Correlation of the model proposed by CORICO program for FAST index

	Coefficient	Definition
0	3.364604924222	Constante
1	-0.597005232463 SpecPow{-Time	SpecPower moyen si non Time
2	-0.337126923601 Time{-SpecPower	Time moyen si non SpecPower
3	0.140874888684 SpecPow]-SpecPower	SpecPower si non SpecPower
4	0.146909035993 Time}Time	Time si moyen Time

FAST_index =3.365 - 0.5970 SpecPow{-Time - 0.3371 Time{-SpecPower
+ 0.1409 SpecPow]-SpecPower + 0.1469 Time}Time   (B.5)

ModelFAST_index
TABLEAU D'ANALYSE DES COEFFICIENTS
Table B.65 Analysis of coefficient of model in Equation B.5

	Coefficient	Difference	t-value	Interaction
1	-0.5970	0.1026	-5.8177	SpecPow{-Time
2	-0.3371	0.0877	-3.8427	Time{-SpecPower
3	0.1409	0.0936	1.5058	SpecPow]-SpecPower
4	0.1469	0.1014	1.4485	Time}Time

Pas de grand levier.
Coefficient de corrélation R : 0.9742396
Coefficient de détermination R^2 : 0.9491429
R^2 ajusté R^2_{adj} : 0.8982857
R^2 prédictif (1 à la fois) Q^2 : 0.9090961   Press 5.494988814857142E-002

TABLEAU D'ANALYSE DE VARIANCE
Table B.66 Analysis of variance of regression for model proposed by CORICO program for FAST index

Source of variation	Sum of square	Df	Mean square	F	P
Régression	0.5737	4	0.1434	18.66	0.007496
Résiduelle	0.3074E-01	4	0.7686E-02		
Totale	0.6045	8			

Erreur Standard d'estimation (SEE) = 8.7667443E-02 , dans l'unité de
FAST_index
Erreur Standard de Prédiction (SEP) = 0.1172070   , dans l'unité de
FAST_index

F critique aux risques d'erreur 0.05, 0.025 et 0.01 :
$F_{0.05} = 6.390$; $F_{0.025} = 9.600$; $F_{0.01} = 15.980$
Lorsque F est supérieur au F critique, on peut, avec un risque d'erreur inférieur au risque choisi, rejeter "l'hypothèse nulle H_0".

B.6 Model regression for average of bottom surface temperature, relative tryptophan loss and FAST index by response surface methodology

Table B.67 Regression anlysis, analysis of variance and lack of fit of average of bottom surface temperature

Regression Statistics	
Multiple R	0.997143
R Square	0.994294
Adjusted R Square	0.984783
Standard Error	1.153113
Observations	9

ANOVA

	df	SS	MS	F	Significance F
Regression	5	695.0733	139.0147	104.5482	0.001456
Residual	3	3.989011	1.32967		
Total	8	699.0623			

	Coefficients	Standard Error	t Stat	P-value	Lower 95%	Upper 95%
Intercept	65.3639	0.667338	97.94727	2.35E-06	63.24013	67.48766
x1	6.442255	0.656877	9.807403	0.002253	4.35178	8.532729
x2	13.62074	0.670535	20.31323	0.000261	11.48679	15.75468
x1x2	3.212273	1.289491	2.491117	0.088397	-0.89146	7.31601
x1^2	-2.45436	1.054659	-2.32716	0.102413	-5.81076	0.902035
x2^2	-1.32378	1.06301	-1.24532	0.301422	-4.70676	2.059187

RESIDUAL OUTPUT

Observation	Predicted Mean (C)	Residuals
1	69.35179	-0.33265
2	80.21949	0.319859
3	70.647	-0.31986
4	56.46728	0.332654
5	50.09609	-0.31986
6	53.92349	0.319859
7	65.61766	1.183839
8	65.61766	-1.38446
9	65.61766	0.200621

ANOVA

Source of Variation	SS	Df	MS	F	P-value	F crit
Between Groups	695.7039	6	115.9506	69.05	0.014344	19.32953
Within Groups	3.358455	2	1.679227			
Total	699.0623	8				

Lack of fit

Source	df	SS	MS	F	F crit
Lack of fit	1	0.630556	0.630556	0.375504	18.5
Pure error	2	3.358455	1.679227		
Residual	3	3.989011	1.32967		

Table B.68 Regression anlysis, analysis of variance and lack of fit of relative tryptophan loss

Regression Statistics	
Multiple R	0.986364
R Square	0.972915
Adjusted R Square	0.927773
Standard Error	4.499968
Observations	9

ANOVA

	Df	SS	MS	F	Significance F
Regression	5	2182.14	436.428	21.55231	0.014768
Residual	3	60.74912	20.24971		
Total	8	2242.889			

	Coefficients	Standard Error	t Stat	P-value	Lower 95%	Upper 95%
Intercept	12.69939	2.604252	4.876405	0.016483	4.411496	20.98728
x1	15.39468	2.563429	6.005502	0.009249	7.236702	23.55265
x2	20.53928	2.616731	7.849213	0.004307	12.21168	28.86689
x1x2	8.705697	5.032175	1.730007	0.182066	-7.30893	24.72032
x1^2	9.254493	4.115754	2.248553	0.110085	-3.84367	22.35266
x2^2	8.824497	4.148343	2.127234	0.123334	-4.37738	22.02638

RESIDUAL OUTPUT

Observation	Predicted %Trp loss	Residuals
1	37.34856	3.231153
2	51.28437	-3.10688
3	27.48894	3.106878
4	6.559204	-3.23115
5	-0.0473	3.106878
6	8.178193	-3.10688
7	13.32998	-0.81017
8	13.32998	0.774614
9	13.32998	0.035558

ANOVA

Source of Variation	SS	Df	MS	F	P-value	F crit
Between Groups	2241.631	6	373.6052	594.1228	0.001681	19.32953
Within Groups	1.25767	2	0.628835			
Total	2242.889	8				

Lack of fit

Source	df	SS	MS	F	F Crit
Lack of fit	1	59.49145	59.49145	94.60583	18.5
Pure error	2	1.25767	0.628835		
Residual	3	60.74912	20.24971		

Table B.69 Regression anlysis, analysis of variance and lack of fit of FAST index

Regression Statistics	
Multiple R	0.928972
R Square	0.862988
Adjusted R Square	0.634636
Standard Error	0.166154
Observations	9

ANOVA

	df	SS	MS	F	Significance F
Regression	5	0.521662	0.104332	3.779189	0.151489
Residual	3	0.082821	0.027607		
Total	8	0.604483			

	Coefficients	Standard Error	t Stat	P-value	Lower 95%	Upper 95%
Intercept	3.233739	0.096158	33.62955	5.78E-05	2.927722	3.539755
x1	0.31988	0.09465	3.379597	0.043104	0.01866	0.6211
x2	0.171315	0.096618	1.773109	0.174321	-0.13617	0.478798
x1x2	-0.03464	0.185805	-0.18641	0.864017	-0.62595	0.556678
x1^2	0.053298	0.151967	0.350721	0.74898	-0.43033	0.536926
x2^2	0.329658	0.153171	2.152228	0.120455	-0.1578	0.817116

RESIDUAL OUTPUT

Observation	Predicted FAST index	Residuals
1	3.606917	0.096787
2	3.790034	-0.09306
3	3.488331	0.093064
4	2.967157	-0.09679
5	3.16275	0.093064
6	3.526397	-0.09306
7	3.246619	-0.09445
8	3.246619	0.136839
9	3.246619	-0.04239

ANOVA

Source of Variation	SS	df	MS	F	P-value	F crit
Between Groups	0.575041	6	0.09584	6.510399	0.139118	19.32953
Within Groups	0.029442	2	0.014721			
Total	0.604483	8				

Lack of fit

Source	df	SS	MS	F	Crit
Lack of fit	1	0.053379	0.053379	3.626027	18.5
Pure error	2	0.029442	0.014721		
Residual	3	0.082821	0.027607		

Appendix C Effect of Salt Concentration, Frequency, and Temperature on Dielectric Properties of Raw and Cooked White Shrimps *Litopenaeus vannamei*

Tanathep Lueangtongkum[1] and Jirarat Anuntagool [1, *]

[1]Department of Food Technology, Faculty of Science, Chulalongkorn University, Phyathai Road, Patumwan, Bangkok, THAILAND

* Corresponding author, Email address: jirarat.t@chula.ac.th

Abstract

The effect of salt concentration (1% - 5%) and temperature (10 °C-85 °C) on dielectric properties of raw and cooked white shrimp *Litopenaeus vannamei* in the microwave frequency range of 300 to 3,000 MHz were studied. The result showed that cooked shrimp had lower water activity, moisture content, ash content, salt content, dielectric constant (ε') and dielectric loss factor (ε'') but higher fat content than raw shrimp. Application of salt solution at higher concentration during the pretreatment step caused a reduction in water activity and moisture content, but an increase in density, protein, fat, ash content, carbohydrate, ε', and ε''. Increasing frequency caused the ε' and ε'' to decrease, but elevating temperature resulted in a decrease in ε' but an increase in ε''. Quadratic models relating dielectric properties with frequency, salt concentration, and temperature for raw and cooked shrimp samples were established.

Keywords: White shrimp, Dielectric properties, Salt, Microwave

C.1 Introduction

Shrimp is one of the most desirable raw materials for the delicacy that is popular in many areas worldwide (Cruz-Suárez, Ricque-Marie, Martínez-Vega, & Wesche-Ebeling, 1993; ErdoĜDu, Balaban, & Chau, 1999; Heu, Kim, & Shahidi, 2003; Karakoltsidis, Zotos, & Constantinides, 1995; Sriket, Benjakul, Visessanguan, & Kijroongrojana, 2007). According to the report in FAO Yearbook of fisheries and aquaculture statistics 2015, shrimp's production was the highest among the crustacean's production from 2009 to 2015. To supply the high demand of shrimp, freezing or canning treatments are among common methods used to increase its shelf life (Ma, Deng, Ahmed, & Adams, 1983). Although freezing preserves product's quality, storing frozen food is inconvenient and requires high energy consumption. On the other hand, sterilization affects the food's texture (Ma et al., 1983) and causes shrinkage (Murakami, 1994) due to long time processing that results in various changes, i.e. myofibrillar protein denaturation, collagen shrinkage (ErdoĜDu et al., 1999) and collagen gelatinization (Takeuchi & Takahashi, 2011). Consequently, canned shrimp is normally soft, tight and stiff (ErdoĜDu et al., 1999).

Microwave heating can generate heat inside the load; hence, it requires less processing time and leads to better quality and nutrient retention (Lassen & Ovesen, 1995; Pandit, Tang, Liu, & Pitts, 2007). Lau and Tang (2002) reported that pickled asparagus pasteurized by microwave with hot water had better quality compared to that pasteurized with hot water. Tang et al. (2008) also reported that microwave heating could heat beef in gravy in 7-Oz tray twice faster than hot water heating alone. These could assure that microwave heating is a promising method for processing shrimp in hermetically sealed container with better quality than the traditional canning method.

However, microwave heating has a major drawback from its uneven heating nature (Lau & Tang, 2002). Experimentation should be carried out to ensure an optimum condition that would result in the best quality product. Modelling is a useful technique to predict the heating pattern which can guarantee a good result with less study resource (Geedipalli, Rakesh, & Datta, 2007). One of the properties required for microwave heating modelling is dielectric properties which describe how materials

interact with electromagnetic energy during dielectric heating. It consists of two components: dielectric constant (ε') and dielectric loss factor (ε''). Dielectric constant shows the ability of a material to store energy when it is subjected to an electric field and dielectric loss factor relates to the ability to dissipate energy in response to an applied electric field commonly results in heat generation (Fellows, 2009).

Dielectric properties of several seafood, e.g. salmon and sturgeon caviar, oyster, salmon fillets, sea cucumber etc., were reported (Al-Holy et al., 2005; Cong et al., 2012; Hu, and Mallikarjunan, 2005; Wang et al., 2008). Zheng et al. (1998) also reported the dielectric properties of shrimp and marinated shrimp. However, there are no studies on the effect of cooking, temperature, frequency, and salt concentration on dielectric properties of shrimp.

This research aimed to investigate the effect of the preparation step on physical properties, composition, and dielectric properties of white shrimp (*Litopenaeus vannamei*) and dielectric properties at various frequencies and temperatures.

C.2 Materials and Methods

C.2.1 White shrimp sample preparation

Raw peeled beheaded white shrimp (70 – 80 shrimp/kg) was bought from a local seafood wholesaler in Pathumthani, Thailand. It was first peeled and beheaded by the vendor and then, packed and kept in a box filled with ice until the time of preparation.

First, it was soaked by the method described in Wachirasiri, Wanlapa, Uttapap, and Rungsardthong (2016) with some modifications. Shrimp was soaked in a solution containing 1% (w/v), 3% (w/v) and 5% (w/v) of iodized salt in tap water with the ratio of shrimp : salt solution of 1 : 1.5 (by weight) in a beaker covered with aluminum foil for 3 h at 4 ± 1 °C in a refrigerator. After being equilibrated, it was drained and some of them was cooked by boiling with the procedure stated in Niamnuy, Devahastin, and Soponronnarit (2008). The boiling solution was prepared using the

same salt concentration as that in the soaking step with the ratio of shrimp: boiling solution or tap water of 1: 2 (by weight) for 5 minutes.

C.2.2 Physical properties and proximate composition

C.2.2.1 Density

The density of the sample was measured by a water substitution method using a 100-mL volumetric cylinder.

C.2.2.2 Water activity

The sample was crushed and its water activity was measured using an AquaLab Model Series 3 TE (Decagon Devices, Pullman, WA, USA).

C.2.2.3 Proximate composition and salt content

Proximate composition (moisture, protein, crude fat, ash and total carbohydrate) and salt content as NaCl was determined according to the methods in AOAC (2000).

C.2.3 Dielectric properties

The samples were equilibrated to reach a desired temperature (10°C to 85°C) for both raw and cooked samples using a refrigerator or a controlled temperature heating bath (Homemade, China). Dielectric properties of equilibrated sample were then measured using the equipment shown in Figure C.1 at the Department of Electrical

Engineering, Faculty of Engineering, King mongkut's Institute of Technology Ladkrabang, Thailand.

The sample was placed above a sponge to ensure that the probe's surface was completely contacted with the sample. The probe used in the system was Agilent 8507E Dielectric Probe (high temperature probe) (Agilent Technologies, Santa Clara, CA, USA) which was calibrated with air and deionized water. It was connected with N9916A FieldFox Handheld Microwave analyzer (Keysight Technologies, Santa Rosa, CA, USA). The spectrum was displayed on a personal computer. 501 values of each property were measured in the range of 300 MHz – 3 GHz.
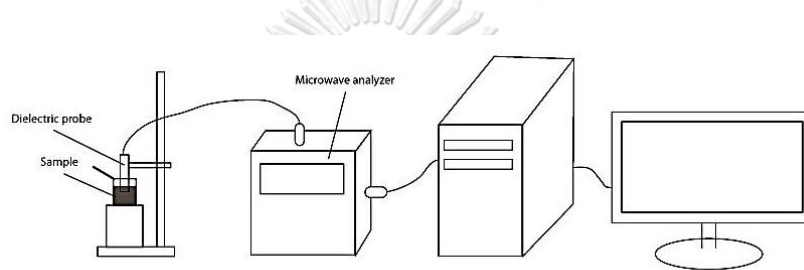
Figure C.1 Schematic drawing of a dielectric property measurement system

C.2.4 Statistical analysis

The effect of preparation condition on the sample's properties and composition was investigated by Analysis of Variance (ANOVA) (P = 0.05) using the IBM SPSS Statistics 22 software. Scatter plots of dielectric properties versus frequency and temperature, as well as mathematical models describing the dielectric properties as affected by salt concentration, frequency, and temperature of raw or cooked sample at 915 MHz and 2450 MHz were generated using the UnscramblerX software version 10.3.

C.3 Results and Discussion

C.3.1 Physical properties and composition

Table C.1 shows some physical properties and composition of the shrimp samples subjected to different treatments. As the salt concentration increased, the shrimp's density was significantly increased. However, the sample's density was not notably affected by cooking.

Table C.1 Physical properties, proximate composition and salt content of white shrimp prepared with different condition

Condition		ρ (g/cm³)	a_w	Moisture (%wb)	Protein (%db)	Fat (%db)	Ash (%db)	Carbohydrates (%db)*	Salt (%db as NaCl)
No soaking,	Raw	0.99 ± 0.00^b	1.00 ± 0.00^{ef}	80.4 ± 0.7^c	91.2 ± 1.6^e	0.91 ± 0.02^b	4.64 ± 0.21^c	3.27 ± 1.57^a	0.77 ± 0.02^b
	Cooked	1.02 ± 0.04^{bc}	1.00 ± 0.00^{ef}	70.8 ± 0.2^a	90.5 ± 2.4^{de}	2.49 ± 0.10^e	3.05 ± 0.01^a	3.97 ± 2.28^a	0.41 ± 0.02^a
Soak with 1% (w/v) NaCl	Raw	0.99 ± 0.00^b	1.00 ± 0.00^f	80.7 ± 0.2^{cd}	87.7 ± 3.2^{cd}	0.91 ± 0.01^b	4.94 ± 0.20^d	6.44 ± 3.42^{ab}	1.70 ± 0.06^c
	Cooked	1.01 ± 0.03^{bc}	1.00 ± 0.00^e	72.0 ± 0.0^b	87.9 ± 1.3^{cd}	2.76 ± 0.09^f	3.74 ± 0.04^b	5.62 ± 1.41^{ab}	1.81 ± 0.04^c
Soak with 3% (w/v) NaCl	Raw	1.03 ± 0.03^{bc}	0.99 ± 0.00^d	81.2 ± 0.2^d	84.7 ± 1.3^{bc}	0.74 ± 0.03^a	8.08 ± 0.27^f	6.48 ± 1.52^{ab}	5.23 ± 0.10^e
	Cooked	1.05 ± 0.04^b	0.99 ± 0.00^c	72.5 ± 0.4^b	83.0 ± 1.9^b	2.32 ± 0.00^d	6.48 ± 0.06^e	8.27 ± 1.86^b	4.86 ± 0.01^d
Soak with 5% (w/v) NaCl	Raw	1.01 ± 0.02^{bc}	0.98 ± 0.00^b	81.1 ± 0.1^d	81.7 ± 0.7^{ab}	1.00 ± 0.04^b	12.0 ± 0.3^h	5.37 ± 0.71^{ab}	9.64 ± 0.17^g
	Cooked	0.86 ± 0.03^a	0.98 ± 0.00^a	72.5 ± 0.3^b	78.7 ± 0.6^a	1.89 ± 0.05^c	10.8 ± 0.1^g	8.62 ± 0.46^b	9.24 ± 0.06^f

a, b, c, ... shows significant difference between values in the same column ($p < 0.05$)

*By difference

The water activity of treated samples was remarkably reduced with increasing salt concentration since salt bound water and decreased its mobility (Rougier, Bonazzi, & Daudin, 2007). Furthermore, cooking also reduced sample's water activity due to lower water content in the cooked sample (Wemmenhove, Wells-Bennik, Stara, van Hooijdonk, & Zwietering, 2016). The reduction of moisture content in the cooked sample could most possibly stem from cooking loss.

The sample's proximate composition and salt content are shown in Table C.1. It was found that moisture content slightly increased in the shrimp treated with higher salt concentration because water holding capacity (WHC) of the sample was higher (Lopkulkiaert, Prapatsornwattana, & Rungsardthong, 2009). However, moisture content in cooked sample was significantly lower than raw sample since cooking resulted in muscle structure's destruction; hence, WHC of the sample decreased (Katsaras & Budras, 1993). The sample treated with higher salt concentration had lower protein content due to salting-out effect (Niamnuy et al., 2008) while cooking did not significantly affect the sample's protein content. The effect of salt in the pretreatment solution on fat content was marginal. Treating the raw sample with higher salt concentration slightly decreased the sample's fat content. However, after cooking, the cooked sample had significantly higher fat content compared to the raw sample. This could be due to the reduction in protein content of the cooked sample, although not significant, and ash content of the cooked sample that, in turn, caused the percentage of the fat and carbohydrates to increase.

Increasing salt concentration in the pretreatment process inevitably and expectedly resulted in higher ash and salt content in the samples. Higher concentration of salt in the pretreatment solution resulted in higher driving force for mass transfer of salt from the solution to meat (Dimakopoulou-Papazoglou & Katsanidis, 2016). However, it is noted that cooking caused the sample's ash and salt content to decrease. This stemmed from the dissolution of salt in the boiling process.

Lastly, treating raw shrimp samples with salt solution caused a non-significant increase in carbohydrate content. But a significant increase in carbohydrate content could be observed in cooked shrimp samples. An increase in carbohydrate content was possibly a result of the decrease in protein content of cooked shrimp.
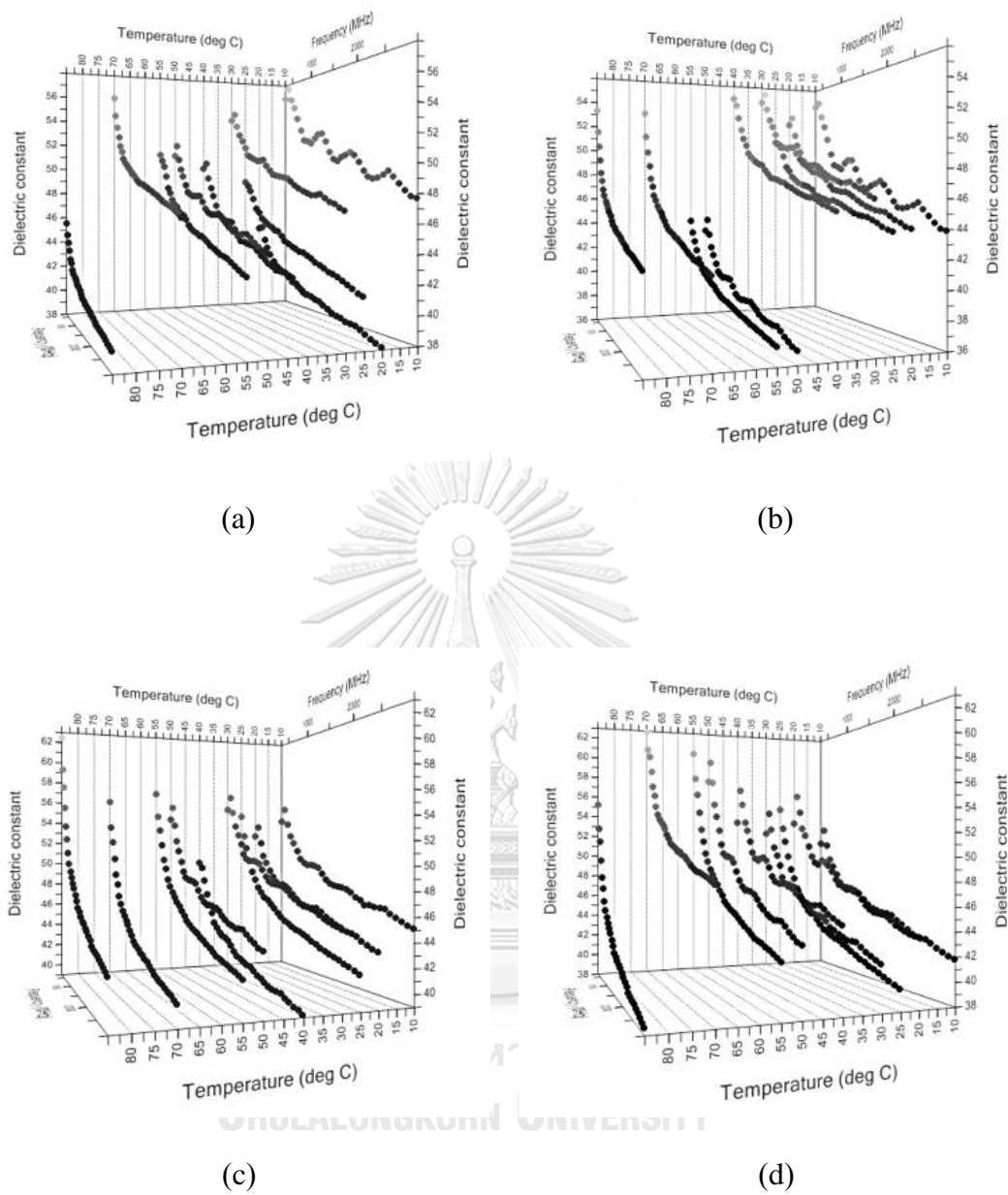
C.3.2 Dielectric constant

Like most food, dielectric constant (ε') of treated white shrimp depends on frequency, salt content (or ash content), and temperature (Venkatesh & Raghavan, 2004). The data of dielectric constant of the shrimp samples treated using different conditions is shown in Figures C.2 and C.3. It was found that cooked samples had significantly lower ε' than raw samples due to lower water activity (Venkatesh & Raghavan, 2004). The second-order polynomial mathematical models describing the relationship between dielectric constant (ε') and frequency (f) in GHz, salt content (S) as salt concentration (% (w/v) iodized salt) used in the preparation step, and temperature (T) in °C of raw and cooked samples were developed and shown in Equations C.1 and C.2, respectively.

จุฬาลงกรณ์มหาวิทยาลัย

CHULALONGKORN UNIVERSITY

(a)

(b)

(c)

(d)
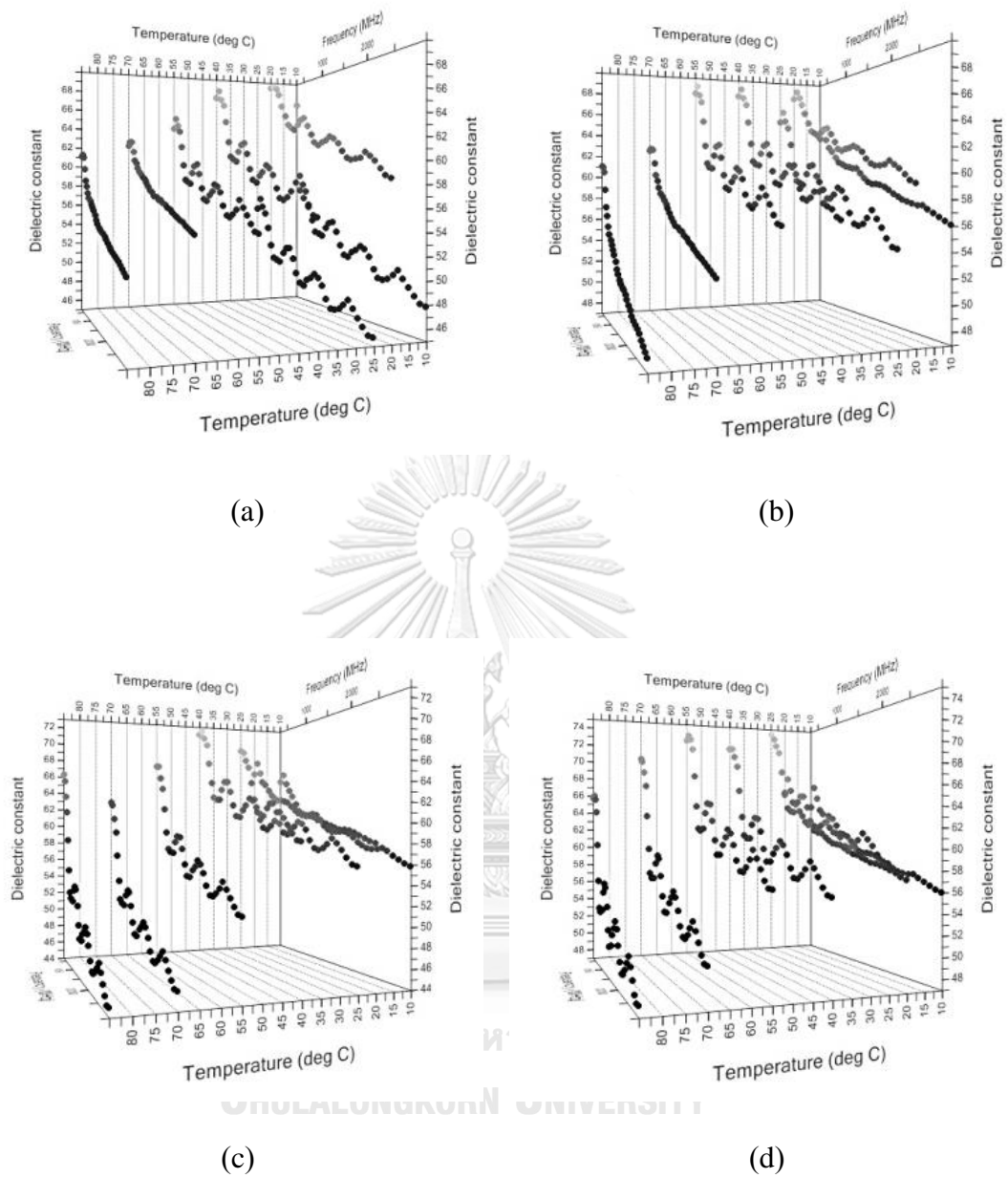
Figure C.2 Dielectric constant of raw shrimp at different salt concentrations (a) No soaking, (b) soak with 1% (w/v) iodized salt, (c) soak with 3% (w/v) iodized salt, (d) soak with 5% (w/v) iodized salt

(a)

(b)

(c)

(d)

Figure C.3 Dielectric constant of cooked shrimp at different soaking and boiling salt concentrations (a) No soaking and boil with tap water, (b) soak and boil with 1% (w/v) iodized salt, (c) soak and boil with 3% (w/v) iodized salt, (d) soak and boil with 5% (w/v) iodized salt

Raw sample;

$$\varepsilon' = 67.441 - 8.153f - 0.691S + 0.209T - 0.142fS - 0.013fT + 1.737f^2 + 0.174S^2$$

$$- 0.003T^2 \quad (R^2_{adj} = 0.859) \tag{C.1}$$

Cooked sample;

$$\varepsilon' = 57.500 - 7.526f - 1.236S - 0.218T - 0.411fS - 0.022fT + 0.021ST + 1.929f^2$$

$$+ 0.285S^2 + 0.002T^2 \quad (R^2_{adj} = 0.571) \tag{C.2}$$

The adjusted regression coefficient of both models was low, thus indicating that the relationship between ε' and the stated parameters was weak. It might have been caused by the inhomogeneity of the sample during dielectric measurement. The equation describing the relationship between ε' and influencing factors of the raw sample showed a substantially higher regression coefficient compared to that of the cooked sample because it was more homogeneous and contained fewer void. The presence of air in the void inside the crushed cooked sample could have affected the ε' value (Venkatesh & Raghavan, 2004).

Equations C.1 and C.2 show a negative coefficient of the frequency term. This indicated that the dielectric constant decreased with increasing frequency. The result agreed with previous studies on other seafood samples such as salmon fillets (Wang, Tang, Rasco, Kong, & Wang, 2008), shucked oysters (Hu & Mallikarjunan, 2005), and non-marinated and marinated shrimp and catfish (Zheng, Huang, Nelson, Bartley, & Gates, 1998). The negative effect of frequency on ε' was shown earlier in the model described by Okiror and Jones (2012) for low acyl gellan gel, and by Dev, Raghavan, and Gariepy (2008) for egg white and egg yolk.

Increasing salt concentration in the preparation step decreased ε' as shown by the negative coefficient of the salt concentration term in Equations (1) and (2). The result was consistent with a previous study by Zheng et al. (1998) which reported the effect of marination on ε' of shrimp and catfish. However, there was no significant difference between the ε' of the sample that was not subjected to soaking in salt solution and the sample treated with 1 % (w/v) NaCl. The ash content in both

samples was approximately equal (Table C.1). The negative effect of salt concentration agreed with the model developed by Zhang et al. (2015) for low acyl gellan gel.

Increasing the sample's temperature during the measurement appeared to decrease ε' because the orderliness of water molecules is disturbed by intermolecular vibration resulted from elevated temperature (Wang et al., 2008). Cong, Liu, Tang, and Xue (2012) and Zheng et al. (1998) also reported the same trend for sea cucumber and marinated shrimp, respectively. The negative effect of temperature on ε' has been reported earlier by Zhang et al. (2015) for low acyl gellan gel. However, the model for raw sample shows that the temperature had a positive effect on ε'. This finding agreed with the model for whole egg described by Zhang, Liu, Nindo, and Tang (2013). The adverse effect of sample's temperature on ε' on raw samples could stem from the denaturation of protein at 50ºC and above. Denaturation of protein caused the release of water molecules from the muscle protein that leads to cooking losses. Higher amount of free water molecules, in turn, caused the ε' to increase.

The interactions of frequency-salt concentration (fS) and frequency-temperature (fT) shows a significant negative effect on ε' for both raw and cooked shrimp samples while the interaction of salt concentration-temperature (ST) had a significant positive effect on ε' of cooked shrimp sample only. This means the net increase in fS or fT can cause a decrease in ε'. The higher magnitude of the coefficient for the fS term indicates that this term has a stronger effect on ε'. The ST interaction did not exert a significant effect on the ε' of raw shrimp, possibly because of the variation in sample's response due to denaturation of protein that was caused by an increase in sample's temperature.

The square of frequency and salt concentration had a significant positive effect on the ε' value of both raw and cooked shrimp samples, while the square of temperature had a negative effect on the ε' value of raw sample but a positive effect on that of cooked sample. However, it could be observed that the coefficient of the square of temperature term is very small, which could mean that the change in temperature squared could exert a little effect the ε' value of the samples.

C.3.3 Dielectric loss factor

Dielectric loss factor (ε'') in an aqueous solution system which contains charged particles comprises two components as shown in Equation C.3

$$\varepsilon'' = \varepsilon''_d + \varepsilon''_\sigma \qquad (C.3)$$

Where ε''_d is dipole loss which involves the activity of dipole molecules e.g. water, and ε''_σ is ionic loss that occurs by ions such as sodium ions and chloride ions dissolved from salt. Therefore, any composition modification that affects the amount of the activity of dipole molecules or ions will inevitably affect ε''. Like dielectric constant, dielectric loss factor of a sample also depends on the frequency, salt content or ash content, and temperature (Venkatesh & Raghavan, 2004). As shown in Figures C.4 and C.5, cooking remarkably reduced ε'' because lowering the moisture content caused by cooking has yielded dielectric loss factor reductions (Prakash, Nelson, Mangino, & Hansen, 1992). The second order polynomial model explaining the relationship between dielectric loss factor (ε'') and frequency (f) in GHz, salt content (S) as salt concentration (% (w/v) iodized salt) used in the preparation step, and temperature (T) in °C of raw and cooked samples was developed and shown in Equations C.4 and C.5.

(a)

(b)

(c)

(d)
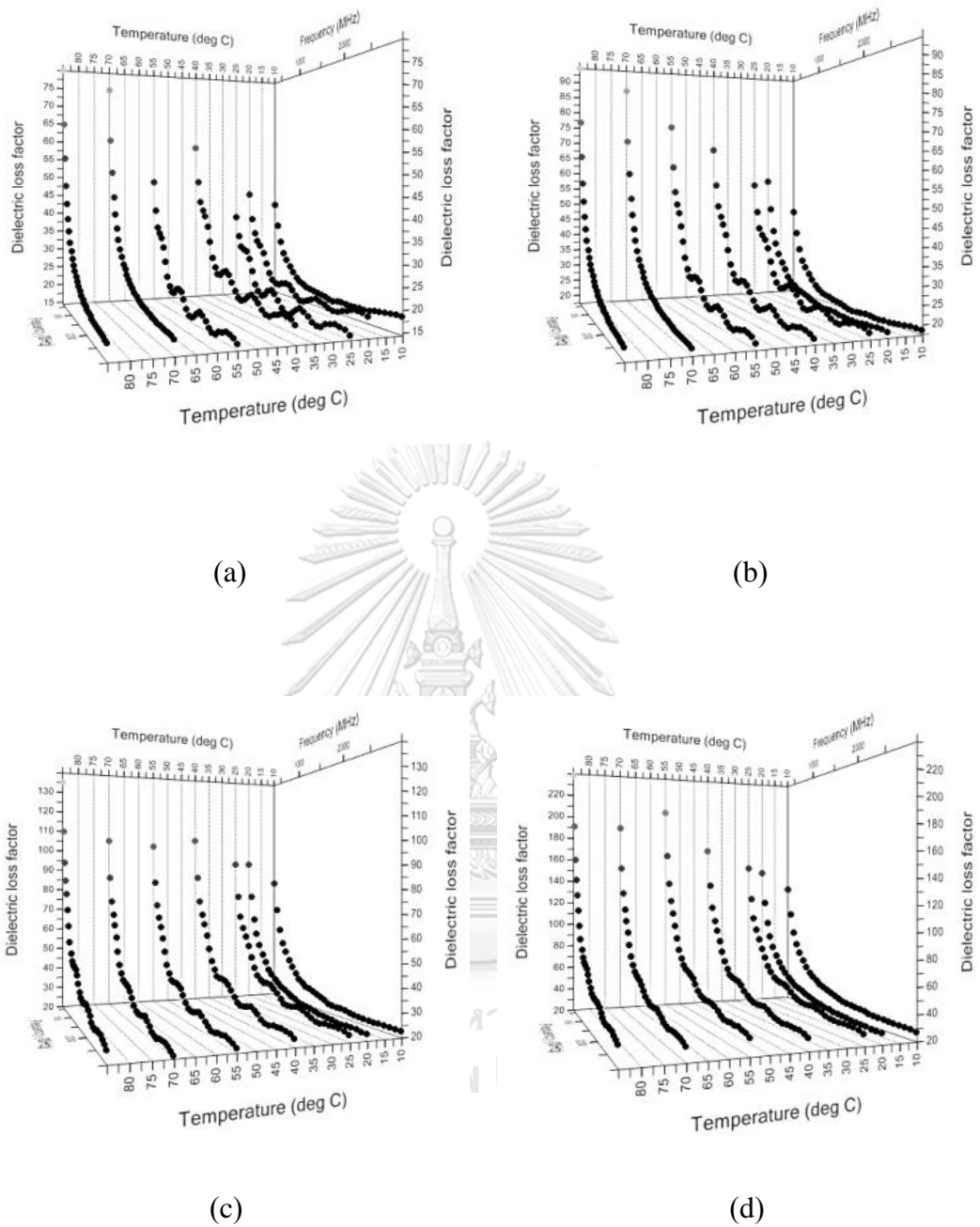
Figure C.4 Dielectric loss factor of raw shrimp at different soaking salt concentrations (a) No soaking, (b) soak with 1% (w/v) iodized salt, (c) soak with 3% (w/v) iodized salt, (d) soak with 5% (w/v) iodized salt

(a)

(b)

(c)

(d)
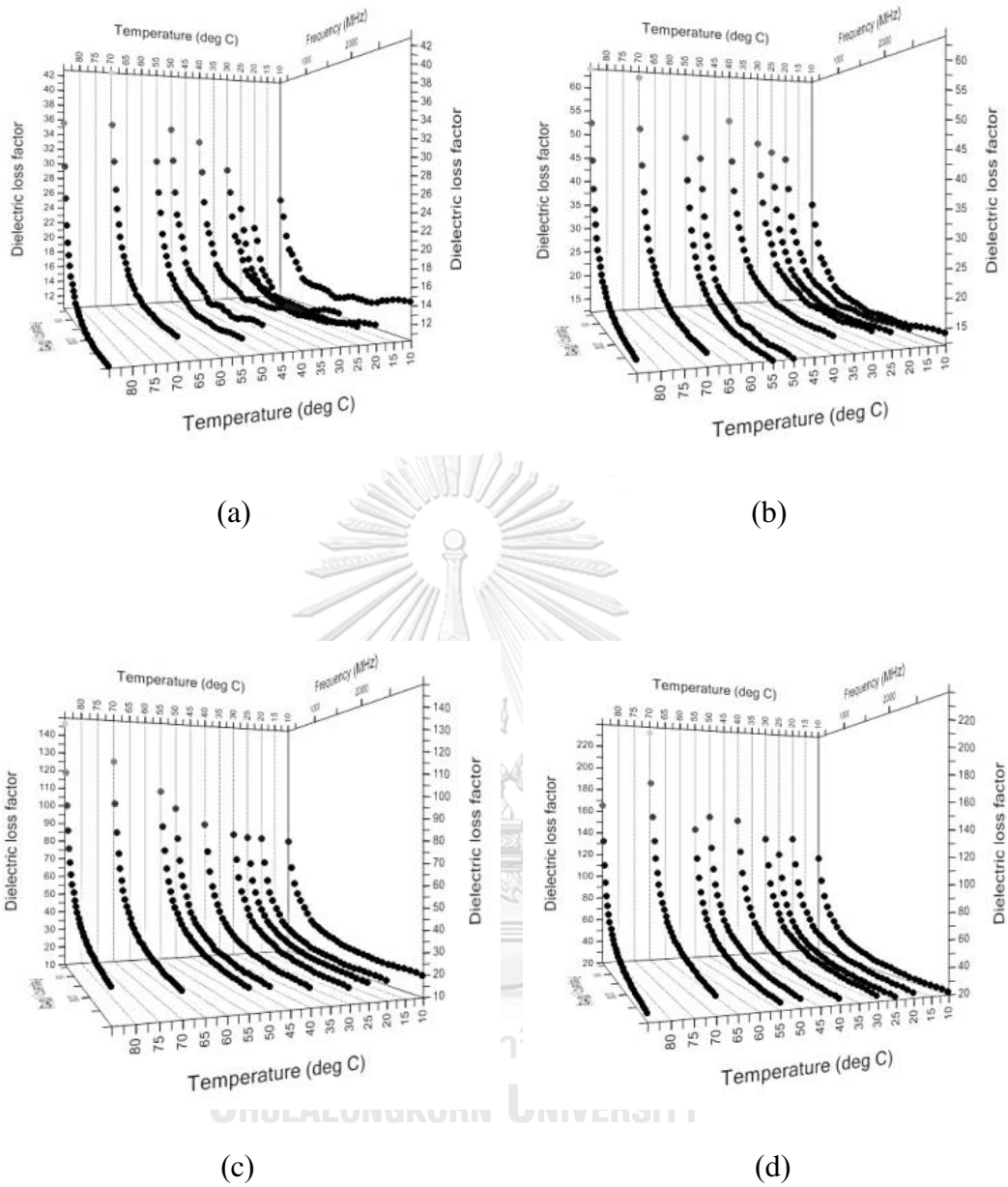
Figure C.5 Dielectric loss factor of cooked shrimp at different soaking and boiling salt concentrations (a) No soaking, boil with tap water, (b) soak and boil with 1% (w/v) iodized salt, (c) soak and boil with 3% (w/v) iodized salt, (d) soak and boil with 5% (w/v) iodized salt

Raw sample;

$$\varepsilon'' = 56.526 - 54.953f + 7.497S + 0.364T - 4.146fS - 0.173fT + 0.034ST$$

$$+ 16.401f^2 + 0.722S^2 \qquad (R^2_{adj} = 0.916) \qquad\qquad (C.4)$$

Cooked sample;

$$\varepsilon'' = 35.337 - 45.321f + 13.417S + 0.313T - 6.879fS - 0.189fT + 0.036ST$$

$$+ 17.726f^2 + 0.295S^2 \qquad (R^2_{adj} = 0.907) \qquad\qquad (C.5)$$

Both mathematical expressions show higher value of correlation coefficient, which indicates that the relationship between ε″ and these parameters was strong. It was found that ε″ decreased with increasing frequency. The level of coefficient indicates that frequency exerted a strong effect on ε″. A slight increase in frequency could decrease ε″ a great extent. As stated in Equation C.3, ε″ is affected by the activity of dipoles and ions, which react differently when subjected to different frequency fields. Dipole loss (ε''_d) is positively correlated with frequency, while the effect of such on ionic loss (ε''_σ) is different (Zhang et al., 2015). The change in ε″ with respect to frequency was consistent with the change in ionic loss, indicating that the ions posed a stronger effect than dipoles did. Zhang et al. (2015) reported that increasing frequency decreased ε″ by impeding the movement of charged particle among the electrical field in food system. This result was consistent with previous studies on seafood, i.e. sea cucumber by Cong et al. (2012), and shucked oyster by Hu and Mallikarjunan (2005). Moreover, Equations C.4 and C.5 also stated the negative effect of frequency on ε″ which is similar to models for low-acyl gellan gel described in Okiror and Jones (2012).

On the other hand, increasing salt content elevated ε″. Although salt reduced free water, resulting in dipole loss, an increase in ions that gave rise to an increase in ionic loss was more outstanding (Zheng et al., 1998). Al-Holy, Wang, Tang, and Rasco (2005) reported that marination increased ε″ of salmon and sturgeon caviar, while Zheng et al. (1998) mentioned that salt addition into shrimp and catfish led to a

surge in sample's dielectric loss factor. The results were also consistent with that reported by Zhang et al. (2013) for egg white and egg yolk and Zhang et al. (2015) for low acyl gellan gel. All models showed that the increase in ε'' was proportional with salt content.

The dielectric loss factor of all samples increased along with temperature. The effect of temperature on ε'' component is diverted; increasing the temperature decreases dipole loss, but increases ionic loss (Al-Holy et al., 2005). Due to high salt content in the sample, ionic loss could play an important role on ε''. This means, in samples with high salt content, increasing the temperature would cause an increase in ε'', rather than a decrease. The increase in temperature results in an increase in ion's energy that drives the ion to travel a greater extent. Wang et al. (2008) and Al-Holy et al. (2005) reported the same effect of temperature on ε'' of salmon fillets and shuck oysters, respectively. The models developed by Okiror and Jones (2012) for low acyl gellan gel agreed with the models proposed in this study as well.

The combined effect of frequency and temperature on ε'' was significant in both models proposed in this study. Okiror and Jones (2012) showed the combined effect of these factors in the ε'' model for low acyl gellan gel and their negative coefficient agreed with this work. Considering other interactions and the square of each parameter in the model, Zhang et al. (2015) also reported the same effect of ST and S^2 terms. It is noted that the effect of temperature-squared on ε'' is insignificant. All models showed good correlation which meant that it could be able to predict ε'' of white shrimp sample treated the same way but different salt content within the range of 0 %(w/v) Iodized salt to 5 %(w/v) Iodized salt.

C.4 Conclusions

The result of this study indicates the effect of cooking and salt concentration used in the preparation step on physical properties, proximate composition, salt content, and dielectric properties of white shrimp. Cooking sample had a reduction in water activity, moisture content, ash content, salt content, dielectric constant and dielectric loss factor but an increase in fat content. Furthermore, using higher salt concentration reduced water activity and moisture content, while increasing density, protein, fat, ash content, salt content, carbohydrate, dielectric constant, and dielectric loss factor. Mathematical models describing the effect of frequency, temperature, and salt content on dielectric properties of raw and cooked white shrimp were successfully developed.

Frequency and temperature also affected dielectric properties. Dielectric constant decreased when higher frequency and temperature applied. Dielectric loss factor decreased with frequency as well but increased with temperature. The model between the dielectric properties with frequency, salt content, and temperature were also developed. Models for raw sample was stronger than those for cooked sample, and dielectric loss factor model had a higher correlation coefficient than that of dielectric constant.

References

Al-Holy, M., Wang, Y., Tang, J., & Rasco, B. (2005). Dielectric properties of salmon (*Oncorhynchus keta*) and sturgeon (*Acipenser transmontanus*) caviar at radio frequency (RF) and microwave (MW) pasteurization frequencies. *Journal of Food Engineering, 70*(4), 564-570. doi:http://dx.doi.org/10.1016/j.jfoodeng.2004.08.046

AOAC. (2000). *Official methods of analysis of AOAC International*. Gaithersburg, Md.: AOAC International.

Cong, H., Liu, F., Tang, Z., & Xue, C. (2012). Dielectric properties of sea cucumbers (*Stichopus japonicus*) and model foods at 915MHz. *Journal of Food Engineering, 109*(3), 635-639. doi:http://dx.doi.org/10.1016/j.jfoodeng.2011.06.012

Cruz-Suárez, L. E., Ricque-Marie, D., Martínez-Vega, J. A., & Wesche-Ebeling, P. (1993). Evaluation of two shrimp by-product meals as protein sources in diets for Penaeus vannamei. *Aquaculture, 115*(1), 53-62. doi:https://doi.org/10.1016/0044-8486(93)90358-6

Dev, S. R. S., Raghavan, G. S. V., & Gariepy, Y. (2008). Dielectric properties of egg components and microwave heating for in-shell pasteurization of eggs. *Journal of Food Engineering, 86*(2), 207-214. doi:10.1016/j.jfoodeng.2007.09.027

Dimakopoulou-Papazoglou, D., & Katsanidis, E. (2016). Mass transfer kinetics during osmotic processing of beef meat using ternary solutions. *Food and Bioproducts Processing, 100*, 560-569. doi:https://doi.org/10.1016/j.fbp.2016.09.001

ErdoĜDu, F., Balaban, M. O., & Chau, K. V. (1999). Mathematical model to predict yield loss og medium and large tiger shrimp (*Penaeus monodon*) during cooking. *Journal of Food Process Engineering, 22*(5), 383-394. doi:10.1111/j.1745-4530.1999.tb00493.x

Fellows, P. J. (2009). 20 - Dielectric, ohmic and infrared heating. In *Food Processing Technology (Third edition)* (pp. 581-609): Woodhead Publishing.

Geedipalli, S. S. R., Rakesh, V., & Datta, A. K. (2007). Modeling the heating uniformity contributed by a rotating turntable in microwave ovens. *Journal of Food Engineering, 82*(3), 359-368. doi:http://dx.doi.org/10.1016/j.jfoodeng.2007.02.050

Heu, M.-S., Kim, J.-S., & Shahidi, F. (2003). Components and nutritional quality of shrimp processing by-products. *Food Chemistry, 82*(2), 235-242. doi:https://doi.org/10.1016/S0308-8146(02)00519-8

Hu, X., & Mallikarjunan, P. (2005). Thermal and dielectric properties of shucked oysters. *LWT - Food Science and Technology, 38*(5), 489-494. doi:http://dx.doi.org/10.1016/j.lwt.2004.07.016

Karakoltsidis, P. A., Zotos, A., & Constantinides, S. M. (1995). Composition of the Commercially Important Mediterranean Finfish, Crustaceans, and Molluscs. *Journal of Food Composition and Analysis, 8*(3), 258-273. doi:https://doi.org/10.1006/jfca.1995.1019

Katsaras, K., & Budras, K.-D. (1993). The Relationship of the Microstructure of Cooked Ham to its Properties and Quality. *LWT - Food Science and Technology, 26*(3), 229-234. doi:https://doi.org/10.1006/fstl.1993.1050

Lassen, A., & Ovesen, L. (1995). Nutritional effects of microwave cooking. *Nutrition & Food Science, 95*(4), 8-10. doi:doi:10.1108/00346659510088654

Lau, M. H., & Tang, J. (2002). Pasteurization of pickled asparagus using 915 MHz microwaves. *Journal of Food Engineering, 51*(4), 283-290. doi:http://dx.doi.org/10.1016/S0260-8774(01)00069-3

Lopkulkiaert, W., Prapatsornwattana, K., & Rungsardthong, V. (2009). Effects of sodium bicarbonate containing traces of citric acid in combination with sodium chloride on yield and some properties of white shrimp (*Penaeus vannamei*) frozen by shelf freezing, air-blast and cryogenic freezing. *LWT -*

Food Science and Technology, 42(3), 768-776. doi:http://dx.doi.org/10.1016/j.lwt.2008.09.019

Ma, L. Y., Deng, J. C., Ahmed, E. M., & Adams, J. P. (1983). Canned Shrimp Texture as a Function of Its Heat History. *Journal of Food Science, 48*(2), 360-363. doi:10.1111/j.1365-2621.1983.tb10743.x

Murakami, E. G. (1994). Thermal Processing Affects Properties of Commercial Shrimp and Scallops. *Journal of Food Science, 59*(2), 237-241. doi:doi:10.1111/j.1365-2621.1994.tb06938.x

Niamnuy, C., Devahastin, S., & Soponronnarit, S. (2008). Changes in protein compositions and their effects on physical changes of shrimp during boiling in salt solution. *Food Chemistry, 108*(1), 165-175. doi:http://dx.doi.org/10.1016/j.foodchem.2007.10.058

Okiror, G. P., & Jones, C. L. (2012). Effect of temperature on the dielectric properties of low acyl gellan gel. *Journal of Food Engineering, 113*(1), 151-155. doi:https://doi.org/10.1016/j.jfoodeng.2012.04.011

Pandit, R. B., Tang, J., Liu, F., & Pitts, M. (2007). Development of a novel approach to determine heating pattern using computer vision and chemical marker (M-2) yield. *Journal of Food Engineering, 78*(2), 522-528. doi:https://doi.org/10.1016/j.jfoodeng.2005.10.039

Prakash, A., Nelson, S. O., Mangino, M. E., & Hansen, P. M. T. (1992). Variation of microwave dielectric properties of hydrocolloids with moisture content, temperature and stoichiometric charge. *Food Hydrocolloids, 6*(3), 315-322. doi:https://doi.org/10.1016/S0268-005X(09)80098-2

Rougier, T., Bonazzi, C., & Daudin, J.-D. (2007). Modeling incidence of lipid and sodium chloride contents on sorption curves of gelatin in the high humidity range. *LWT - Food Science and Technology, 40*(10), 1798-1807. doi:https://doi.org/10.1016/j.lwt.2006.11.004

Sriket, P., Benjakul, S., Visessanguan, W., & Kijroongrojana, K. (2007). Comparative studies on chemical composition and thermal properties of black tiger shrimp (Penaeus monodon) and white shrimp (Penaeus vannamei) meats. *Food Chemistry, 103*(4), 1199-1207. doi:https://doi.org/10.1016/j.foodchem.2006.10.039

Takeuchi, Y., & Takahashi, H. (2011). Research on the softness of Grass Prawn *Penaeus monodon* tissue by retort sterilization. *NIPPON SUISAN GAKKAISHI, 77*(5), 887-895. doi:10.2331/suisan.77.887

Tang, Z., Mikhaylenko, G., Liu, F., Mah, J.-H., Pandit, R., Younce, F., & Tang, J. (2008). Microwave sterilization of sliced beef in gravy in 7-oz trays. *Journal of Food Engineering, 89*(4), 375-383. doi:http://dx.doi.org/10.1016/j.jfoodeng.2008.04.025

Venkatesh, M. S., & Raghavan, G. S. V. (2004). An Overview of Microwave Processing and Dielectric Properties of Agri-food Materials. *Biosystems Engineering, 88*(1), 1-18. doi:https://doi.org/10.1016/j.biosystemseng.2004.01.007

Wachirasiri, K., Wanlapa, S., Uttapap, D., & Rungsardthong, V. (2016). Use of amino acids as a phosphate alternative and their effects on quality of frozen white shrimps (*Penaeus vanamei*). *LWT - Food Science and Technology, 69*, 303-311. doi:http://dx.doi.org/10.1016/j.lwt.2016.01.065

Wang, Y., Tang, J., Rasco, B., Kong, F., & Wang, S. (2008). Dielectric properties of salmon fillets as a function of temperature and composition. *Journal of Food Engineering, 87*(2), 236-246. doi:http://dx.doi.org/10.1016/j.jfoodeng.2007.11.034

Wemmenhove, E., Wells-Bennik, M. H. J., Stara, A., van Hooijdonk, A. C. M., & Zwietering, M. H. (2016). How NaCl and water content determine water activity during ripening of Gouda cheese, and the predicted effect on inhibition of Listeria monocytogenes. *Journal of Dairy Science, 99*(7), 5192-5201. doi:https://doi.org/10.3168/jds.2015-10523
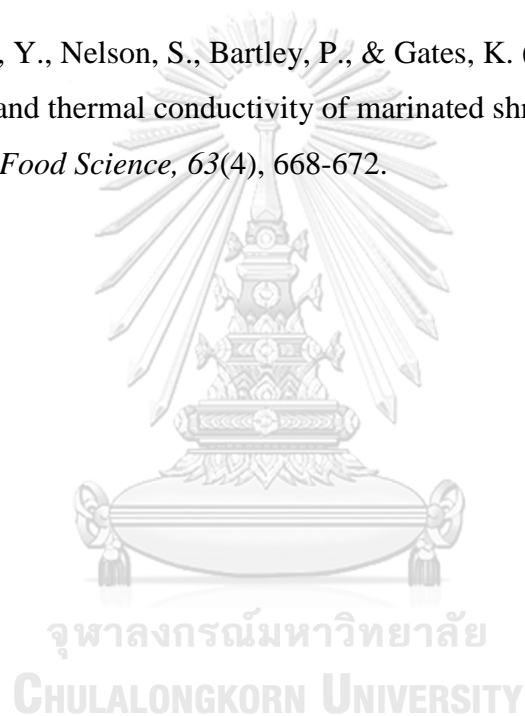
Zhang, W., Liu, F., Nindo, C., & Tang, J. (2013). Physical properties of egg whites and whole eggs relevant to microwave pasteurization. *Journal of Food Engineering, 118*(1), 62-69. doi:https://doi.org/10.1016/j.jfoodeng.2013.03.003

Zhang, W., Luan, D., Tang, J., Sablani, S. S., Rasco, B., Lin, H., & Liu, F. (2015). Dielectric properties and other physical properties of low-acyl gellan gel as relevant to microwave assisted pasteurization process. *Journal of Food Engineering, 149*, 195-203. doi:https://doi.org/10.1016/j.jfoodeng.2014.10.014

Zheng, M., Huang, Y., Nelson, S., Bartley, P., & Gates, K. (1998). Dielectric properties and thermal conductivity of marinated shrimp and channel catfish. *Journal of Food Science, 63*(4), 668-672.

VITA

NAME	Tanathep Leungtongkum
DATE OF BIRTH	11 December 1992
PLACE OF BIRTH	Bangkok
INSTITUTIONS ATTENDED	Chulalongkorn University
HOME ADDRESS	120/89 Tiwanon-Pakkret Rd., Pakkret, Pakkret, Nonthaburi 11120

จุฬาลงกรณ์มหาวิทยาลัย
CHULALONGKORN UNIVERSITY